Photometric binaries in Magellanic Cloud star clusters

Thesis submitted to fulfill the requirements for the
award of the degree of,

Doctor of Philosophy in Astronomy

by

Anjana Mohandasan

(Ph.D. Cycle: XXXVI, 2020-2023,
Matricola No. 2021934)

Under the supervision of,

Prof. Antonino P. Milone

Dipartimento di Fisica e Astronomia “Galileo Galilei”

Università Degli Studi Di Padova

Vicolo dell’Osservatorio, 3, 35125, PD, Italy

Dedicated to the admirers of stars,
to all those who look beyond!

Abstract

"*It takes two to tango...*"

As it happens, this saying holds even in the case of stars!

Binary stars, with their potential to promote evolutionary scenarios at odds with standard single stellar models, have been long recognised as fascinating and important objects in stellar astrophysics. Higher interaction cross-section and the evolutionary relations with various intriguing objects, ranging from massive stars to progenitors of gravitational waves, enable binaries to have a lasting impact on their neighborhoods. Binaries and their progenies, which are often massive, have pivotal roles in the chemical and dynamical evolution of star clusters and even galaxies.

Star clusters host a substantial amount of binaries, many of them being primordial. In the dense environment of Globular Clusters (GCs), which are some of the oldest objects in the **U**niverse, the elastic scatterings of binaries carry great significance. Binaries play a crucial role in the energy distribution in star clusters often through three-body interactions. They are important in determining cluster parameters such as age, radius, and mass function. Many of the exotic objects that have been frequently detected in the vast expanse of GCs, such as Blue straggler stars (BSSs) or cataclysmic variables, have formation scenarios that can be traced to binary interactions in star clusters.

Studying binaries and associated stellar populations can reveal vital information about the life and eventual fate of a cluster. However, most of the studies on binaries are restricted to Galactic clusters which limits the range of accessible cluster parameters such as masses, ages, and densities. To broaden the cluster parameter range and better understand their impact on binary formation and evolution, we must look beyond the Galaxy.

Magellanic Cloud (MC) dwarf galaxies offer an extragalactic environment with its GCs spanning a wide range of ages and a mass range that is not spanned by both Galactic open and globular clusters. Additionally, they are close enough to study resolved stellar populations. The images collected with the Hubble Space

Telescope are used to study fourteen star clusters of the MC dwarf galaxies that cover an age interval between ~ 0.6 and 2.1 Gyr and masses of $10^4 - 10^5$ $M_\odot$, which is poorly investigated in the context of binaries.

Photometry is used to estimate the fraction of binary systems composed of two main-sequence (MS) stars, as well as the fraction of candidate BSSs. Colour magnitude diagram (CMD) analysis of star clusters facilitates a statistically robust detection of binaries spanning a large range of stellar parameters, such as primary star mass and mass ratio, with limited observation time in two filters. The fraction and distribution of binary fractions in terms of cluster and stellar parameters are also investigated. Moreover, the structural parameters of the cluster, including the core radius, central density, mass function, and total mass are also estimated.

The fraction of binaries with a mass ratio larger than 0.7 was found to range from ∼7% in the cluster NGC 1846 to ∼20% in the cluster NGC 2108. The radial and luminosity distribution was observed to change from one cluster to another. However, on combining the results from all the clusters, the binaries are found to follow a flat distribution with the mass of the primary star and show no significant correlation with the mass ratio of the companion stars in the binary. Dynamically younger clusters were found to form a flat radial distribution while dynamically older clusters demonstrated evidence of segregation towards the center. A novel approach was devised to detect low mass-ratio binaries which are deemed inaccessible for binary fraction analysis due to photometric errors and their proximity to the MS stars.

The results on binaries in the examined MC clusters are combined with those from 67 Galactic GCs and 78 open clusters (OCs), which were subjected to a homogeneous binary fraction analysis. We find a significant anti-correlation between the binary fraction in the core and the mass of the host cluster. The observed trend is consistent with analytical studies on cluster cores which imply that as cluster mass increases, so does the collision rate, driving the binary disruption processes. However, star clusters with similar masses were discovered to exhibit a wide range of binary fractions. In contrast, there is no evidence of a relationship between the fraction of binaries and either the cluster or dynamic age.

Binaries share evolutionary links with many stellar populations. The potential relation between binary fraction and the occurrence of other stellar populations, notably that of the BSSs, was investigated. However, no evidence of a relation was found between them in the case of the analysed MC star clusters of young and intermediate age. The lack of correlation was similar to what has been observed in the case of young Galactic OCs and contrary to the strong correlation observed in the case of old Galactic GCs. Interestingly, the radial distribution of BSSs showed evidence of a moderate correlation with the dynamical age of the cluster.

A population of stars was discovered above the Red Clump (RC) region of the cluster. Their number is quantified with respect to the number of stars in the (RC) and thus obtained fraction is explored for their potential relation with different physical parameters of the cluster. To shed light on their formation scenarios, their fraction is explored with respect to the MS binary fraction and BSS fraction.

An accurate binary fraction determination holds immense gravity in stellar and cluster studies. As of now, 159 clusters belonging to both Milky Way and MC have been homogeneously analysed in the context of binaries. With new and upcoming telescopes and enhanced data reduction techniques, the scope of the proposed study is certain to expand. Robust studies of binaries are sure to arise, revealing many secrets about these fascinating objects.

Contents

Abbreviations

AS	**A**rtificial **S**tar
BSS	**B**lue **S**traggler **S**tar
CV	**C**ataclysmic **V**arible
CTE	**C**harge **T**ransfer **E**fficiency
CMD	**C**olour **M**agnitude **D**iagram
FoV	**F**ield of **V**iew
GC	**G**lobular **C**luster
HST	**H**ubble **S**pace **T**elescope
LMC	**L**arge **M**agellanic **C**loud
LMXB	**L**ow **M**ass **X**-ray **B**inary
MC	**M**agellanic **C**loud
MS	**M**ain **S**equence
MSFL	**MS F**iducial **L**ine
MSFL	**MS T**urn **O**ff
MW	**M**ilky **W**ay
MSP	**M**illi **S**econd **P**ulsars
MPs	**M**ultiple **P**opulations
OC	**O**pen **C**luster
PSF	**P**oint **S**pread **F**unction
RC	**R**ed **C**lump
RCB	**R**ed **C**lump **B**inary
RGB	**R**ed **G**iant **B**ranch
SMC	**S**mall **M**agellanic **C**loud

Symbols

A	A-parameter
C	Completeness
$E(B-V)$	Extinction
$[Fe/H]$	Metallicity
F_{bin}	Binary fraction
F_{BSS}	BSS fraction
F_{RCB}	RCB fraction
$(m-M)_0$	Distance Modulus
$\bar{M}$	Average M_1
M_1	Primary star mass
M_2	Secondary star mass
M_l	M_1 corresponding to the lower limit of the analysis region
M_u	M_1 corresponding to the upper limit of the analysis region
$\mu(R)$	Density function
q	Mass ratio parameter
r	Spearman's correlation rank coefficient
R	Radial distance
R_c	Core radius
R_{hm}	Half mass radius
R_t	Tidal radius
ρ	Density
t_{rh}	Half mass relaxation time
V_{bin}	Equivalent binary fraction
ξ_M	Mass function

Chapter 1

Introduction

1.1 Binary stars

In the late 18th century, while conducting his studies on the spatial distribution of stars in the Milky Way (MW) to infer the shape of the Galaxy, Sir William Hershel with the skilful aid of his sister Carolina Hershel, noticed that a large number of stars appeared in pairs. He found that the pairing was not due to differential parallaxes or spatial projections of two spatially separate stars. After studying their motions in detail, he confirmed they appeared to revolve around each other and termed them binary systems. Isolated and independent observations of binary stars date back to as early as the second half of the 17th century. However, Hershel's robust observations which fitted perfectly in the then newly proposed theoretical framework of Sir. Isaac Newton, was the seminal discovery that encouraged exploration into a new and exciting field of stellar astrophysics, i.e., the binary stars.

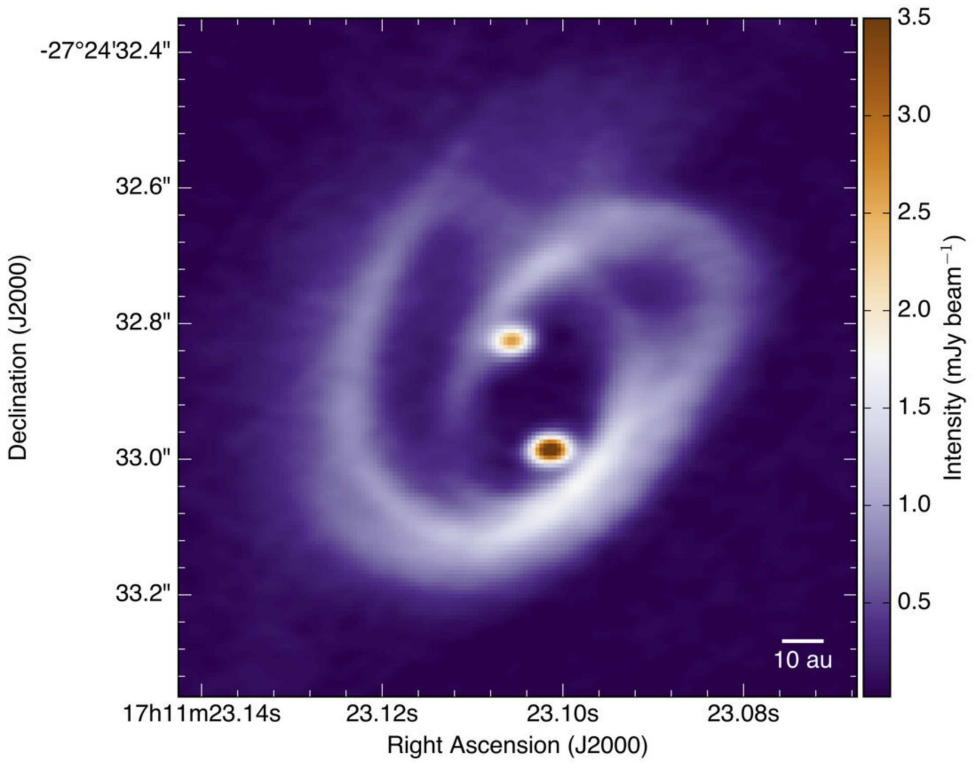

FIGURE 1.1: High-resolution ALMA image of the binary system [BHB2007]11 of a small star cluster belonging to the Barnard 59 core in Pipe Nebula molecular cloud (Alves et al., 2019).

Binary stars refer to a system of two stars that are gravitationally bound and orbit around their common centre of mass. Many stars, especially in the solar neighbourhood, are found to appear in binary systems (Raghavan et al., 2010; Duquennoy and Mayor, 1991). The Sun itself is speculated to be part of a binary that later dissolved (Siraj and Loeb, 2020). While being formed in collapsing molecular clouds, disk fragmentation tempts stars to emerge in multiple systems, out of which binaries are the most populous group. Figure 1.1 shows the high-resolution Atacama Large Millimetre/submillimeter Array (ALMA) images of the young binary system [BHB2007]11 that is still under formation. It clearly shows the accretion filaments that feed the two protesters in the centre of the circumbinary disk. Binary stars can be formed in the later stages of a star's life as well. Massive stars can gravitationally capture a passing star and form binaries, though such events

are quite rare.

Since the beginning of the twentieth century, binaries have been studied rigorously both on the observational and theoretical frontiers, which provided valuable insights into the stellar structure and evolution. Binaries were found to provide well-constrained mass–luminosity (Kuiper, 1938) and mass–radius relations (Huang and Struve, 1956). The variability in their light curves and relative motions remains one of the most accurate ways to measure stellar parameters such as mass, radius, and temperature.

Proximity and gravitational attractions between the companion stars in a binary is an apt recipe for a variety of evolutionary pathways which are unachievable by standard single stellar evolution models. Closer and tightly bound hard binaries can influence each other's evolution by even transferring mass while soft binaries have weak gravitational interactions and barely interfere with each other's evolution. Complex interactions ought to happen as the companion stars evolve which leads to an array of interesting objects.

Formation scenarios of planetary nebulae, intermediate luminous transients, supernovae, gamma-ray bursts, and gravitational wave progenitors, among others, are closely linked with binary evolution. Most massive stars form in multiple systems and a binary system is found to be their preferred choice (Sana et al., 2012). Models suggest binarity alters the temperatures, luminosities, and elemental abundances, on the surface and interior, of massive stars. The rates and mechanisms of their mass loss and their ultimate core-collapse fates are directly linked to the conditions present at their formation in a binary (Dorn-Wallenstein and Levesque, 2020). Under specific conditions, binarity induces the onset of certain nuclear reactions leading to the formation of Type Ia supernova explosions

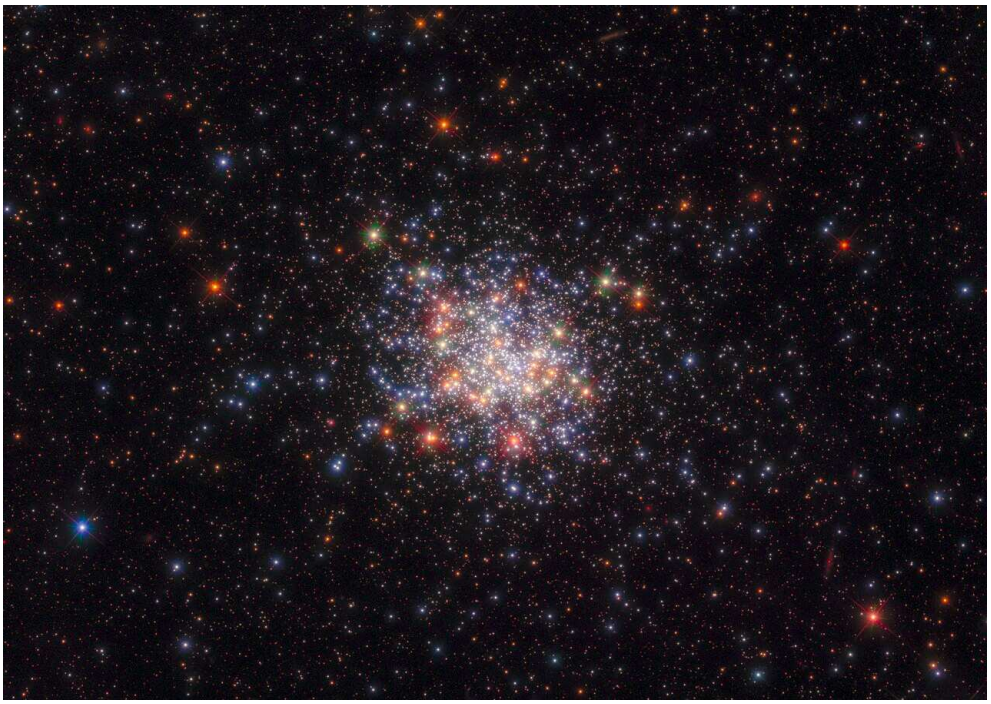

FIGURE 1.2: Hubble space telescope image of the Large Magellanic Cloud cluster NGC1755 (esahubble.org).

from low-mass stars in binaries, which also serve as a standard candle in astronomy. Massive early-type stars have powerful stellar winds that interact with the interstellar medium. These processes immensely contribute to the abundance and distribution of heavy elements observed in the interstellar medium.

Binaries are peculiar in many ways that it is safe to say when observations disagree with the theory, there ought to be a binary involved. And, the peculiar evolution binaries and their progenies, which are often massive, have inadvertent ramifications in the chemical and dynamical evolution of star clusters and galaxies as well.

1.2 Star clusters and binary stars

Star clusters form one of the most spectacular spectacles in the night sky. Luminous clusters such as Hyades, Pleiades, or Omega Centauri have been observed through centuries. They are luminous groups of stars that are held together by their mutual gravitational attraction. They are useful tools in distance calibration and in measuring the age and evolution of galaxies. Cluster members are expected to be formed from the same molecular clouds and have similar ages and metallicities. The coeval members are expected to be at the same distance and move as a single unit through the galaxy. However, recent studies have shown that star clusters host multiple populations of stars with differences in elemental abundances and/or distinct sequences in photometric diagrams (Milone and Marino, 2022). Binaries are expected to play a key role in this phenomenon. Nevertheless, their importance as an astrophysical laboratory for stellar evolution and dynamics studies remains unchallenged.

Star clusters are categorised into two major classes; Open clusters (OCs) and Globular clusters (GCs). OCs are loosely bound aggregates of hundreds or thousands of stars. They consist of Population I stars and are relatively younger and less massive compared to GCs. GCs are one of the oldest objects in the universe and host Population II stars. Hence, they are excellent tools to probe galactic archaeology. With a few thousand to a million members, they have stronger mutual gravitational attraction which gives them a globular shape. Being one of the densest environments, star clusters are home to a variety of intriguing objects. Among them, binaries hold a position that is both fundamental and significant (Ishak, 2019). Both open and globular clusters host a substantial number of binaries, many of them primordial in nature (Hut et al., 1992). Binaries have a major role to play

in the ever-ensuing dynamics of the clusters and their various stellar populations (Lanzoni et al., 2016). Additionally, the determination of various cluster parameters such as age, luminosity function, radius, and mass benefit greatly from the understanding of binarity in the system (Mohandasan et al., 2024; Cordoni et al., 2023).

Binaries have higher interaction cross-sections compared to single stars. Through frequent interactions with other objects in the cluster, they form an efficient mechanism for kinetic energy distribution (Fregeau et al., 2004). This binary-burning phase of the cluster is the longest phase of cluster evolution in which most of the observed clusters are expected to be (Heggie, 1975). The elastic scattering interactions of binaries are effective in withstanding the impeding gravitational collapse in the centre, thereby, defining the dense cluster core (Heggie and Hut, 2003). Aarseth and Hills (1972) found that even if there are no binaries initially in the cluster, they can be formed swiftly and can take possession of a considerable amount of the binding energy of the cluster within a few mean crossing times. The growth in binding energy is often accompanied by the formation of triple systems by capturing single stars that pass by. These interactions can guide the binary stellar evolution by altering the orbital parameters, assisting the escape and exchange of the binary members.

The interaction rate of binaries in clusters can be significant enough to cause the destruction of soft binaries even in low-density stellar systems. Raghavan et al. (2010) suggest binaries, especially the ones with higher cross sections and hence a higher interaction rate, will lose companions to dynamical stripping with age. Soft binaries in clusters are tremendously influenced by the tidal effects which modify their orbital periods and reduce their eccentricities (Duquennoy and Mayor, 1991). Hard binaries, on the other hand, become even harder with the ongoing

interactions (Heggie, 1975). The high rate of scattering transforms the dense cluster neighbourhood into an ideal cauldron for the production of exotic objects. In recent decades, Blue Straggler Stars (BSSs, Piotto et al., 2004), Cataclysmic Variables (CVs, Cool et al., 1995), Low-Mass X-ray Binaries (LMXBs, Kim et al., 2006), and Millisecond Pulsars (MSPs, Edmonds et al., 2002) have been detected in close binary systems in star clusters. In addition, their evolution is better understood against the backdrop of binary fractions in the cluster.

The evolution of binaries in a cluster largely depends on two factors: i) the secular binary stellar evolution and ii) their interaction with other cluster members. Secular binary evolution can depend on the mass and mass ratio of the companion stars. Environmental parameters and internal dynamics of the cluster greatly influence the formation, destruction, and segregation of binaries. Cluster core provides an excellent place of birth for binaries but there is no guarantee that they can stay there for long. The high rate of interactions that facilitated the birth of binaries can very well toss them to the outskirts. Gravity, on the other hand, segregates the cluster members to the core, thus trying to retain the core density. This sinking is more prominent in the case of massive stars, and binaries more than often comprise the most massive cluster members (Sana et al., 2012). The binaries with kinetic energy comparable to that of a typical cluster star are the main variables in the binary fraction. Their amount and influence on cluster evolution can significantly depend on the environment.

Being massive, binaries and their progeny are subjected to dynamical sinking in star clusters. Processes in star clusters leave lasting imprints in their amount and distribution. By exploring the binary fractions belonging to diverse cluster environments in terms of different stellar and cluster parameters, we can peek into the dynamics underway.

1.3 Detection methods

Several techniques are deployed to detect binaries. The techniques employed should be specific to the characteristics of the types of binaries being studied. The first binaries to be detected were visual. They are systems in which the angular separation between the companion stars in a binary is wide enough for the telescope to resolve them. These are usually soft binaries with large separations between them and periods of a few decades. Another approach is to study the spectral lines emitted by a binary system. In close binaries, the orbital velocity of the companion stars will be significant enough to produce detectable Doppler shifts which are detectable from their spectra. Astrometric measurements of the wobbling of the luminous companion in a binary are also found useful in verifying the presence and estimating the structural parameters of the inconspicuous companion.

Photometric variability (Kaluzny et al., 1996) in the light curve of photometric or eclipsing binaries is one of the most common binary detection methods. It is quite useful in detecting binaries with their orbital plane lying in the line of sight of the observer. When they undergo eclipses, their light curve reaches a discernable minimum. Occultation causes a periodicity in the light curve which can be used to estimate mass, radius, and distance to these binaries with unprecedented accuracy. Figure 1.3 denotes the typical light curve of an eclipsing binary. The method is specific for systems with large brightness differences.

Radial velocity variability analysis is another prominent method to detect binaries (Latham, 1996). This method is frequently employed to analyse binaries comprising massive stars. Radial velocities of the companions are commonly measured employing Doppler spectroscopy of the spectral lines emitted by the stars. Figure

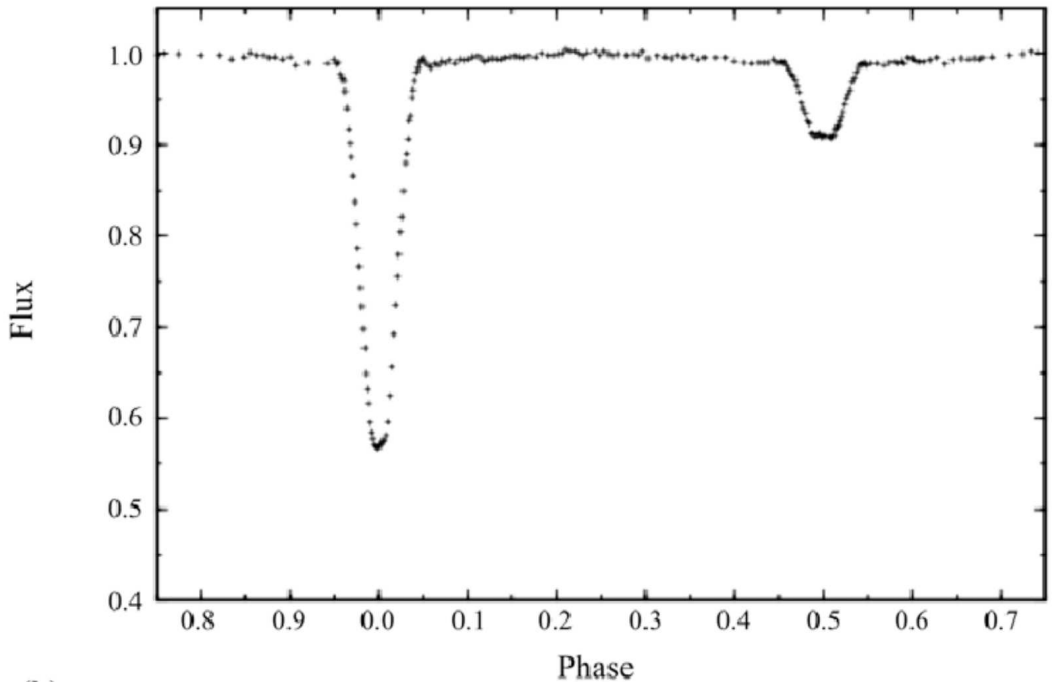

FIGURE 1.3: Binary detection using photometric variability. The figure denotes the dip in the light curve of a non-contact binary system (Skelton and Smits, 2009).

1.4 shows the variation in the line of sight component of the radial velocity of a typical binary system. Solid and hollow points denote the different components of the binary system. However, accurate radial velocity estimation requires a long observation time.

Among the various techniques in literature to identify and characterise binary systems, the method based on the colour-magnitude diagram (CMD) provides an efficient approach. CMD is a form of Hertzsprung Russel Diagram where the luminosity is represented by either apparent or absolute magnitude and the temperature is represented by the colour index. CMDs of star clusters have been extensively employed to study stellar populations in them (Milone et al., 2009; Ferraro et al., 1999a; Cordoni et al., 2022; Milone et al., 2023b; Tailo et al., 2021; Dondoglio et al., 2022) including unresolved main sequence (MS) binaries (Rubenstein and Bailyn, 1997). Unlike the previously mentioned methods, the said approach is not

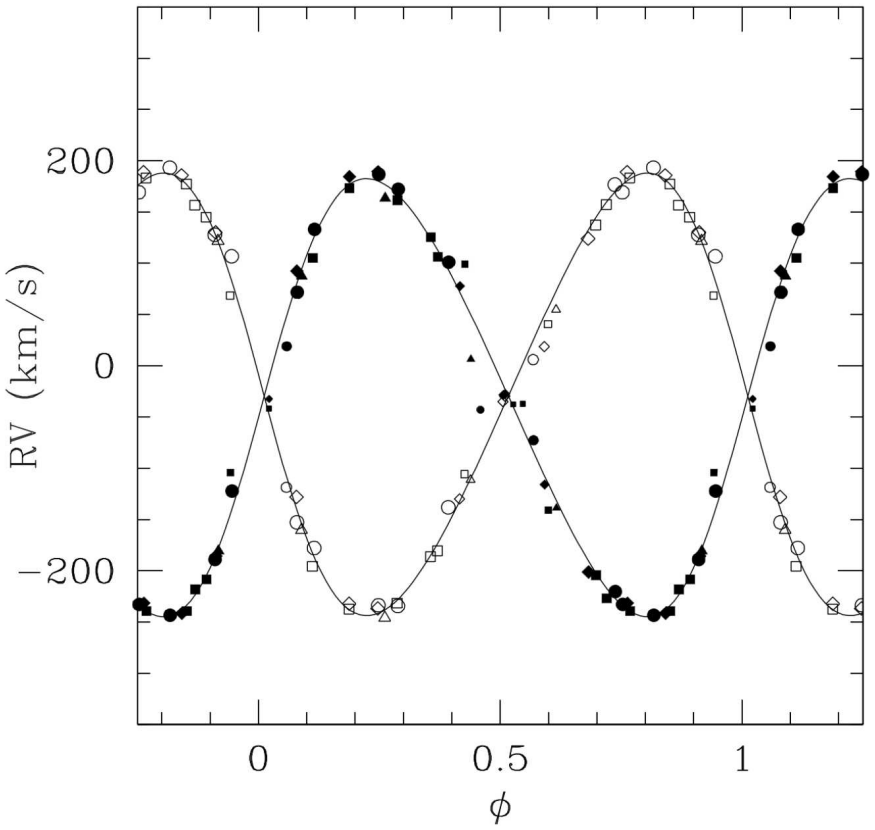

FIGURE 1.4: The plot demonstrates the radial velocity variations observed for binary system (Sana et al., 2001).

biased toward systems with higher brightness, radial separation, or eccentricity. Rather, it is effective in studying binaries that span a wide range of structural parameters such as the mass of the primary star (M_1), mass-ratio of the companion stars (q), or radial region of occurrence in the cluster (Bolte, 1992). Additionally, this method is statistically robust and observationally cheap as a limited observation time in two filters alone is sufficient to examine the multitude of binaries and other stellar populations in the cluster which belongs to a large parameter space (Hut et al., 1992).

Even with the highest resolution instruments, it is hard to resolve single stars in binary in dense stellar systems such as GCs. Therefore, they appear as a single star of enhanced magnitude in telescopic images (Refer to Chapter 4 for details). In the

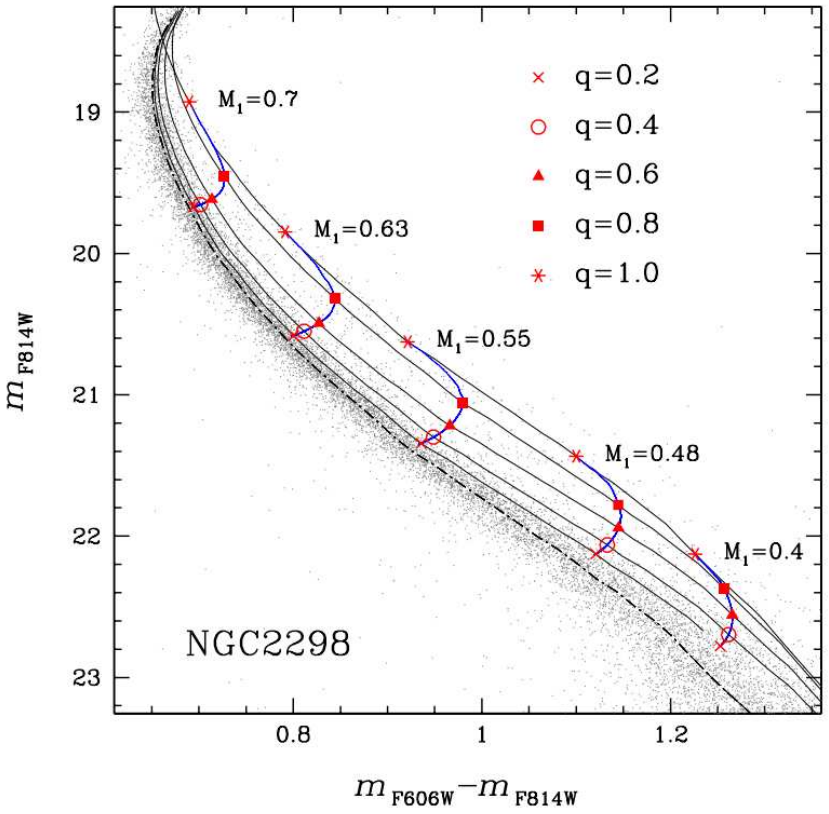

FIGURE 1.5: Colour magnitude diagram used for binary analysis. Locus of binaries belonging to different mass-ratios, q, and primary star masses, M_1, are indicated in the figure (Milone et al., 2012).

CMD of a cluster, MS-MS binaries populate the region in the red side of the main-sequence-fiducial-line (MSFL). Figure 1.5 demonstrates the binary populations in the CMD of the Galactic GC NGC2298 (Milone et al., 2012). The position of binaries in the CMD is a function of M_1 and q, as shown in the figure. Similarly, we can simultaneously analyze a large number of binaries with different primary star masses and mass ratios and calculate their fraction in the cluster using cluster CMD. The distribution of binaries with respect to M_1, q, and radial distance from the cluster centre provides vital inferences about the dynamics underway in the cluster.

Photometric errors, differential reddening, blending, and spatial-dependent variations of the photometric zero points are among the major challenges for accurately

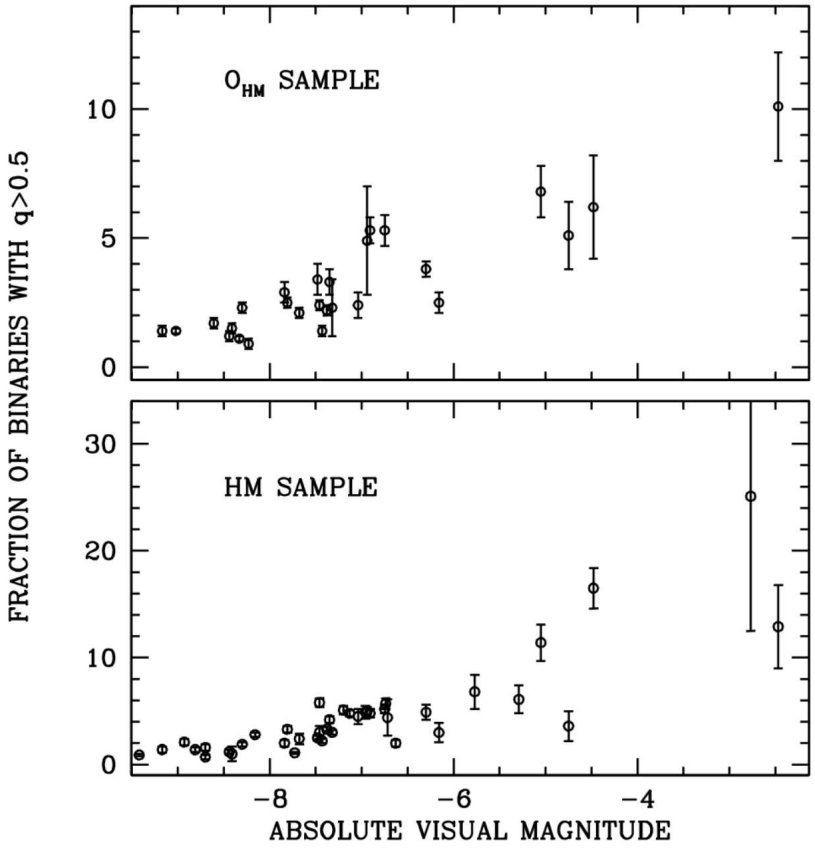

FIGURE 1.6: Variation of binary fraction as a function of the mass of the cluster. The plot is based on observations of 50 Galactic globular clusters (*Upper panel*) outside their half-mass radii (*Lower panel*) and between their core radii and half-mass radii (Milone et al., 2008).

determining photometric binaries. Field stars that sneak into the cluster region of the telescopic field of view (FoV) pose another hurdle. Hence, this approach necessitates high-precision photometry, astrometry, and high-resolution images. These requirements are achievable in the era of the Hubble Space Telescope (HST) and advanced data reduction software. The methods adopted to rectify such effects will be discussed in Chapter 2 and Chapter 4.

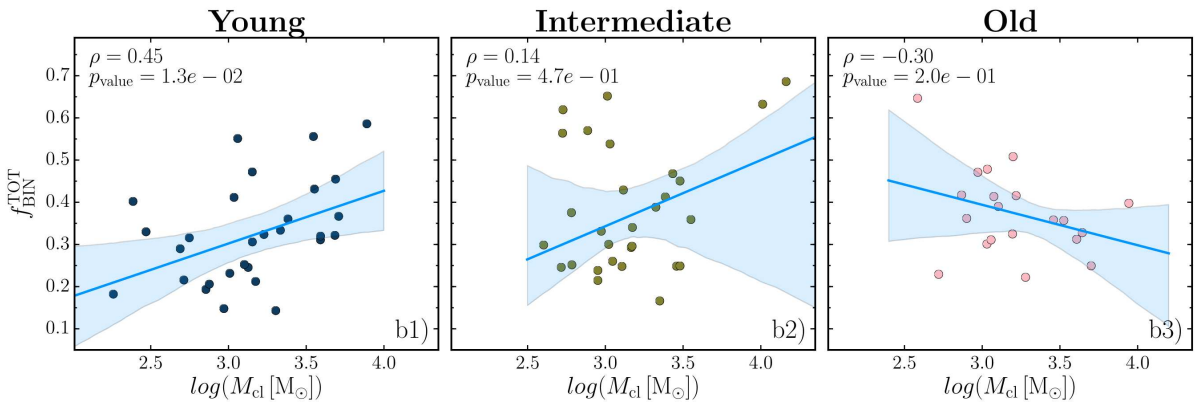

FIGURE 1.7: Variation of binary fraction as a function of the mass of the cluster. The plot is based on observations on 78 Galactic Open Clusters (Cordoni et al., 2023). Clusters in different panels span different age ranges.

1.4 Binary fraction and distribution

Pioneering studies on photometric binaries can be seen in the work of Bolte (1992), Aparicio et al. (1991), and Romani and Weinberg (1991). The first investigation of a large sample of clusters was done by Sollima et al. (2007), who studied the binaries in 13 low-density Galactic GCs and derived the binary fractions in the cluster cores. They found an anti-correlation between the relative age of the cluster and binary fraction. An extensive survey of photometric binaries in 67 Galactic GCs was conducted by Milone et al. (2012) and Milone et al. (2016), using the images collected with the Advanced Camera for Survey (ACS) aboard HST. They did not observe any link between age and binary fraction. However, the fraction of binaries in the cluster core was found to anti-correlate with the cluster mass, as shown in Figure 1.6. Similar to Galactic GCs, studies on Galactic OCs also show a reduction in binary fraction with an increase in cluster mass and no relation with the age of the cluster (Sollima et al., 2010).

Theoretical models have predicted the importance of binary ionisation processes in determining the binary fraction, particularly in relaxed stellar systems (Sollima,

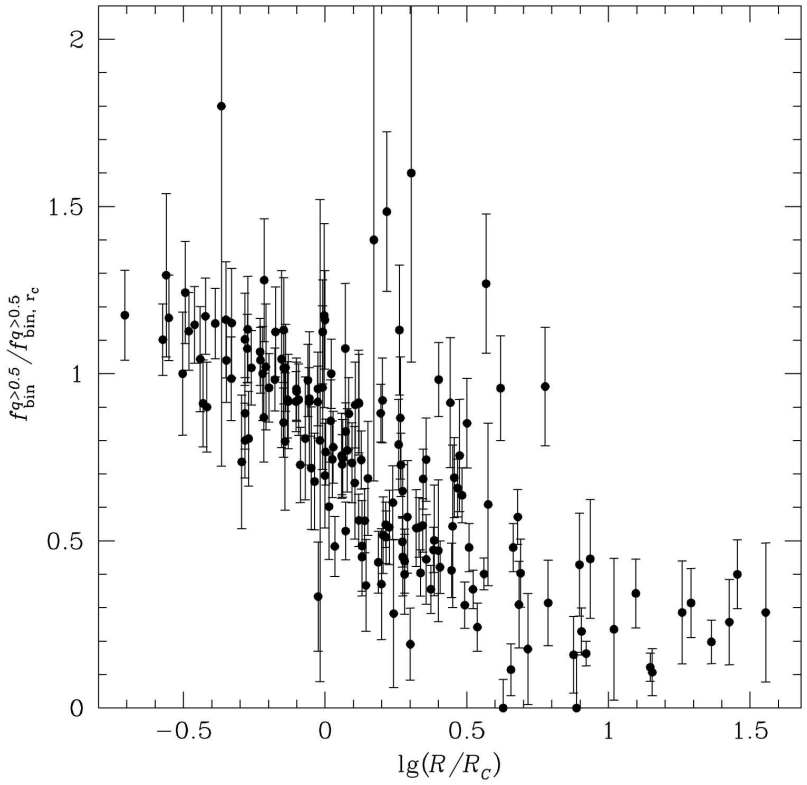

FIGURE 1.8: The figure shows the binary fraction as a function of radial distance for a sample of 59 Galactic globular clusters (Milone et al., 2012).

2008). A massive system has a higher probability of collisional interactions, often with colliding stars of higher kinetic energy (Battinelli and Capuzzo-Dolcetta, 1991). Collisional interactions can result in binary disruption or mergers and reduce the binary fraction. An extensive Gaia-based study on 78 Galactic OCs has shown the variation of binary fraction with cluster mass can be a function of age. Figure 1.7 shows the binary fraction decreases with increasing mass in the case of the relaxed systems, while young and intermediate clusters show an increase.

Different processes can influence the formation and survival of binaries in a cluster, such as collision, fragmentation, and tidal disruption (Heggie and Hut, 2003). Binaries of different masses, mass-ratios, and the ones pertaining to different regions in the cluster, such as cluster centres or outskirts, are not equally affected by these processes. For example, the high-mass binaries, whether it be due to higher

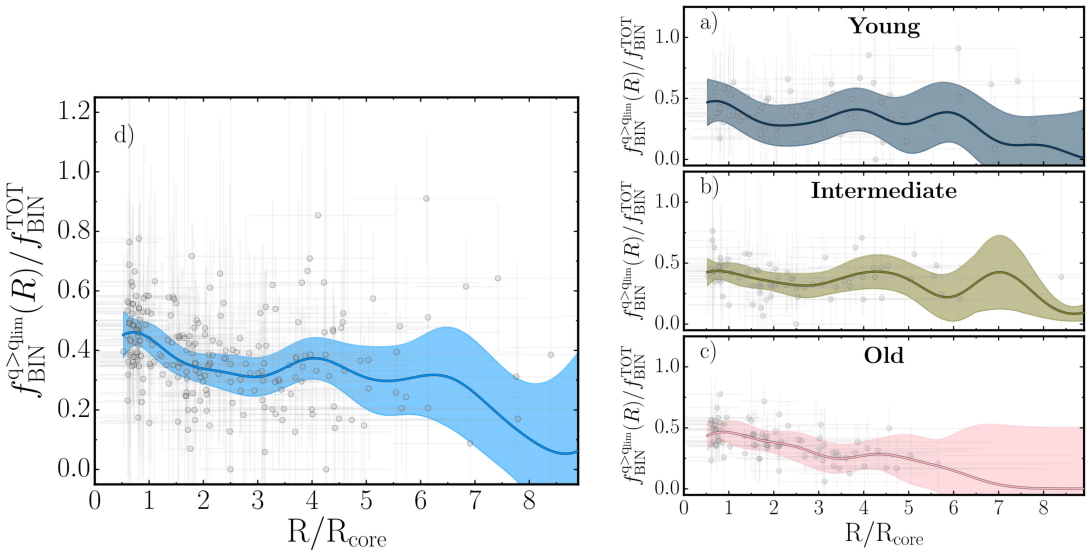

FIGURE 1.9: (*left panel*) Radial distribution of MS binaries in Galactic open star clusters (Cordoni et al., 2023). (*right panels*) The radial distribution in younger, older, and intermediate age clusters is plotted separately. Y axes in each panel show the normalised binary fraction.

primary star mass or high mass-ratio between the companion stars in a binary, tend to form in tightly bound systems unlike the low-mass ones and are more resistant to disruption by interaction with other cluster members (Heggie, 1975). However, high-mass-ratio binaries have a higher chance of fragmenting and turning into low-mass-ratio binaries. Additionally, high-mass binaries are prone to dynamic friction and sink to the cluster centre whereas the low-mass counterparts are eventually pushed to the outskirts. This mass segregation increases the probability of collisional interaction, especially in the cluster core, and can be a function of the dynamical state of the cluster (Ferraro et al., 2012). The domineering processes determine the amounts of binaries belonging to a certain mass, mass-ratio, and radial region. Conversely, by understanding the preferred mass, mass-ratio, and radial distribution of binaries, we can infer the governing processes in the system.

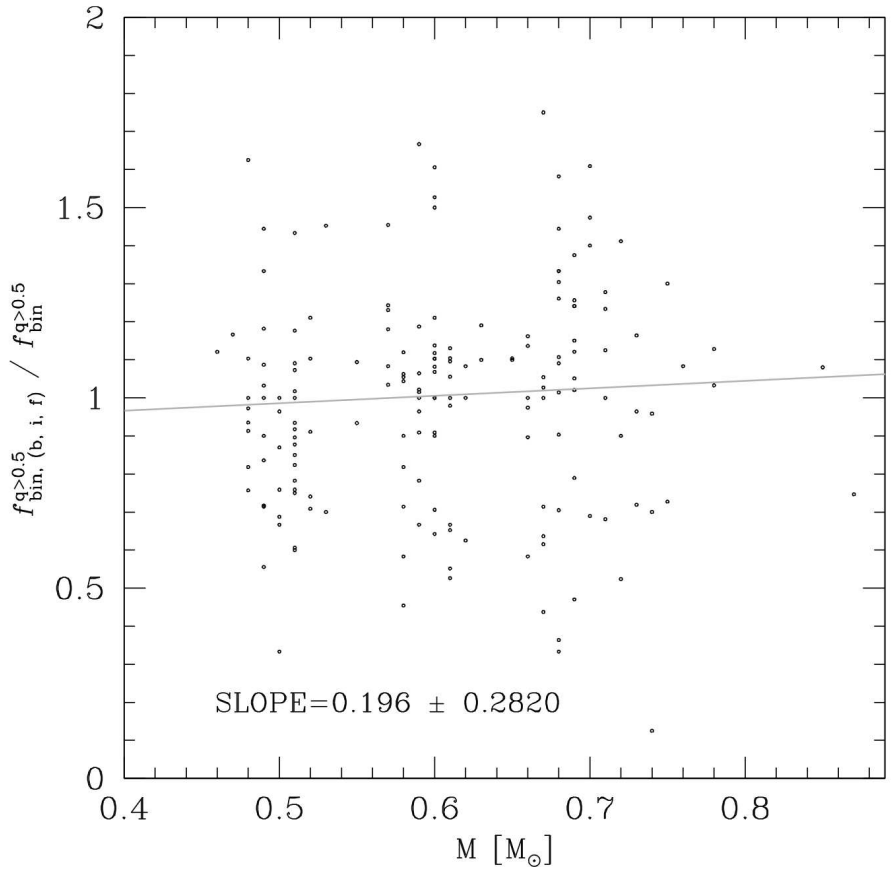

FIGURE 1.10: Variation of binary fraction as a function of the mass of the primary star in old Galactic globular clusters. Y-axes show the normalised binary fraction corresponding to the mass bin in the x-axes. Refer to Milone et al. (2012) for more details.

The radial distribution of binaries in Galactic GCs was observed to have a preference towards the cluster centre (Sollima et al., 2007). Figure 1.8 shows the normalised radial distribution of binary fraction 59 old Galactic GCs (Milone et al., 2012). For feasibility in comparison, the normalisation of the radial range and the binary fraction is done with respect to the core of the clusters. A significant population of binaries appears to have segregated to the centre. The left panel of Figure 1.9 demonstrates the radial distribution observed in the case of Galactic OCs (Cordoni et al., 2023). The blue strip shows the mean distribution of 78 young Galactic OCs in a confidence interval defined by the standard deviation. On dividing in terms of their relative ages, differences can be discerned in the relative

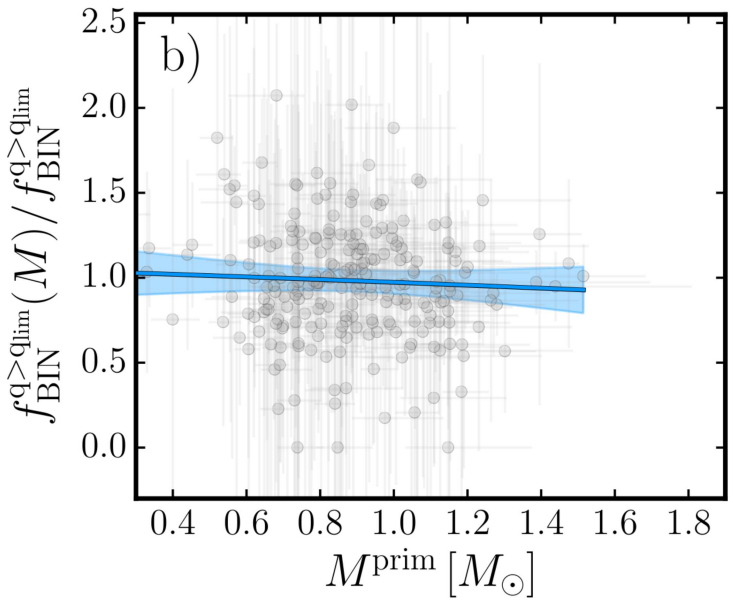

FIGURE 1.11: Variation of binary fraction as a function of the mass of the primary star in Galactic open clusters (Cordoni et al., 2023). Y-axes denote the normalised binary fraction corresponding to the mass bin denoted in the x-axe. q_{lim} is the minimum q accessible in the cluster.

distribution of younger and older clusters in the sample set, as shown in the right panels. Dynamical sinking in systems of different relaxation states is predicted to be responsible for such a difference in the radial distribution of binaries (Geller et al., 2013).

The distribution of binary fraction with respect to the mass of the primary star was observed to be flat in the case of Galactic GCs (Milone et al., 2012). Figure 1.10 shows the lack of correlation between binary fraction and primary star mass for 59 old Galactic GCs. A similar analysis in Galactic OCs resulted in a similar lack of correlation (Cordoni et al., 2023), as shown in Figure 1.11. On exploring the variation of binary fraction with the mass-ratio of the companion stars, no correlation was observed in the case of Galactic GCs (Milone et al., 2012) or Galactic OCs (Cordoni et al., 2023). Figure 1.12 and Figure 1.13 show the patterns observed for the dataset of 59 Galactic GCs and 78 Galactic OCs, respectively.

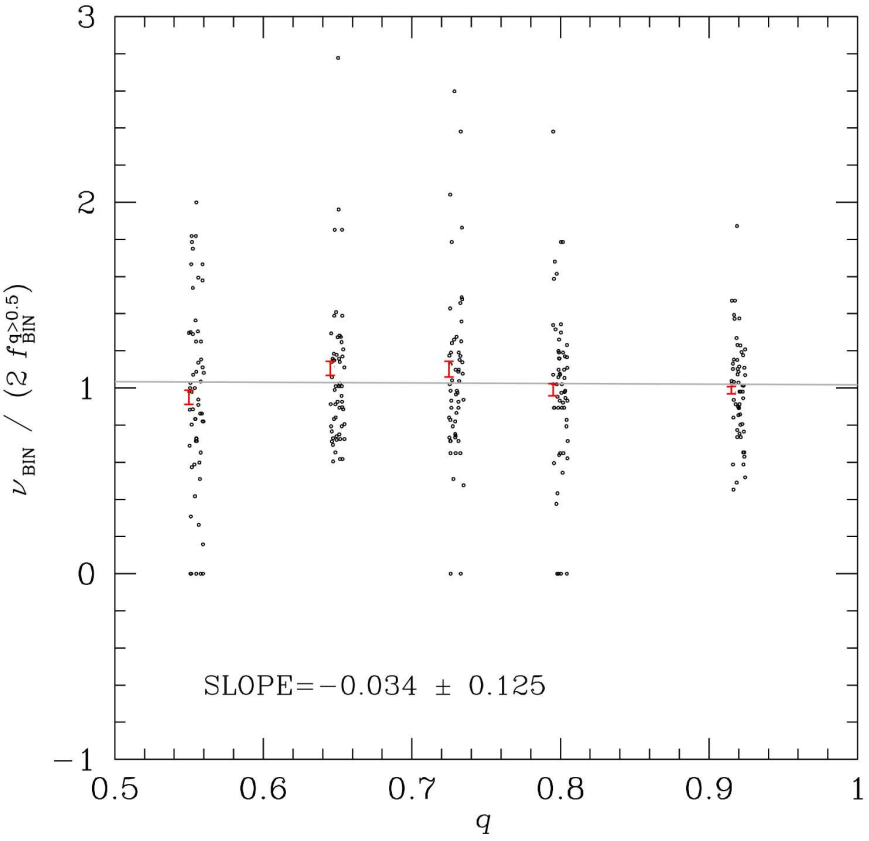

FIGURE 1.12: Binary fraction in Galactic globular clusters as a function of mass ratio parameter, q (Milone et al., 2012).

1.5 Exotic objects in star clusters

Binary stellar evolution has great significance in stellar evolution studies. Depending on the type of interaction between the companion stars in a binary, they can give rise to a variety of evolutionary pathways. Numerical analysis has shown that the frequent interactions between cluster members can drive the disruption of soft binaries and the hardening of hard binaries (Heggie, 1975). Though stars in a non-contact binary system do not deviate much from standard evolutionary scenarios, mass transfer in contact binaries results in progenies that are at odds with single stellar evolutionary models. The higher interaction rates in cluster environments have a substantial influence on these scenarios.

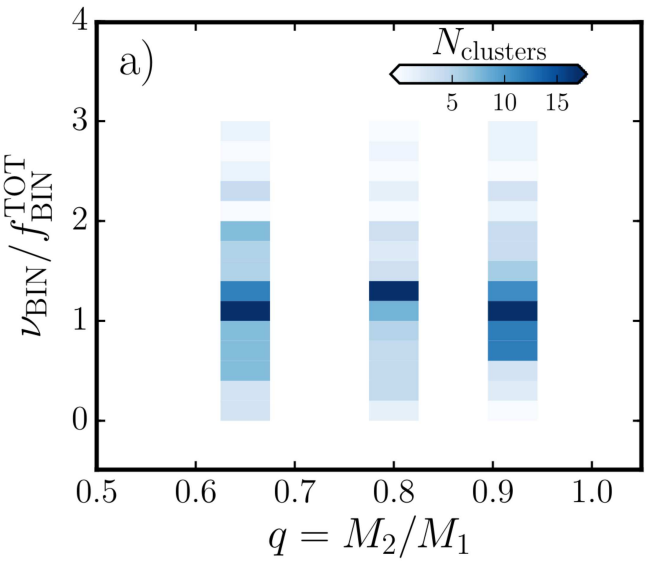

FIGURE 1.13: Binary fraction in Galactic open clusters as a function of mass ratio parameter, q (Cordoni et al., 2023). Y-axes denote the normalised value of equivalent binary fraction in each q bin.

Binaries with compact companions usually demonstrate strong accretion scenarios. When the compact companion is either a black hole or neutron star, and the other one is a lower-mass star, either a MS star, giant, or white dwarf, it forms a LMXB. The accretion disk produces radiation in X-ray wavelength, making it one of the brightest objects in the X-ray sky. The powerful outflows produced have a great impact on the surrounding environment and interstellar medium (Fijma et al., 2023). A white dwarf that accretes from a low-mass companion in a close binary system forms CVs. MSPs form in binary systems containing a neutron star and an evolving companion star, where mass accretion eventually spins up the neutron star. About 50% of the identified MSP population belongs to GCs (Ferraro, 2006).

The dense environments of GCs promote strong dynamic interactions between its members, including collisions. Compared to the Galactic disk where such binaries can only form through the evolution of primordial binaries, dynamical interactions

in GCs can lead to the formation of several different binary systems suitable to produce exotic objects (Ferraro, 2006) which are often detected in the vast expanses of GCs. These binary by-products can be strongly affected by the cluster dynamics, thus serving as a diagnostic tool for the dynamical evolution of GCs.

BSSs constitute the most abundant stellar population among the exotic objects observed in star clusters. Two competing scenarios are proposed to explain their formation, i.e., binary accretion and stellar collision, both are related to the binary frequency in the cluster. In the dynamical clock framework of star clusters (Ferraro et al., 2009), the radial distribution of BSSs is presented as an effective tool to map the evolution of the hosting star cluster. Binaries along with their massive progenies such as BSSs are prone to dynamical friction which leads to their eventual migration towards cluster centers. Depending on the degree of migration observed in the cluster, as demonstrated by their radial distributions, the dynamical state of the system can be inferred (Lanzoni et al., 2016).

Photometry has been successfully used to probe exotic stellar populations. BSSs span a distinguishable sequence in the CMD of a star cluster and can be studied efficiently. Studies on Galactic GCs have shown a strong correlation between binary fraction and BSS fraction (Milone et al., 2012) while such a trend was absent in young Galactic OCs (Cordoni et al., 2023).

1.6 Problem statement

Several works on photometric binaries explore the effect of stellar parameters on binary fraction. Some of these works compare a large number of clusters (Sollima et al., 2007; Milone et al., 2012, 2016; Cordoni et al., 2023) such that the influence

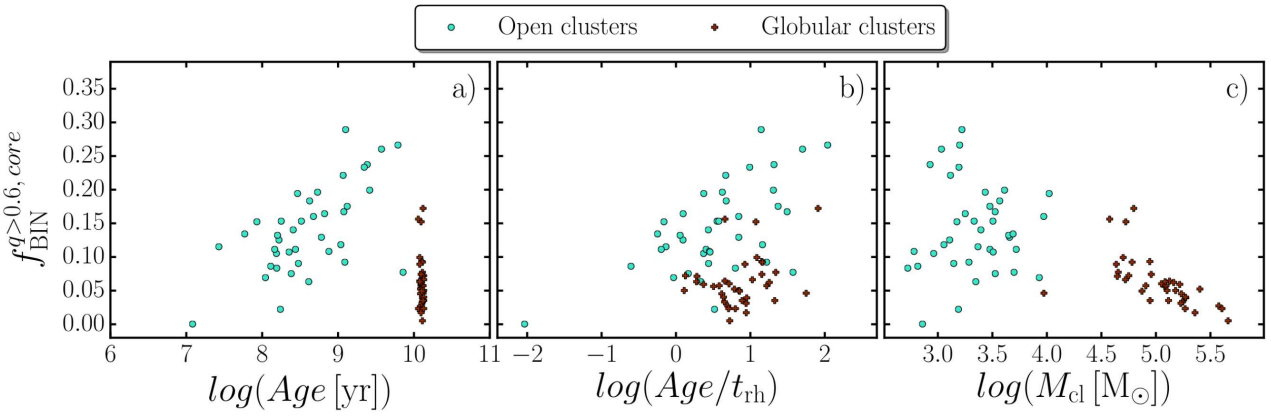

FIGURE 1.14: Binary fraction as a function of age, dynamical age, and mass of Galactic clusters, in logarithmic scale (Cordoni et al., 2023).

of cluster parameters on binary fraction can be investigated. Yet, they face a major limitation of being constrained to Galactic environments.

Given the higher signal-to-noise ratio (SNR), studies on Galactic clusters can obtain better photometry compared to their extragalactic counterparts. However, Galactic GCs share similar ages and environmental parameters. Most of them are older than $\sim$10 Gyr and quite massive (Dotter et al., 2010). Hence, it is challenging to investigate the dependence of binary fractions on cluster age and study the binary systems where one component is more massive than $\sim 0.8 M_\odot$ (Sollima et al., 2007; Milone et al., 2012, 2016). On the contrary, the investigation of binaries in Galactic OCs is limited to low-mass clusters with masses smaller than $\sim 10^4$ $M_\odot$ (e.g. Cordoni et al., 2023; Jadhav et al., 2021).

Figure 1.14 demonstrates core binary fraction in clusters as a function of mass, age, and dynamical age. The studied clusters belong to a statistically robust and homogeneously analysed sample of Galactic OCs (Cordoni et al., 2023) and Galactic GCs (Milone et al., 2012, 2016), as denoted in the figure in blue and black dots, respectively. A gap is evident in age and mass intervals can be observed which can be filled using the GCs in MC. MC clusters offer an extragalactic environment

while being close enough to study resolved stellar populations in them. Theoretical studies have shed light on the role of cluster mass and age in directing binary destruction processes (Sollima et al., 2008). Filling the mentioned mass and age gaps and checking the veracity of these claims is indispensable.

The present work surpasses these limitations on mass and age by analysing fourteen star clusters in the Large and Small Magellanic Clouds (LMC and SMC). The selected clusters span an age interval between ∼0.6 and 2.1 Gyrs and masses between 10^4 and 10^5 $M_\odot$. Clusters in MC evolved in an environment, with different parameters such as density and concentration, than the Galactic case. We aim to study and quantify the population of binary stars and other exotic stellar populations in them and compare them with the results obtained for Galactic open and globular clusters. We strive to understand the influence of different stellar, cluster, and environmental parameters in the formation and evolution of these stellar populations, and the dynamical implications they carry.

Study objectives and thesis outline

The study aims to explore the MS binaries and related stellar populations in MC star clusters. I want to understand the effect of stellar, cluster, and environmental parameters on the binary fraction and distribution in the cluster. Particularly, my investigation will revolve around the following,

- The global fraction of MS binaries in the MC star clusters.
- The dependency of the binary fraction on stellar parameters such as primary star mass, mass-ratio, and radial range of occurrence.
- The dependency of the binary fraction on cluster parameters such as age, mass, and dynamical age.

- The fraction of BSSs in the clusters and their dependence on MS binary fraction and cluster parameters.

This thesis is organised into 9 chapters, including the present chapter (Chapter 1), where we explored the previous studies on binary stars in star clusters, their detection methods, and the dynamical relevance of their fraction and distribution. This chapter describes the need for the study, the problem statement, the objectives of the study, and a brief thesis outline. We have selected 14 MC GCs for this study. We have used HST data for this study which has been subjected to state-of-the-art data reduction techniques, and differential reddening correction, among others. The used data source and data reduction approaches are detailed in Chapter 2. Thus obtained CMD is used to estimate cluster parameters through mass function and density profiles, as will be discussed in Chapter 3. Afterwards, we calculated the global binary fraction in each of the clusters. Chapter 4 describes the binary fraction analysis methodology in detail while Chapter 5 summarises the distribution of binaries in the analyzed clusters. In this part of the chapter, we try to understand the mass, mass-ratio, and radial distribution of binaries in MC GCs and their relation with Galactic clusters. Notably, the selected MC clusters allow us to extend the cluster parameter range for binary analysis. Therefore, I want to explore the dependency of binary fractions on cluster parameters such as age, mass, and dynamical age, by combining the results from the MC GCs with homogeneous analysis performed on Galactic clusters. Apart from binaries, we have focused on other stellar populations in star clusters such as BSS in Chapter 6 and red clump stars in Chapter 7. We explore the potential relation between the fraction of these populations and with MS binary fraction in the cluster. We also look at these relations or the lack of them in contrast to the results through homogeneous studies

in Galactic clusters. Conclusions and research contributions of the current work and practical implications are summarised in Chapter 8.

Chapter 2

Data sources and reduction

High-resolution images are required to investigate resolved star populations in extragalactic clusters. Space telescopes are free of atmospheric distortions and can view at wavelengths inaccessible to ground-based telescopes. As a result, they are the most suitable instruments for resolving and studying stellar populations in crowded environments such as GCs. High-precision astrometry and photometry obtained from HST data are used to study binaries and related stellar populations in the analysed MC GCs. Details of data sources and processing techniques are described in this section.

2.1 Data Source

This work investigates fourteen MC star clusters younger than ∼2 Gyr that span an interval of mass (10^4 and 10^5 solar masses) which has been poorly explored in the context of binaries [1]. To obtain robust results, our sample does not include clusters

[1]This extract is taken from Section 2 of Mohandasan et al. (2024).

younger than ∼0.6 Gyr. Indeed, these star clusters exhibit split MSs associated with stellar populations with different rotation rates (Milone and Marino, 2022, and references therein), which can alter our binary fraction analysis.

I have used HST observations in Optical, Ultraviolet, and Infrared filters to study MC GCs. The clusters are observed with the Wide Field Channel (WFC) of the ACS and the Ultraviolet and Visible channel (UVIS) of the Wide Field Camera 3 (WFC3) on board HST. ACS/WFC has an angular resolution of 0.05 arcsec/pixel and a field of view (FoV) of 202 $\times$ 202 $arcsec^2$. In the case of WFC3/UVIS, the angular resolution is 0.04 arcsec/pixel and FoV is 162 $\times$ 162 $arcsec^2$. The features of the employed HST channels ensured detailed images of the studied GCs with a wide enough coverage of the cluster and field regions.

The details of the used HST observations are summarised in Table 2.1. The images are corrected for the effect of the poor Charge Transfer Efficiency (CTE) by using the method described in Anderson and Bedin (2010).

2.2 Data Reduction

High-precision photometry and astrometry, essential for an accurate binary analysis, are derived using the state-of-the-art data reduction programs developed by Jay Anderson (e.g. Anderson and King, 2000; Anderson et al., 2008), which are based on the effective point spread function (ePSF) fitting [2]. We used the FORTRAN software package KS2, which is an upgraded version of the program kitchen_sync (Anderson et al., 2008) that entails three different methods to measure the positions and magnitudes of stars. Method I measures the stars in each

[2]This section is taken from Section 2 of Mohandasan et al. (2024).

TABLE 2.1: The table contains the details of the images used for the study.

Cluster-ID	Filter	Instrument	N×Exposure Time	Date	Program	PI
ESO057SC075	F435W	ACS/WFC	55s + 2×340s	Nov 17 2006	10595	P. Goudfrooij
	F555W	ACS/WFC	25s + 2×340s	Nov 17 2006	10595	P. Goudfrooij
	F814W	ACS/WFC	15s + 2×340s	Nov 17 2006	10595	P. Goudfrooij
ESO057SC030	F475W	WFC3/UVIS	120s + 600s + 720s	August 16 2012	12257	L. Girardi
	F814W	WFC3/UVIS	30s + 2×700s	August 16 2012	12257	L. Girardi
KMHK316	F475W	ACS/WFC	2×665s	June 10 2016	14204	A. P. Milone
	F814W	ACS/WFC	42s + 533s	June 10 2016	14204	A. P. Milone
NGC1651	F475W	WFC3/UVIS	120s + 600s + 720s	Oct 16 2011	12257	L. Girardi
	F814W	WFC3/UVIS	30s + 2×700s	Oct 16 2011	12257	L. Girardi
NGC1718	F475W	WFC3/UVIS	120s + 600s + 720s	Dec 02 2011	12257	L. Girardi
	F814W	WFC3/UVIS	30s + 2×700s	Dec 02 2011	12257	L. Girardi
NGC1751	F336W	WFC3/UVIS	3580s	13 Oct 2011	12257	L. Girardi
	F435W	ACS/WFC	2×90s + 2×340s	18 Oct 2006	10595	P. Goudfrooij
	F555W	ACS/WFC	8s + 40s + 2×340s	18 Oct 2006	10595	P. Goudfrooij
	F814W	ACS/WFC	8s + 200s + 2×340s	18 Oct 2006	10595	P. Goudfrooij
NGC1783	F275W	WFC3/UVIS	9048s	16 Sep 2019	15630	N. Bastian
	F336W	WFC3/UVIS	3580s	12 Oct 2011	12257	L. Girardi
	F343N	WFC3/UVIS	2×3095s + 2×9258s	15 Jan 2021	16255	E. Dalessandro
	F435W	ACS/WFC	90s + 2×340s	Jan 14 2006	10595	P. Goudfrooij
	F555W	ACS/WFC	40s + 250s + 2×340s	Jan 14 2006	10595	P. Goudfrooij
	F814W	ACS/WFC	8s + 170s + 2×340s	Jan 14 2006	10595	P. Goudfrooij
NGC1806	F336W	WFC3/UVIS	3580s	12 Oct 2011	12257	L. Girardi
	F343N	WFC3/UVIS	2945s	14 Sep 2016	14069	N. Bastian
	F435W	ACS/WFC	90s + 2×340s	Sep 29 2005	10595	P. Goudfrooij
	F555W	ACS/WFC	40s + 2×340s	Sep 29 2005	10595	P. Goudfrooij

TABLE 2.2: Continuation of Table 2.1.

Cluster-ID	Filter	Instrument	N×Exposure Time	Date	Program	PI
	F555W	ACS/WFC	300s	Aug 12 2003	9891	G. Gilmore
	F814W	ACS/WFC	8s + 2×340s	Sep 29 2005	10595	P. Goudfrooij
	F814W	ACS/WFC	200s	Aug 12 2003	9891	G. Gilmore
NGC1846	F160W	WFC3/NIR	2843s	17 Apr 2011	12219	A. P. Milone
	F336W	WFC3/UVIS	9156s	17 Apr 2011	12219	A. P. Milone
	F343N	WFC3/UVIS	2945s	4 Apr 2016	14069	N. Bastian
	F435W	ACS/WFC	90s + 2×340s	Jan 12 2006	10595	P. Goudfrooij
	F555W	ACS/WFC	40s + 2×340s	Jan 12 2006	10595	P. Goudfrooij
	F555W	ACS/WFC	300s	Oct 08 2003	9891	G. Gilmore
	F814W	ACS/WFC	8s + 2×340s	Jan 12 2006	10595	P. Goudfrooij
	F814W	ACS/WFC	200s	Oct 08 2003	9891	G. Gilmore
NGC1868	F336W	WFC3/UVIS	2×831s + 830s	Dec 22 2016	14710	A. P. Milone
	F656N	WFC3/UVIS	1429s	Dec 22 2016	14710	A. P. Milone
	F814W	WFC3/UVIS	90s + 666s	Dec 22 2016	14710	A. P. Milone
NGC1872	F555W	ACS/WFC	115s	Sep 21 2003	9891	G.Gilmore
	F814W	ACS/WFC	90s	Sep 21 2003	9891	G.Gilmore
NGC2108	F435W	ACS/WFC	90s + 2×340s	Aug 22 2006	10595	P. Goudfrooij
	F555W	ACS/WFC	40s + 2×340s	Aug 22 2006	10595	P. Goudfrooij
	F555W	ACS/WFC	250s	Aug 16 2003	9891	G. Gilmore
	F814W	ACS/WFC	8s + 2×340s	Aug 22 2006	10595	P. Goudfrooij
	F814W	ACS/WFC	170s	Aug 16 2003	9891	G. Gilmore
NGC2203	F336W	WFC3/UVIS	2200s	Oct 08 2011	12257	L. Girardi
	F475W	WFC3/UVIS	120s + 2×700s	Oct 08 2011	12257	L. Girardi
	F814W	WFC3/UVIS	30s + 550s + 2×700s	Oct 08 2011	12257	L. Girardi
NGC2213	F475W	WFC3/UVIS	120s + 600s + 720s	Nov 29 2011	12257	L. Girardi
	F814W	WFC3/UVIS	30s + 2×700s	Nov 29 2011	12257	L. Girardi

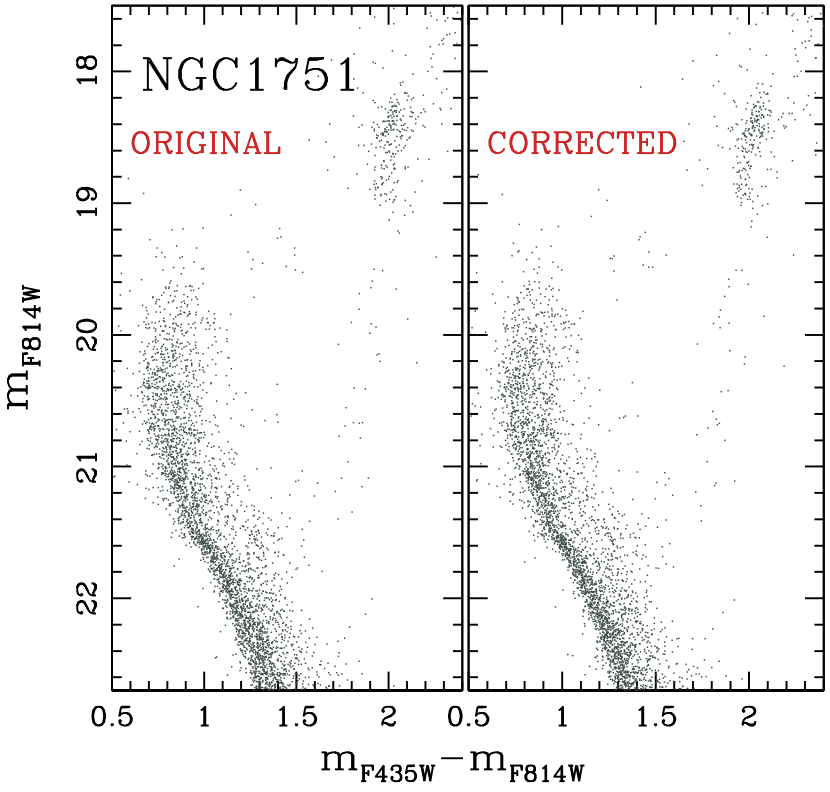

FIGURE 2.1: Differential reddening correction. The figure comparison of the CMD of the star cluster NGC 1751 (*left panel*) before and (*right panel*) after the correction for differential reddening (Mohandasan et al., 2024).

image, independently, by using the best available ePSF model. The results are then averaged to derive the best estimates of magnitude and position. This method provides the best photometry for relatively bright stars that define distinct peaks in a 5×5 pixel raster. Method II measures each star using aperture photometry, after subtracting all the neighboring stars. It works well for faint stars that do not have enough photons to be aptly fitted by the ePSF. Method III is similar to method II in terms of analysis and it works well in very crowded regions. We refer to papers by Sabbi et al. (2016), Bellini et al. (2017), and Milone et al. (2023a) for details on KS2.

Since we are interested in stars with high-precision photometry, we excluded all

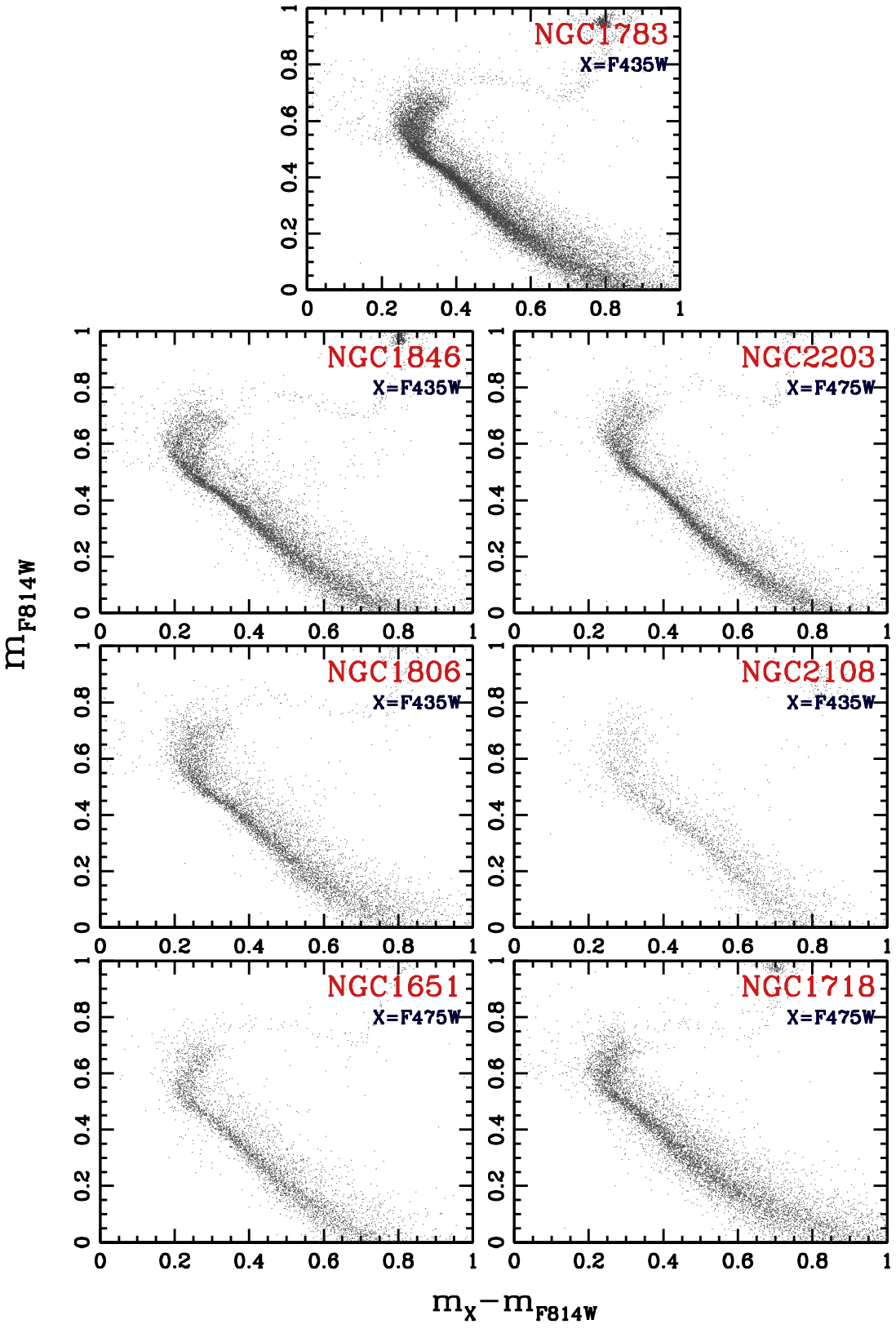

FIGURE 2.2: Collection of CMDs for the investigated star clusters. For each cluster, we plot the F814W magnitude against the X−F814W colour, where the X filter is quoted in the corresponding panel.

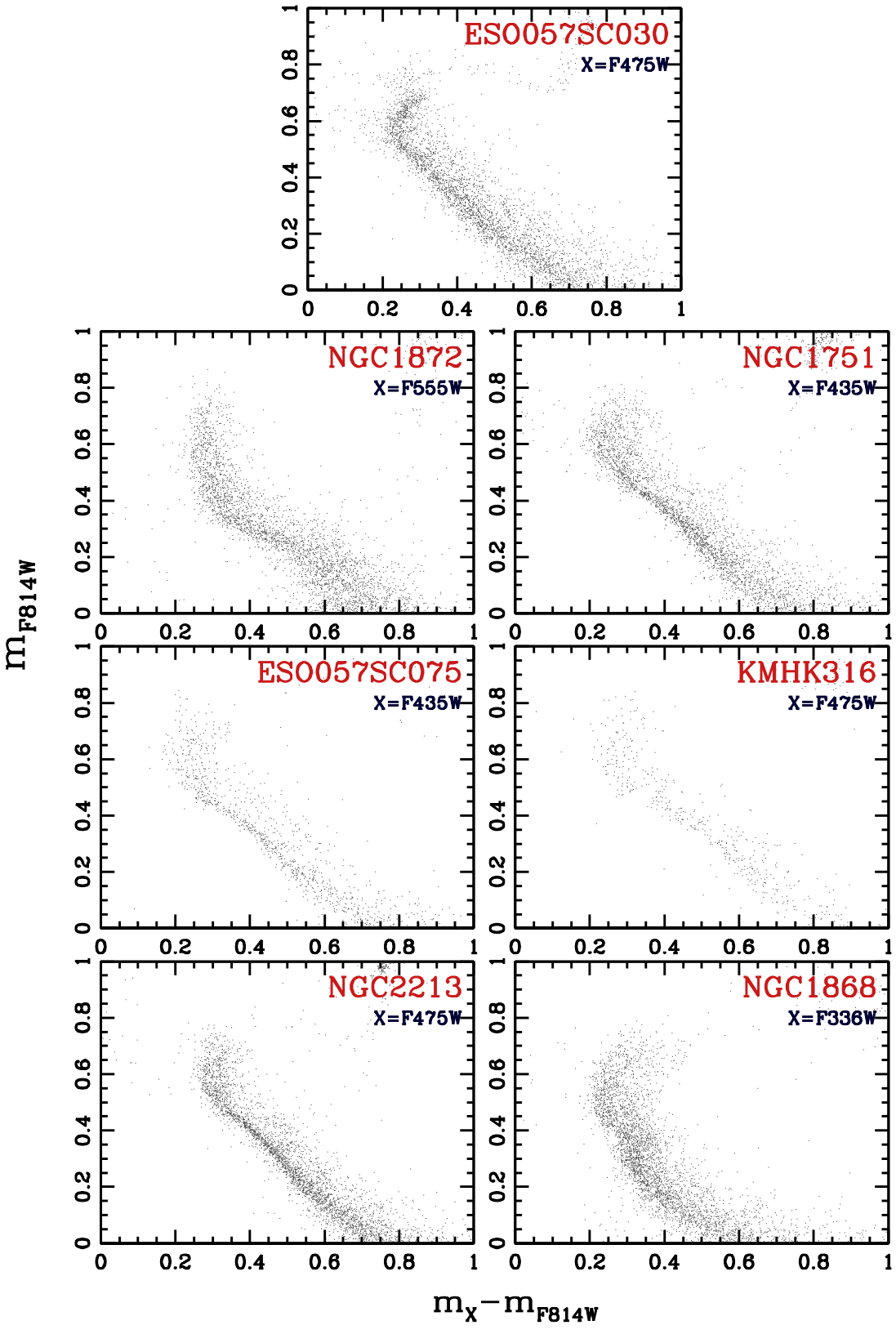

FIGURE 2.3: Continuation from Figure 2.2.

the sources that were poorly fitted by the PSF model and the stars with large root mean square values in positions. To select these stars, we used the computer programs and the methods provided by Milone et al. (2012). The stellar coordinates are corrected for geometric distortion by using the solutions by Anderson and King (2006) and Bellini et al. (2011). The photometry has been calibrated to the Vega magnitude system as in Milone et al. (2023a) using the zero points provided by Space Telescope Science Institute (STScI) [3]. The photometry was corrected for the effects of differential reddening by using the methods by Milone et al. (2012) and Legnardi et al. (2023). As an example, Figure 2.1 compares the original CMD of NGC 1751 (left) with the CMD corrected for differential reddening (right). Finally, we derived the ages, metallicities, distances, and reddening of the studied clusters by comparing the CMDs with isochrones, as in Cordoni et al. (2023). We used the isochrone from the Dartmouth Stellar Evolution Database [4] which were only available for clusters older than 1 Gyr. MESA Isochrones and Stellar Tracks [5] were used for clusters younger than 1 Gyr. The use of isochrones from different sources had a negligible effect on the binary analysis as will be discussed in Section 4.3. The reddening coefficients for the different filters are provided by Aaron Dotter (private communication).

Figure 2.2 and 2.3 demonstrate the CMDs obtained after data reduction and differential reddening corrections for the analysed MC GCs.

[3] https://www.stsci.edu/hst/instrumentation/acs/data-analysis/zeropoints
[4] http://stellar.dartmouth.edu/models/isolf_new.html
[5] http://waps.cfa.harvard.edu/MIST/

Chapter 3

Estimation of cluster parameters

In this section, we discuss the methods used to calculate different physical parameters of the cluster. We have derived the density profile and mass function of the studied MC clusters and inferred the values of the core radius, half-mass radius, central density, and mass of each of them. These quantities are employed to characterise binaries and related stellar populations.

3.1 Density profiles of the clusters

To estimate the density profile of each star cluster, we used the procedure illustrated in Figure 3.1 for the cluster NGC 1751 [1]. We first derived the number of stars with mass greater than $0.9M_{\odot}$ in different annuli in the HST FoV and then corrected those numbers for completeness. The obtained numbers are normalised by the areas of the annuli to get the number density profile of the cluster.

[1] This section is taken from Section 3.1 of Mohandasan et al. (2024).

TABLE 3.1: Parameters of the best-fitting density profile.

Cluster ID	EFF profile fit					King's profile fit			
	μ_0 [arcsec^{-2}]	a [arcsec^{-1}]	γ	R$_c$ [arcsec]	bg [arcsec^{-2}]	K [arcsec^{-2}]	R$_c$ [arcsec]	R$_t$ [arcsec]	R$_{hm}$ [arcsec]
ESO057SC075	1.07 ± 0.03	14.1 ± 1.2	1.80 ± 0.13	15 ± 4	0.06	1.23 ± 0.02	15.9 ± 0.4	159 ± 13	30
ESO057SC030	4.49 ± 0.06	15.5 ± 0.9	1.54 ± 0.08	19 ± 2	0.45	5.29 ± 0.08	19.6 ± 0.3	142 ± 6	31
KMHK316	2.75 ± 0.19	5.6 ± 0.7	1.06 ± 0.05	9 ± 1	0.33	2.41 ± 0.05	9.7 ± 0.3	145 ± 20	22
NGC1651	3.31 ± 0.01	19.3 ± 0.3	2.10 ± 0.03	19 ± 2	0.14	4.23 ± 0.04	20.6 ± 0.2	146 ± 4	32
NGC1718	7.15 ± 0.07	12.6 ± 0.3	1.89 ± 0.03	13 ± 1	0.20	7.89 ± 0.06	14.2 ± 0.2	168 ± 8	30
NGC1751	2.83 ± 0.05	14.1 ± 0.7	1.44 ± 0.04	18 ± 1	0.26	3.40 ± 0.04	19.8 ± 0.2	128 ± 3	28
NGC1783	4.82 ± 0.03	33.3 ± 0.9	2.34 ± 0.07	30 ± 8	0.26	7.27 ± 0.13	34.7 ± 0.4	161 ± 4	41
NGC1806	3.92 ± 0.02	27.3 ± 0.9	2.30 ± 0.09	25 ± 8	0.36	5.43 ± 0.07	26.2 ± 0.3	138 ± 4	33
NGC1846	1.89 ± 0.02	22.0 ± 0.9	1.73 ± 0.06	24 ± 3	0.10	2.29 ± 0.05	26.9 ± 0.5	208 ± 13	44
NGC1868	6.17 ± 0.06	11.7 ± 0.3	2.39 ± 0.04	10 ± 2	0.07	7.48 ± 0.04	11.1 ± 0.1	115 ± 4	21
NGC1872	8.48 ± 0.21	9.4 ± 0.5	1.51 ± 0.06	12 ± 1	0.82	10.09 ± 0.20	12.5 ± 0.3	83 ± 4	16
NGC2108	2.81 ± 0.04	13.3 ± 0.5	1.43 ± 0.04	17 ± 1	0.29	3.15 ± 0.03	17.5 ± 0.2	143 ± 5	29
NGC2203	2.42 ± 0.01	30.8 ± 0.8	3.03 ± 0.09	23 ± 17	0.02	3.60 ± 0.06	27.3 ± 0.4	148 ± 5	36
NGC2213	3.59 ± 0.07	12.2 ± 0.6	2.24 ± 0.08	11 ± 3	0.06	4.20 ± 0.05	11.8 ± 0.2	145 ± 10	24

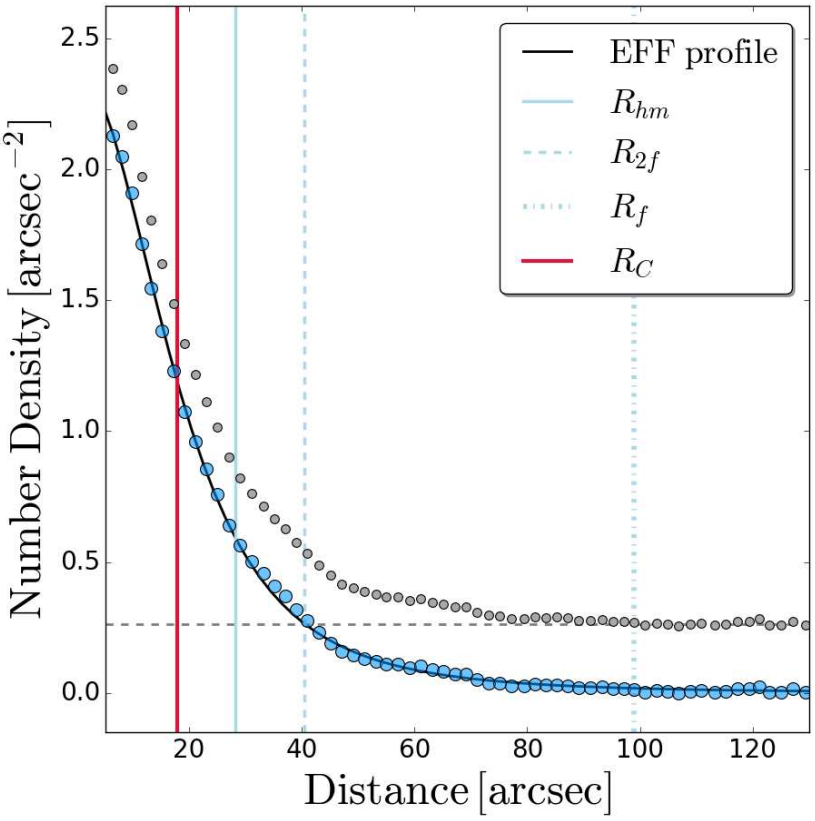

FIGURE 3.1: Grey points correspond to the observed density profile of the cluster NGC1751. The grey dotted horizontal line denotes the contribution from field contamination. The profile in blue is obtained after subtracting the background contamination from the actual density estimate, and it is fitted with the EFF profile (Mohandasan et al., 2024).

We derived the parameters of the EFF profile (Elson et al., 1987) that provide the best fit with the observed density profile. Specifically, we adopted the relation:

$$\mu(R) = \mu_0(1 + \frac{R^2}{a^2})^{-\frac{\gamma}{2}} + bg, \tag{3.1}$$

where μ_0 is the central density, a is the scaling factor, γ is the power law factor, and bg is the constant that accounts for the contamination from field stars (Santos

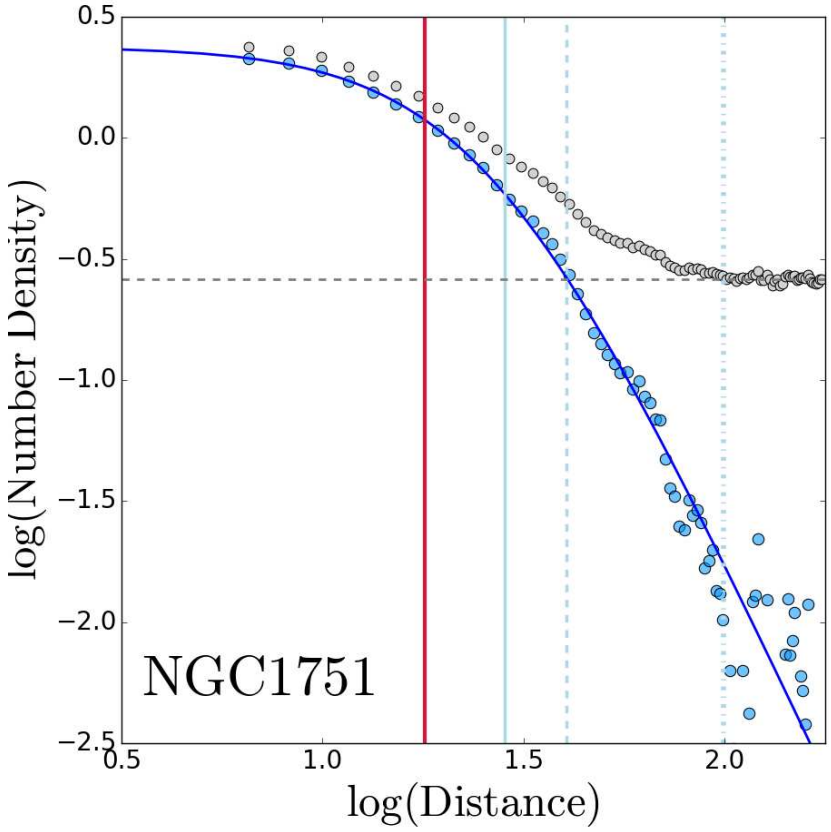

FIGURE 3.2: Logarithmic version of the density profile in Figure 3.1 (Mohandasan et al., 2024).

et al., 2020). The core radius, R_c, is derived by the relation,

$$R_c = a(2^{\frac{2}{\gamma}} - 1)^{\frac{1}{2}}. \tag{3.2}$$

Figure 3.1 shows the EFF density profile that provides the best fit with the observed density profile from the cluster NGC 1751. Figure 3.2 shows the corresponding plot in the logarithmic scale. The grey and blue points denote the number density distribution with and without the contamination from field stars. Blue points are obtained by subtracting bg from the grey points, where the black horizontal line denotes the level of bg. The corresponding radius is R_f. The radius at which the

TABLE 3.2: Average density and concentration of the cluster.

Cluster ID	ρ_{R_c} $[arcsec^{-2}]$	$\rho_{R_{hm}}$ $[arcsec^{-2}]$	C_1	C_2
ESO057SC075	0.84	0.61	1.02	0.29
ESO057SC030	3.54	2.84	0.88	0.21
KMHK316	2.10	1.45	1.20	0.38
NGC1651	2.63	2.02	0.89	0.23
NGC1718	5.60	3.64	1.11	0.36
NGC1751	2.23	1.81	0.85	0.20
NGC1783	3.84	3.31	0.73	0.14
NGC1806	3.12	2.74	0.75	0.13
NGC1846	1.48	1.12	0.93	0.26
NGC1868	4.92	3.39	1.05	0.31
NGC1872	6.69	5.76	0.86	0.16
NGC2108	2.22	1.72	0.93	0.23
NGC2203	1.93	1.57	0.80	0.19
NGC2213	2.84	1.90	1.11	0.34

number density becomes two times bg is denoted as R_{2f}.

For comprehensiveness, we derived the King profile (King, 1962) parameters that provide the best-fit with the observed density profile. The results are listed in Table 3.1. The average density of the core and the cluster region till R_{hm}, denoted as $\rho_{R_{hm}}$ and ρ_{R_c} respectively, are reported in Table 3.2. The table also features the normal concentration parameter, $C_1 = log(R_t/R_c)$, and the modified concentration parameter, $C_2 = log(R_{hm}/R_c)$, of the analysed MC cluster.

TABLE 3.3: Parameters of the mass function along with the total mass of the cluster (Mohandasan et al., 2024).

Cluster ID	α	$\bar{M}$ [M$\odot$]	$M_{Cluster}$ [M$\odot$]	t_{rh} [Gyrs]
ESO057SC075	-1.56 $\pm$ 0.11	0.77	9.86 $\times$ 10^3	0.27
ESO057SC030	-2.15 $\pm$ 0.04	0.95	8.77 $\times$ 10^4	0.51
KMHK316	-2.09 $\pm$ 0.06	1.17	1.42 $\times$ 10^4	0.12
NGC1651	-1.53 $\pm$ 0.07	1.00	3.72 $\times$ 10^4	0.46
NGC1718	-1.95 $\pm$ 0.04	0.99	7.64 $\times$ 10^4	0.50
NGC1751	-1.74 $\pm$ 0.04	1.04	3.05 $\times$ 10^4	0.30
NGC1783	-1.48 $\pm$ 0.05	0.79	8.15 $\times$ 10^4	1.15
NGC1806	-1.38 $\pm$ 0.12	1.15	4.67 $\times$ 10^4	0.50
NGC1846	-1.29 $\pm$ 0.07	0.81	4.12 $\times$ 10^4	0.68
NGC1868	-1.28 $\pm$ 0.13	1.23	1.61 $\times$ 10^4	0.14
NGC1872	-2.81 $\pm$ 0.05	1.13	8.24 $\times$ 10^4	0.14
NGC2108	-2.30 $\pm$ 0.06	1.11	4.34 $\times$ 10^4	0.31
NGC2203	-1.63 $\pm$ 0.04	0.79	3.35 $\times$ 10^4	0.58
NGC2213	-1.96 $\pm$ 0.06	1.13	2.44 $\times$ 10^4	0.21

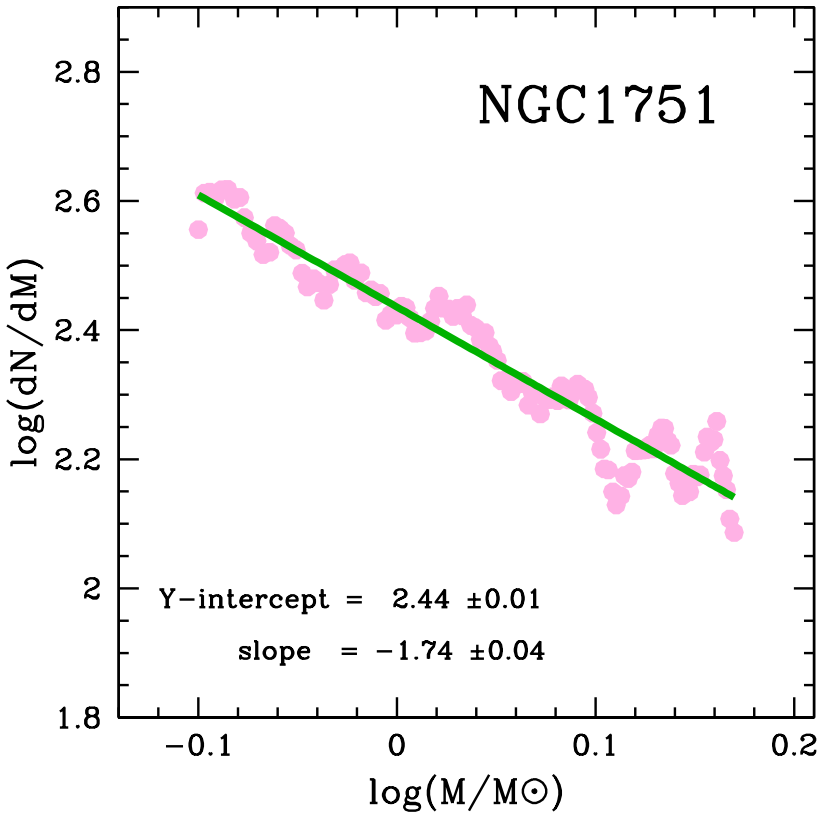

FIGURE 3.3: The mass function of clusters is determined using $log(dN/dM)$ v/s $log(M)$ plots. The green line is the least square fit of the observed mass distribution, denoted in pink.

3.2 Mass functions and masses of the clusters

To derive the mass functions of each cluster, we used the procedure by Cordoni et al. (2023) [2]. We derived the number of MS stars within the radial distance of R_{2f}, divided them into intervals of equal mass, and normalised this quantity to the mass bin. The star counts are corrected for completeness and only stars with completeness values larger than 0.5 are taken into account.

We fitted the observed mass function with the following relation obtained from Trenti et al. (2010):

$$\xi_M = \xi_0 M^{-\alpha}. \tag{3.3}$$

[2]This section is taken from Section 3.2 of Mohandasan et al. (2024).

To estimate the total mass of the cluster, $M_{Cluster}$, we integrated the mass function over the entire mass interval provided by the best-fit isochrone. Moreover, we accounted for the cluster stars with a radial distance larger than R_{2f} by using the cluster EFF profile and assuming a homogeneous radial distribution for stars with different masses.

Finally, we estimated the half-mass relaxation time by using the following equation,

$$t_{rh} = \frac{0.138 M_{Cluster}^{1/2} {R_{hm}}^{3/2}}{G\bar{M} ln(0.11 M_{Cluster}/\bar{M})}, \tag{3.4}$$

where G is the universal gravitational constant, $\bar{M}$ is the average mass of a star, and R_{hm} is the half-mass radius (Spitzer, 1987). The results are provided in Table 3.3.

Chapter 4

Binary fraction

4.1 Binaries in star clusters

Binary stars are the most populous multiple systems and star clusters host a significant amount of them. Their number in a cluster is influenced by the physical parameters and is subject to the dynamics underway. Sollima et al. (2007) studied the binary fraction in the core of 13 low-density Galactic GCs and found a minimum fraction of 6%. They also projected a global fraction ranging from 10% to 50% depending on the clusters. Later, a statistically robust survey on 59 old and massive Galactic GCs found that the fraction can go as low as 1% (Milone et al., 2012). Sollima et al. (2010) conducted a similar study on five high-latitude Galactic OCs and found a minimum binary fraction of 11% within the core. With a global fraction estimate ranging from 35% to 70%, the OCs have been found to hold a significantly higher fraction of binaries than GCs as predicted by theoretical models and N-body simulations (Sollima et al., 2010). They credit this result to the dominance of binary destruction processes that progress with age, mass, or

density. These results are consistent with radial velocity surveys in the solar neighbourhood, which have also shown the fraction can go as high as 33% (Raghavan et al., 2010).

To better our understanding of binaries, it is imperative to have homogeneous studies on clusters belonging to different environments and wide ranges of physical parameters. To this effort, we have studied the MS binary fraction in 14 young and intermediate-age MC GCs spanning a mass range unexplored by Galactic studies. The adopted methodology and results are described in this session.

4.2 Methodology

Star clusters are dense systems. Surviving in such environments requires the stars in a binary to be in close proximity [1]. Even with the high-resolution power of HST, it is hard to resolve the individual stars in such systems. Hence, the binaries are perceived as single stars of enhanced luminosity, where the observed flux will be the combination of the fluxes of the companion stars.

Suppose we are observing a binary system where the magnitudes and fluxes of the companion stars are m_1 and m_2, and F_1 and F_2, respectively. Then, the magnitude of the binary system is:

$$m_{bin} = m_1 - 2.5log(1 + \frac{F_2}{F_1}), \tag{4.1}$$

where subscripts 1 and 2 denote the primary and secondary stars, respectively, with the primary star being the more massive component of the binary system.

[1] This session is taken from Section 4 of Mohandasan et al. (2024).

TABLE 4.1: Parameters for the best fitting isochrone (Mohandasan et al., 2024).

Cluster ID	Age [Gyr]	[Fe/H] [dex]	$(m-M)_0$ [mag]	E(B-V) [mag]	RA h m s	DEC d m s
ESO057SC075	1.90	-0.40	18.49	0.06	06 13 27.26	-70 41 45.0
ESO057SC030	2.10	-0.50	18.40	0.17	05 42 17.65	-71 35 28.2
KMHK316	0.90	-0.30	18.35	0.12	04 56 37.46	-68 09 55.8
NGC1651	1.70	-0.40	18.70	0.14	04 37 32.23	-70 35 10.8
NGC1718	1.90	-0.50	18.53	0.23	04 52 25.89	-67 03 06.6
NGC1751	1.75	-0.50	18.55	0.15	04 54 11.99	-69 48 27.1
NGC1783	1.60	-0.39	18.75	0.07	04 59 08.97	-65 59 13.8
NGC1806	1.50	-0.40	18.78	0.10	05 02 11.72	-67 59 08.0
NGC1846	1.70	-0.50	18.25	0.12	05 07 34.15	-67 27 36.7
NGC1868	1.45	-0.40	18.45	0.06	05 14 35.91	-63 57 15.1
NGC1872	0.60	-0.40	18.31	0.18	05 13 11.29	-69 18 44.9
NGC2108	1.00	-0.30	18.40	0.14	05 43 56.54	-69 10 52.9
NGC2203	1.55	-0.30	18.55	0.10	06 04 42.62	-75 26 16.1
NGC2213	1.70	-0.40	18.50	0.10	06 10 42.13	-71 31 45.9

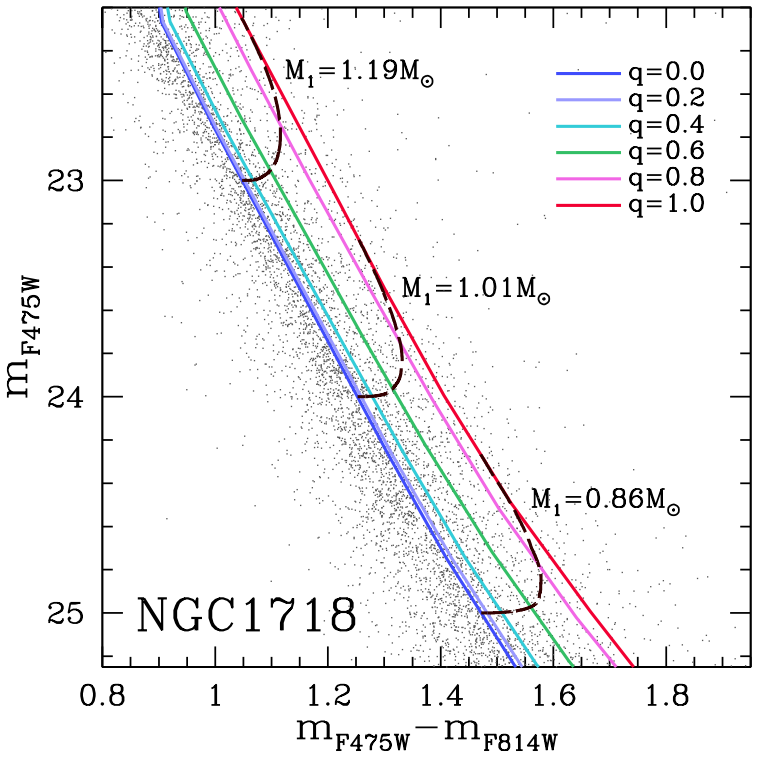

FIGURE 4.1: CMD of NGC 1718 zoomed around the upper MS (Mohandasan et al., 2024). The colored continuous lines are the fiducial lines of binary systems with different mass ratios, as indicated in the inset. The dashed lines represent the locus of binaries with primary masses of 1.19, 1.01, and 0.86 solar masses and mass ratios between 0 and 1.

In a simple stellar population, the fluxes of MS stars depend on stellar mass and follow a given mass-luminosity relation. Hence, the luminosity of a binary system depends on the mass ratio between the companion stars:

$$q = \frac{M_2}{M_1}, \tag{4.2}$$

where, $0 < q \leq 1$.

As illustrated in Figure 4.1, MS-MS binaries populate the CMD region on the red and bright side of the MSFL, with equal-mass binaries defining a fiducial line that is parallel to the MSFL but is shifted by -0.7526 mag in brightness.

The fiducial lines are derived from the observed MS stars of the cluster NGC 1718, which is taken as a test case for demonstration. Specifically, we selected the well-measured candidate MS stars and divided this sample into intervals of 0.5 mag in the F475W band. The MSFL is derived by linearly interpolating the median colours and magnitudes of the stars in each bin. The standard deviation of the colours of stars in each bin, σ, is considered a proxy for the average colour error of the stars in that bin.

For a fixed mass of the primary star, the binaries with $q < 1$ distribute on a curved line between the MSFL and the equal-mass binary fiducial line. Due to observational errors, it is not possible to disentangle binaries with small mass ratios from single stars in the observed CMD. The colours and magnitudes of the binaries with different mass ratios are determined with the mass-luminosity relation provided by the best-fitting isochrones provided by Dotter et al. (2008); Dotter (2016). The latter is derived by comparing the CMD of each cluster with a grid of solar-scaled isochrones that account for different ages, metallicities ([Fe/H]), distance modulus ((m−M)$_0$), and reddening (E(B−V), see Milone et al., 2009, for details). The distance to the cluster is calculated from (m−M)$_0$. The values of age, [Fe/H], (m−M)$_0$, and E(B−V) that provide the best match with the observed data are listed in Table 4.1.

The ages obtained in our work are in agreement, at 1-σ level, with those by Sun et al. (2018), who compared the observed CMDs with the Padova group's PARSEC 1.2S isochrones (Bressan et al., 2012). The average age difference is 190 Myr, which is comparable with the age error of ~ 200 Myr provided by Sun et al. (2018). The distance modulus, (m−M)$_0$, derived in our work differ, on average, by 0.18 mag with those from Sun et al. (2018).

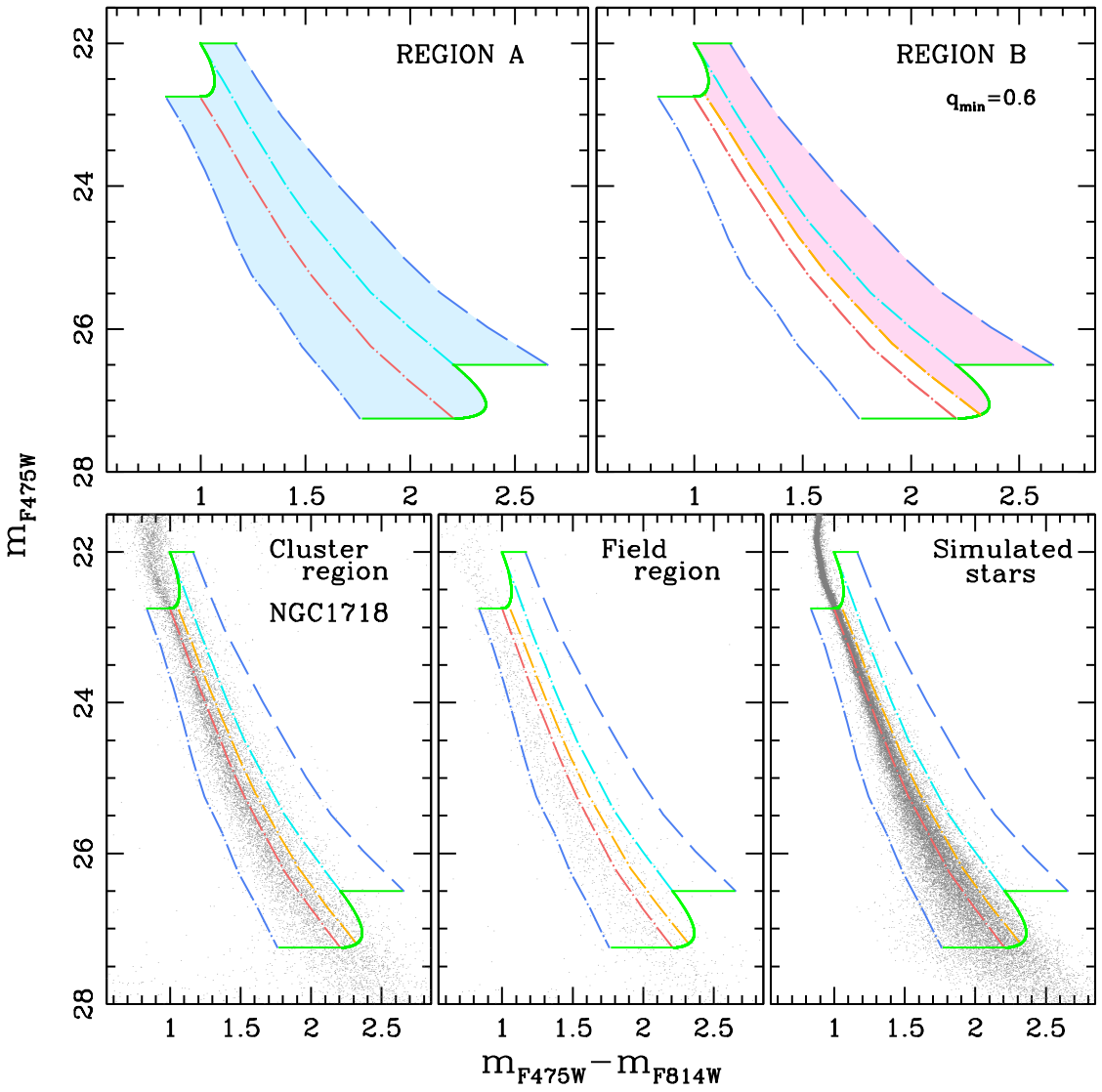

FIGURE 4.2: The figure summarises the method that was used to analyse MS-MS binaries in NGC 1718 (Mohandasan et al., 2024). *Top-left panel*: Region A of the $m_{\rm F475W}$ vs. $m_{\rm F475W} - m_{\rm F814W}$ CMD, which is shaded with light-blue colour. *Top-right panel*: Region B, a subsection of Region A, is shaded with pink. *Bottom-left*: CMDs of stars in the cluster region. *Bottom-centre*: Field region. *Bottom-right:* Simulated CMD. See text for details.

The method for deriving the fraction of binaries is illustrated in Figure 4.2 in the case of cluster NGC 1718. We divided the CMD into two regions. The region A includes all the single stars in the studied luminosity interval and the binary systems with a primary star in the same magnitude range. It is limited to the left by

the blueshifted MSFL, which is blueshifted by three times the colour observational error (σ) is introduced. The right boundary corresponds to the fiducial line of equal-mass binaries redshifted by three times the colour error. The upper and lower boundaries are the sequences of binaries where the mass ratio ranges from zero to one and the primary stars exhibit magnitudes of $m_{\rm F475W} = m^{\rm bright}_{\rm F475W}$ and $m^{\rm faint}_{\rm F475W}$, respectively. Here, $m^{\rm bright}_{\rm F475W}$ and $m^{\rm faint}_{\rm F475W}$, corresponding to masses M_u and M_l, are the bright and faint limit of the studied luminosity interval. Then, $m^{\rm bright}_{\rm F475W}$ is selected such that region A does not intervene with the turnoff region, and the selected $m^{\rm faint}_{\rm F475W}$ assures the completeness of the magnitude range of analysis remains above 0.5. Region B is the portion of Region A that is predominantly populated by binaries with $q \geq q_{min}$. The value of $q_{\rm min}$ is chosen with the criterion that the fiducial line of binaries with $q = q_{\rm min}$ is redder than the MSFL shifted by σ to the red. In Figure 4.2, the MSFL and the fiducial of equal-mass binaries are represented with red and cyan dot-dashed lines, respectively, in all panels. The blue dot-dashed and blue-dashed lines mark the left and right colour boundaries of region A, displaced by three times the colour error from the fiducial and equal mass binary lines, respectively. Green curves represent the mass limit of analysis, i.e., binaries with certain primary mass and the mass ratio with secondary mass ranging between 0 and 1. Orange lines represent the unequal mass binary line, i.e., binaries with a mass ratio, $q = 0.6$.

Moreover, to derive the fraction of binaries, we defined two regions in the HST FoV: 1) The cluster-region that extends from the dense cluster centre to R_{2f}. 2) Starting from R_{2f}, the field-region stretches to the outermost parts of the HST FoV. Figure 4.3 demonstrates the cluster-region and field-region in the case of the cluster ESO057SC075. As an example, the bottom-left and bottom-middle panels of Figure 4.2 show the CMDs of stars in the cluster-region and the field-region of

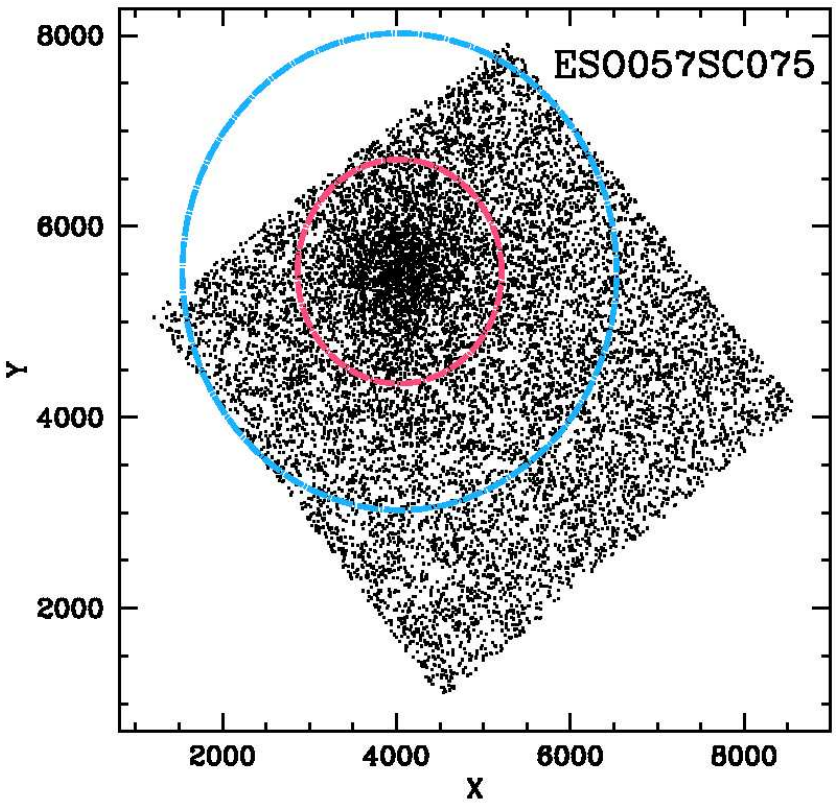

FIGURE 4.3: Spatial distribution of stars in the cluster ESO057SC075. The region within the red circle is the cluster region and the designated region outside the blue circle is the field region.

NGC 1718, respectively.

The binary fraction is derived using the Equation 1 of Milone et al. (2012):

$$F_{\rm bin}^{q\geq q_{\rm min}} = \frac{N_{\rm cluster}^{\rm B} - N_{\rm field}^{\rm B}}{N_{\rm cluster}^{\rm A} - N_{\rm field}^{\rm A}} - \frac{N_{\rm art}^{\rm B}}{N_{\rm art}^{\rm A}}. \tag{4.3}$$

Here, $N_{\rm cluster}^{\rm A}$ and $N_{\rm cluster}^{\rm B}$ are the number of stars in the cluster-region, corrected for completeness (Refer to subsection 4.2.3), in the regions A and B of the CMD, respectively. $N_{\rm field}^{\rm A}$ and $N_{\rm field}^{\rm B}$ are the corresponding number of stars in the field-region normalised by the ratio between the respective areas of the cluster and field region (Refer to subsection 4.2.1). $N_{\rm art}^{\rm A}$ and $N_{\rm art}^{\rm B}$ are the numbers of artificial stars

that populate the regions A and B of the CMD. The artificial star binary fraction is denoted by the term $\frac{N_{\rm art}^{\rm B}}{N_{\rm art}^{\rm A}}$ of the Equation 4.3. This term accounts for the fraction of single stars that populate region B of the CMD due to large photometric errors or chance superposition of their images with other single stars (Refer subsection 4.2.2 for details).

4.2.1 Field star contamination

Contamination of the telescopic images by foreground stars and background galaxies is a serious concern in CMD analysis of binaries. Field stars are ideally separated using the difference in their proper motion with respect to cluster stars. Proper motion separation requires observations in two epochs. Given the smaller distances, such approaches are frequently used in the case of Galactic clusters. In the case of MC clusters, a good enough proper motion disentanglement requires observations that are at least a decade apart. Since such data sets are not available for the clusters under study, we are adopting a statistical subtraction approach.

Within the small HST FoV, we can assume the field star distribution to be uniform in cluster-region and field-region. The field stars appearing in cluster-region may contribute to the stars present in regions A and B of the cluster-region CMD. A CMD is plotted for stars in the field-region as shown in the lower middle panel of Figure 4.2, and the number of stars in regions A and B is found using the same method followed for cluster stars. The area of the field-region and cluster-region need not be the same in the telescopic FoV and a scaling factor is introduced to account for the said difference in their relative areas. Further, another scaling is done to account for the reduction in star count due to incompleteness in data (Refer to subsection 4.2.3). Thus obtained number of field stars in regions A and

B, denoted by N^A_{field} and N^B_{field} respectively, are subtracted from the observed star count in region A and B of cluster-region CMD as shown in Equation 4.3.

4.2.2 Scattering correction

Photometric errors and scattering can cause the images of single stars to superimpose on each other and thereby approach the magnitude of a binary system. The amount of such 'chance-superposition binaries' has to be estimated and omitted for an accurate binary fraction determination. Since it is hard to discern the real and blended source in the CMD, a statistical approach using an Artificial star (AS) set has been adopted (Milone et al., 2012; Anderson et al., 2008).

We performed AS tests to estimate the photometric errors, the level of completeness of our sample, and the fraction of blended sources that contaminate the CMD region populated by binaries. To do so, we used the method by Anderson et al. (2008) and Milone et al. (2009). For each cluster, we generated a catalogue of 100,000 ASs with instrumental magnitudes between -4 and -13.7 in the F814W bands. The colours of each AS are derived from the empirical fiducial line of MS stars. For the ASs, we adopted the same radial distribution and luminosity function as the real stars and reduced them using the same PSF model and procedure adopted for real stars. Moreover, we used the same criteria as for real stars to select the sample of relatively isolated ASs that are well-fitted by the PSF. Completeness is derived for each star as in Milone et al. (2009) (see their section 2.2), by accounting for its magnitude and radial distance from the cluster centre. The points with large deviations in their initial and final measurements of position and magnitude in respective filters were also discarded. Subjected to the same reduction method as real stars, the statistically rich AS set can mimic the behaviour of

single star images in real data that underwent chance superposition and appeared as binary.

A CMD is constructed using the reduced ASs within the cluster radius limits, as demonstrated in the lower right panel in Figure 4.2. The number of ASs appearing in regions A and B of the AS CMD, N_{art}^{A} and N_{art}^{B} respectively, is calculated in the same way as in cluster star CMD (refer to section 4.2). The chance superposition binary fraction is obtained by taking the ratio of these two quantities, which is then subtracted from the field star-corrected binary fraction of the cluster, as in Equation 4.3.

4.2.3 Completeness correction

For a given resolution power, faint stars have a lower probability of being detected as separate objects and measured accurately compared to brighter objects. This is particularly evident in dense regions such as cluster centres or the vicinity of other bright objects. This effect, pertaining to the data reduction step of the analysis, causes the star count to be smaller than the actual number. To account for this reduction in star count, a quantity called the Completeness Ratio, C, is introduced. Ideally, C has a value of one for bright objects and it reduces to zero with an increase in crowding and a decrease in stellar luminosity.

C is defined as the ratio between the number of objects that are successfully resolved to the number of input objects that are present. Practically, C is calculated using simulated sources, such as the AS set discussed in the previous section. AS set is subjected to the same data reduction procedures and selection criteria as real stars. With ASs, we are also in a unique position of having access to both input and output files of data reduction, which is quite useful in calculating C. The ASs are

divided into small magnitude bins of $0.1mag$ width and the number of stars in each bin that satisfy certain selection criteria (Milone et al., 2012) is calculated before and after the data reduction. Completeness is calculated in each magnitude bin by taking the ratio of the star counts obtained before and after the data reduction. The measured C in each bin is expressed as a function of the mean magnitude of the bin. By scaling the observed star count in a certain magnitude range by the corresponding C, we can obtain the original star count.

Since the cluster stars and field stars belong to different density environments, C has to be calculated separately for each region. C is calculated within a radius of R_{2f} for cluster-region and outside a radius of R_f for field-region of analysis. The variation of C in cluster-region and field-region of NGC1718, as a function of magnitude, is reported in Figure 4.4. On average, the C is high for lower values of magnitudes and it reduces significantly for larger values of magnitude, specifically after a m_{F475W} magnitude of 26.5. In the latter regions, it is evident that the completeness for field-region stars is higher than cluster-region stars, as the latter is densely populated.

4.3 Binary fraction in Magellanic Cloud star clusters

Following the procedure described in previous sections, we derived the fraction of binaries with a mass ratio, $q \geq 0.7$ for each of the analysed MC GCs. Moreover, in the clusters where the binaries are better distinguishable from single stars, namely NGC 1718, NGC 1751, NGC 1783, NGC 1846, NGC 1868, NGC 2203, and NGC 2213. We also studied binaries with $q \geq 0.6$. The results are listed in Table 4.2, where we provide the fraction of binaries within the radial distance of R_{hm} and the analysed stellar-mass interval, given by the difference between the

TABLE 4.2: Fraction of binaries for all studied clusters. We provide the radius of the studied region and the stellar-mass interval (Mohandasan et al., 2024).

Cluster ID	$F_{bin,R_{hm}}^{q>0.6}$	$F_{bin,R_{hm}}^{q>0.7}$	$F_{bin,R_c}^{q>0.6}$	$F_{bin,R_c}^{q>0.7}$	M_u $[M\odot]$	M_l $[M\odot]$
ESO057SC075	———	0.150 ± 0.013	———	0.220 ± 0.029	1.25	0.72
ESO057SC030	———	0.123 ± 0.010	———	0.103 ± 0.017	1.16	0.65
KMHK316	———	0.105 ± 0.023	———	0.108 ± 0.039	1.46	0.89
NGC1651	———	0.110 ± 0.010	———	0.117 ± 0.016	1.29	0.81
NGC1718	0.122 ± 0.010	0.108 ± 0.008	0.125 ± 0.021	0.128 ± 0.017	1.24	0.73
NGC1751	0.221 ± 0.022	0.175 ± 0.017	0.213 ± 0.031	0.171 ± 0.024	1.21	0.74
NGC1783	0.113 ± 0.010	0.094 ± 0.007	0.118 ± 0.013	0.103 ± 0.009	1.33	0.80
NGC1806	———	0.115 ± 0.010	———	0.112 ± 0.013	1.39	0.86
NGC1846	0.105 ± 0.011	0.074 ± 0.009	0.113 ± 0.017	0.080 ± 0.013	0.98	0.66
NGC1868	0.112 ± 0.018	0.093 ± 0.014	0.108 ± 0.042	0.107 ± 0.033	1.32	0.87
NGC1872	———	0.111 ± 0.020	———	0.135 ± 0.030	1.56	1.06
NGC2108	———	0.241 ± 0.018	———	0.237 ± 0.026	1.44	0.76
NGC2203	0.085 ± 0.009	0.075 ± 0.007	0.080 ± 0.013	0.074 ± 0.010	1.33	0.65
NGC2213	0.132 ± 0.016	0.119 ± 0.012	0.146 ± 0.028	0.133 ± 0.023	1.27	0.66

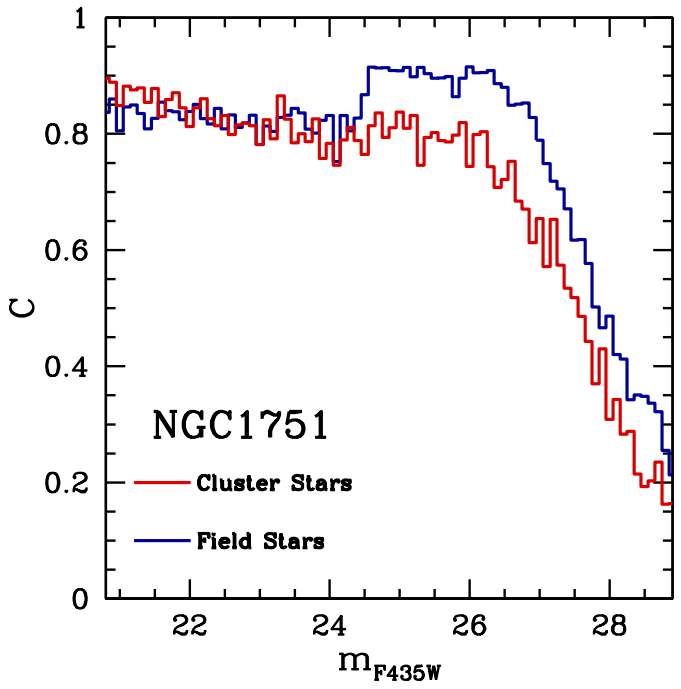

FIGURE 4.4: Completeness value is plotted as a function of magnitude in filter $F475W$, for cluster NGC2108. The blue continuous curve denotes the trend for stars in the field-region and the red curve denotes the one for the cluster-region.

corresponding M_u and M_l values. The binary fraction ranges between $\sim$ 0.07 in NGC 1846, to $\sim$ 0.24, in NGC 2108.

Table 4.2 also provides the fraction of binaries within the core of each cluster, which has a minimum of 7% in NGC 2203 to a maximum of 24% in NGC2108. For most clusters, namely ESO057SC075, KMHK0316, NGC1651, NGC1718, NGC1783, NGC1846, NGC1868, NGC1872, and NGC2213, the core binary fraction is greater than the one within the half mass radius. This indicates the relative concentration of binaries in the centre compared to the MS single stars.

The results of 12 out of the 14 analysed clusters are derived using the isochrones from Dartmouth Stellar Evolution databases [2], which are available for ages greater than 1 Gyr. In the cases of KMHK 316 and NGC 1872, which are younger than 1

[2]http://stellar.dartmouth.edu/models/

Gyr, we used the MIST isochrones [3]. To investigate possible systematic errors in the binary fraction due to the difference in the used isochrone, we calculated the fraction of binaries in three clusters, of different ages, by using both types of isochrones. In the ~ 1 Gyr old cluster NGC 2108, the fraction of binaries within R_C and R_{hm} that we derived using the Dartmouth and the MIST isochrones differ by less than 1%, whereas in NGC 1868 (age of $\sim$1.5 Gyr) and ESO 057SC030 (age of $\sim$2 Gyr) the fraction of binaries derived from the two sets of isochrones varies by $\sim$0.6% and $\sim$0.3%, respectively. Since such differences are much smaller than the corresponding observational errors, we conclude the results are not significantly affected by the adopted isochrones.

4.4 Summary

The MS binary fraction in young and intermediate-age MC GCs is successfully computed within core and half mass radii of the cluster for mass ratios greater than 0.7, and 0.6 whenever possible. Fraction has been subjected to corrections for field star contaminations, scattering effects, and incompleteness of the data set. Within half mass radius and for a mass-ratio greater than 0.7, the fraction ranges from 7% in NGC1846 to 24% in NGC2108. The fraction increases in the cluster core for most of the clusters, with a minimum of 7% in NGC 2203 to a maximum of 24% in NGC2108. The obtained fractions are higher than the results obtained from a homogeneous study on old and massive Galactic GCs (Milone et al., 2012) where the minimum was around 1%. Similar studies on young and less massive Galactic OCs have obtained a maximum fraction of 40% (Cordoni et al., 2022).

[3] https://waps.cfa.harvard.edu/MIST/

Chapter 5

Properties of binary fraction

The structural and dynamical parameters of the star clusters, such as age, mass, and dynamical age, can determine the ambient conditions in the cluster. They are used to determine the average kinetic energy of the members, their interaction cross-section, collision rates, and mass segregation. Further stellar parameters of the binary system play a major role in determining the stability of the system and its interaction with other cluster members, which has ramifications in its neighbourhood. To understand the same, we explore the distribution of binaries with respect to different stellar and cluster parameters in the analysed MC GCS, as detailed in the following sections.

5.1 Binary fraction and cluster parameters

Several studies focused on Galactic clusters have explored the dependence of binary fractions on the physical parameters of the clusters. Sollima et al. (2007) studied 13 low-density Galactic GCs and found that the relative fraction of binaries

in the core has a dependence on their ages. They propounded that the disruption process ensuing in the core reduces the binary fraction with time. However, Milone et al. (2012) did not report any evident relation between binary fraction and age or relative age for the large sample of 59 old Galactic GCs. Nevertheless, they did find an anti-correlation between cluster mass and binary fraction. Raghavan et al. (2010) found a decrease in binarity with age for binaries in solar neighbourhoods, especially for the ones with higher interaction cross sections, and no dependence on its metallicity. A statistically robust study of 78 Galactic OCs by Cordoni et al. (2023) suggests the anti-correlation between binary fraction and cluster mass is a characteristic of older stellar systems. Sollima et al. (2010) studied five Galactic GCs and found a similar anti-correlation between binary fraction and mass and no dependence on cluster age. They suggest the binary disruption process is the dominant process that drives binary fractions in stellar systems.

In the case of the analysed MC GCs, the binary fraction exhibits no significant correlations with cluster age and metallicity, as shown in the left and right panels of Figure 5.1. This conclusion is supported by Spearman's rank correlation coefficients of 0.2 and -0.2, respectively. Similarly, there was no correlation between binary fraction and other cluster parameters such as mass, density, or concentration. However, the distribution of binary fractions with the dynamical age of the clusters shows some interesting patterns. As demonstrated in Figure 5.2, some clusters show a linear anti-correlation in their binary fraction with dynamical age. These clusters, ESO057SC075, KMHK316, NGC1751, NGC1868, NGC2108, and NGC2213 are clusters with lower masses in the data set, from $\sim 10^4$ to 4×10^4, as evident from the colour coding of the points with respect to the cluster mass, while massive clusters appear to have a binary fraction less than 0.15. There is a decrease in binary fraction in low mass clusters with each mean revolution time,

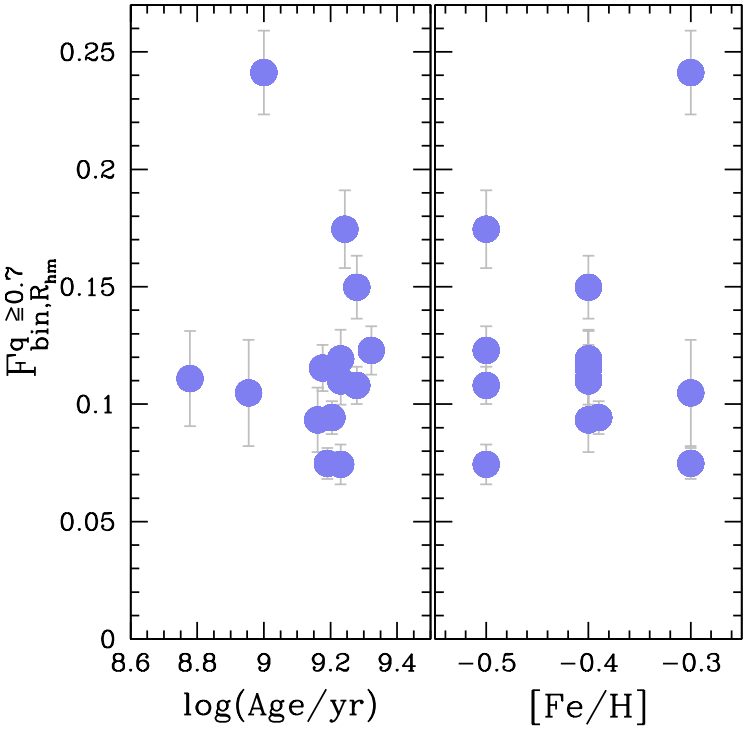

FIGURE 5.1: Binary fraction and cluster parameters. Fraction of binaries with q≥0.7 and within the R_{hm} of the cluster is plotted against the age (*left panel*) and iron abundance (*right panel*) of the host cluster Mohandasan et al. (2024).

indicating the progress of binary disruption interactions.

5.2 Binary fraction and the mass of the primary star

To investigate the binary fraction in different intervals of primary-star mass, we divided the studied magnitude interval into five magnitude bins of equal width [1]. NGC 1846 and NGC 1872 are remarkable exceptions where we only used four bins as the magnitude intervals were smaller. To infer the masses of the stars in a magnitude bin, we used the mass-luminosity relations inferred from the best-fitting isochrones. We estimated the fraction of binaries with q $\geq$ 0.7 and $r \leq R_{hm}$

[1]The following extract is taken from Section 5.1 of Mohandasan et al. (2024).

TABLE 5.1: χ^2 and $P-value$ derived for the relations between the binary fraction and the stellar mass, mass ratio, and radial distribution (Mohandasan et al., 2024).

Cluster ID	Mass distribution		q distribution		Radial distribution	
	χ^2	$P-value$	χ^2	$P-value$	χ^2	$P-value$
ESO057SC075	7.1×10^{-4}	0.40	11.6×10^{-3}	0.02	11.0×10^{-4}	0.05
ESO057SC030	2.3×10^{-4}	0.70	10.0×10^{-3}	0.00	3.0×10^{-4}	0.14
KMHK316	10.1×10^{-4}	0.72	4.1×10^{-3}	0.30	2.9×10^{-4}	0.91
NGC1651	4.0×10^{-4}	0.45	0.3×10^{-3}	0.60	1.3×10^{-4}	0.45
NGC1718	3.0×10^{-4}	0.32	15.0×10^{-3}	0.00	2.0×10^{-4}	0.07
NGC1751	10.9×10^{-4}	0.45	12.2×10^{-3}	0.00	0.6×10^{-4}	0.93
NGC1783	4.8×10^{-4}	0.05	6.1×10^{-3}	0.00	1.2×10^{-4}	0.10
NGC1806	0.8×10^{-4}	0.95	4.2×10^{-3}	0.00	2.5×10^{-4}	0.21
NGC1846	3.0×10^{-4}	0.29	0.4×10^{-3}	0.44	1.9×10^{-4}	0.10
NGC1868	12.4×10^{-4}	0.17	22.6×10^{-3}	0.00	3.8×10^{-4}	0.20
NGC1872	1.2×10^{-4}	0.96	3.6×10^{-3}	0.10	10.5×10^{-4}	0.19
NGC2108	45.3×10^{-4}	0.00	2.7×10^{-3}	0.27	0.5×10^{-4}	0.96
NGC2203	1.9×10^{-4}	0.37	5.2×10^{-3}	0.00	0.3×10^{-4}	0.80
NGC2213	4.0×10^{-4}	0.69	20.2×10^{-3}	0.00	1.6×10^{-4}	0.30

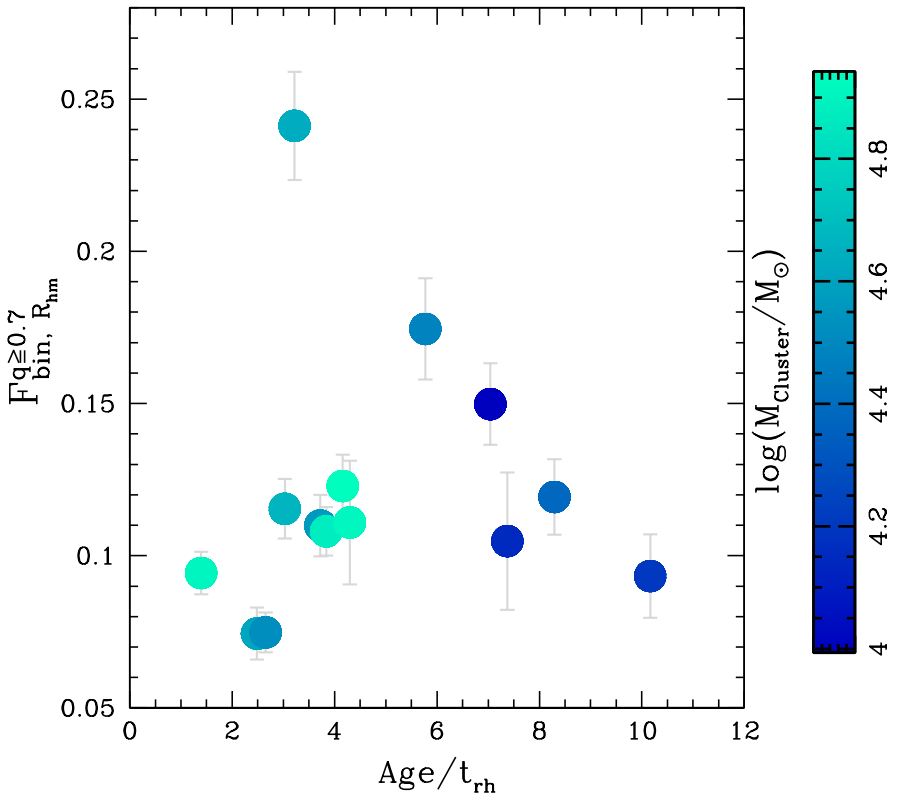

FIGURE 5.2: Variation of binary fraction and dynamical age of the cluster. The points are colour-coded according to the mass of the cluster on a logarithmic scale.

in each bin and plotted this quantity as a function of the mean mass of the primary stars in that bin, as illustrated in Figure 5.3 and Figure 5.5. A visual inspection of this figure suggests that the behaviour of $F^{q\geq0.7}_{bin,R_{hm}}$ as a function of the stellar mass varies from cluster to cluster.

Furthermore, for each cluster, we derived the χ^2 value with respect to the average binary fraction, and the corresponding $P-value$, which indicates the deviation from a flat distribution. We calculated the χ^2 values according to the relation, $\chi^2 = \sum_0^N(((Y-\bar{Y})^2)/N)$. The latter is estimated using 1,000 Monte Carlo simulations. In each simulation, we assumed a flat binary fraction corresponding to the observed average binary fraction and the same number of stars as in the observed CMD. The $P-value$ is defined as the fraction of simulations with χ^2 values greater

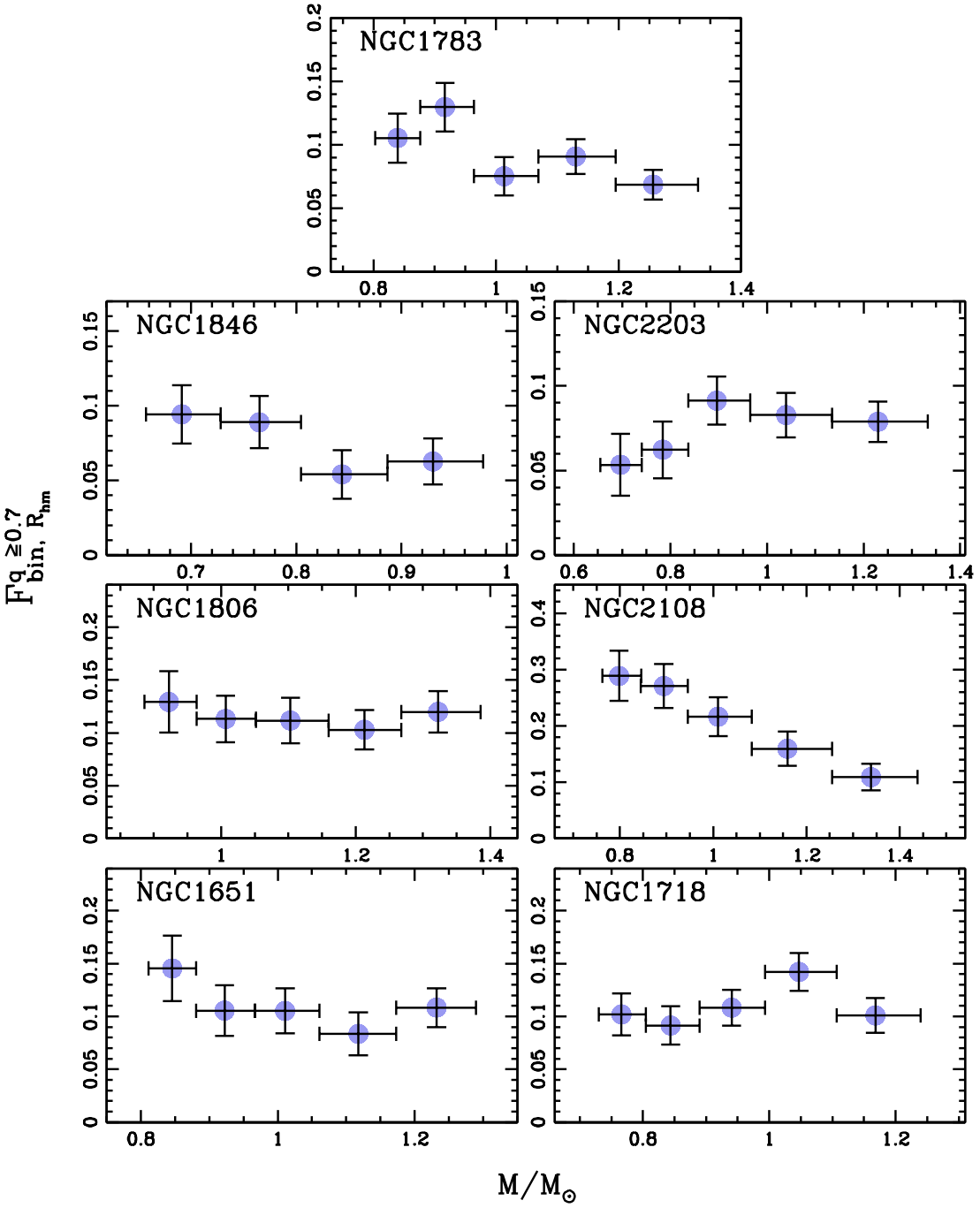

FIGURE 5.3: Binary fraction distribution with mass of the primary star. The fraction of binaries with a mass ratio greater than 0.7 and within the half-mass radius of the cluster is plotted against the mass of the primary star. Horizontal bars denote the extent of each mass bin.

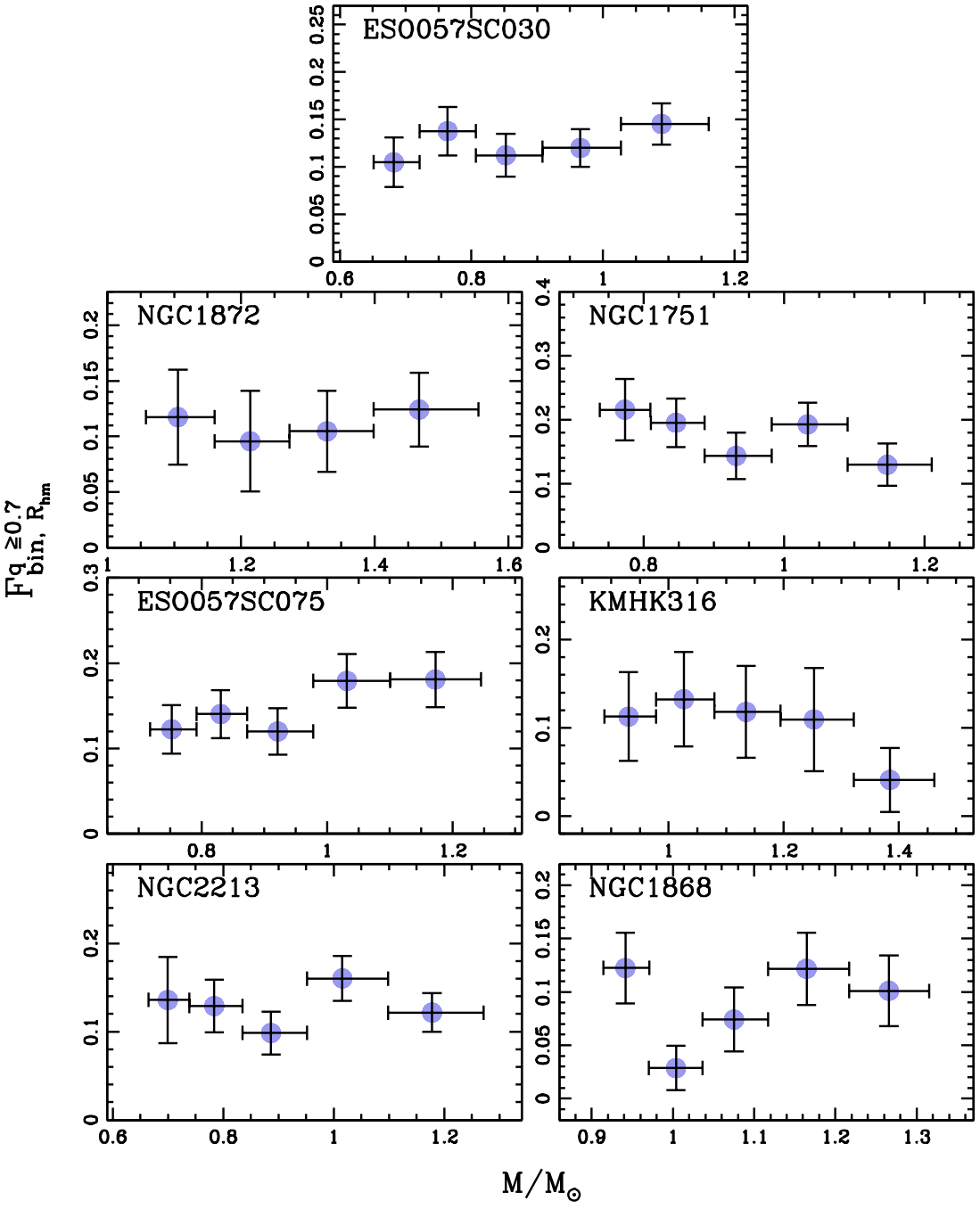

FIGURE 5.4: Continuation from Figure 5.3.

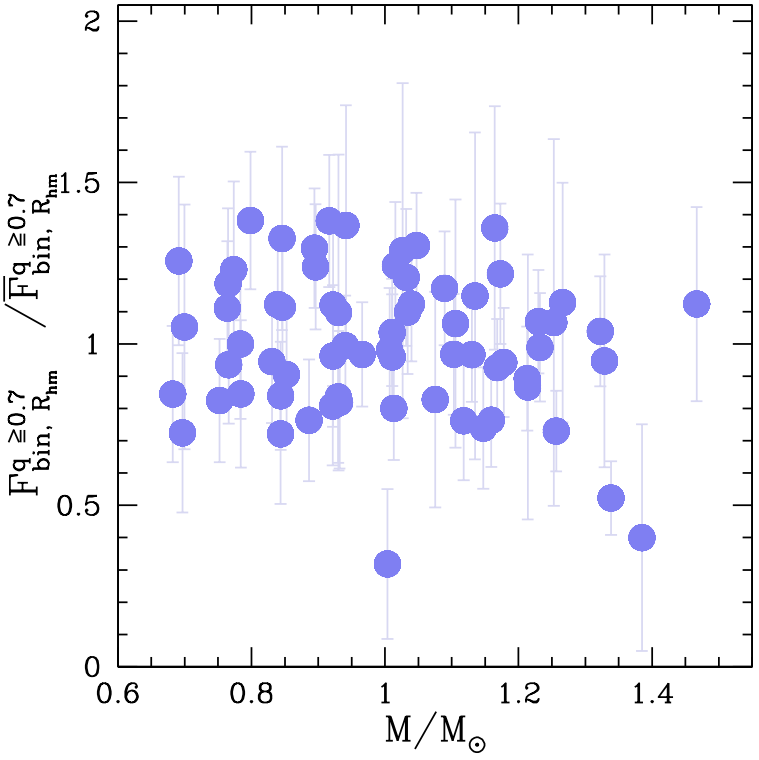

FIGURE 5.5: Mass distribution of binaries. The figure demonstrates the variation of binary fractions with mass ratios larger than 0.7 as a function of the mass of the primary star, for all the studied Magellanic Cloud clusters. The binary fraction is normalised to the average binary fraction in each mass bin (Mohandasan et al., 2024).

than the observed χ^2. The χ^2 and $P-values$ are listed in Table 5.1.

Various clusters manifest a trend very close to flat distribution, as evident in NGC1806 ($P-value$ ~1). Conversely, NGC2108 ($P-value$ of ~0) shows a decrease in the binary fraction with increasing mass of the primary star.

To further compare the results from the different clusters, we calculated the average binary fraction ($\overline{F}^{q\geq0.7}_{\mathrm{bin,R_{hm}}}$) in the different mass bins and plotted the $F^{q\geq0.7}_{\mathrm{bin,R_{hm}}}/\overline{F}^{q\geq0.7}_{\mathrm{bin,R_{hm}}}$ ratio as a function of the mean mass of the primary stars in a particular bin. The results obtained from combining the distributions from all the analysed clusters are plotted in Figure 5.5, where we observe that the general trend is that of a flat distribution with a Spearman's rank correlation coefficient of -0.1. The obtained

trend is in agreement with the results obtained from homogeneous studies on 59 old and massive Galactic GCs (Milone et al., 2012) and 78 young and less massive Galactic OCs (Cordoni et al., 2023).

5.3 Relations between the binary fraction and the mass ratio

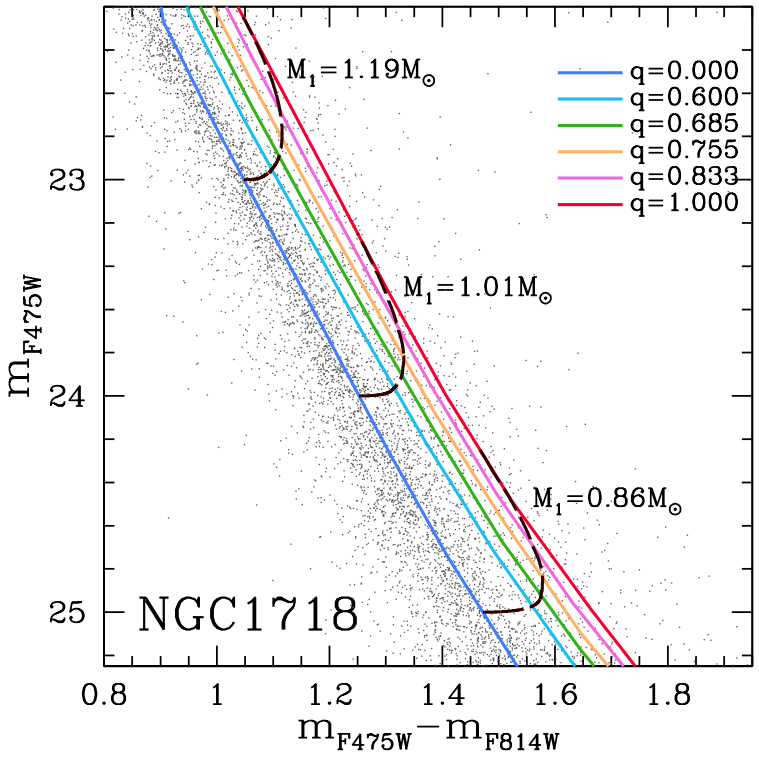

FIGURE 5.6: $m_{\rm F475W}$ vs. $m_{\rm F475W} - m_{\rm F814W}$ CMD of NGC 1718. Different unequal mass fiducial lines used to derive the fraction of binaries in different mass-ratio bins are denoted in the figure. See the text for details.

There are several studies on the mass-ratio distribution of binaries, many of them with contradictory results. Through a statistically robust study on 59 old and massive Galactic GCs, Milone et al. (2012) found a flat mass-ratio distribution for MS binaries. A homogeneous study on 78 young and less massive OCs also

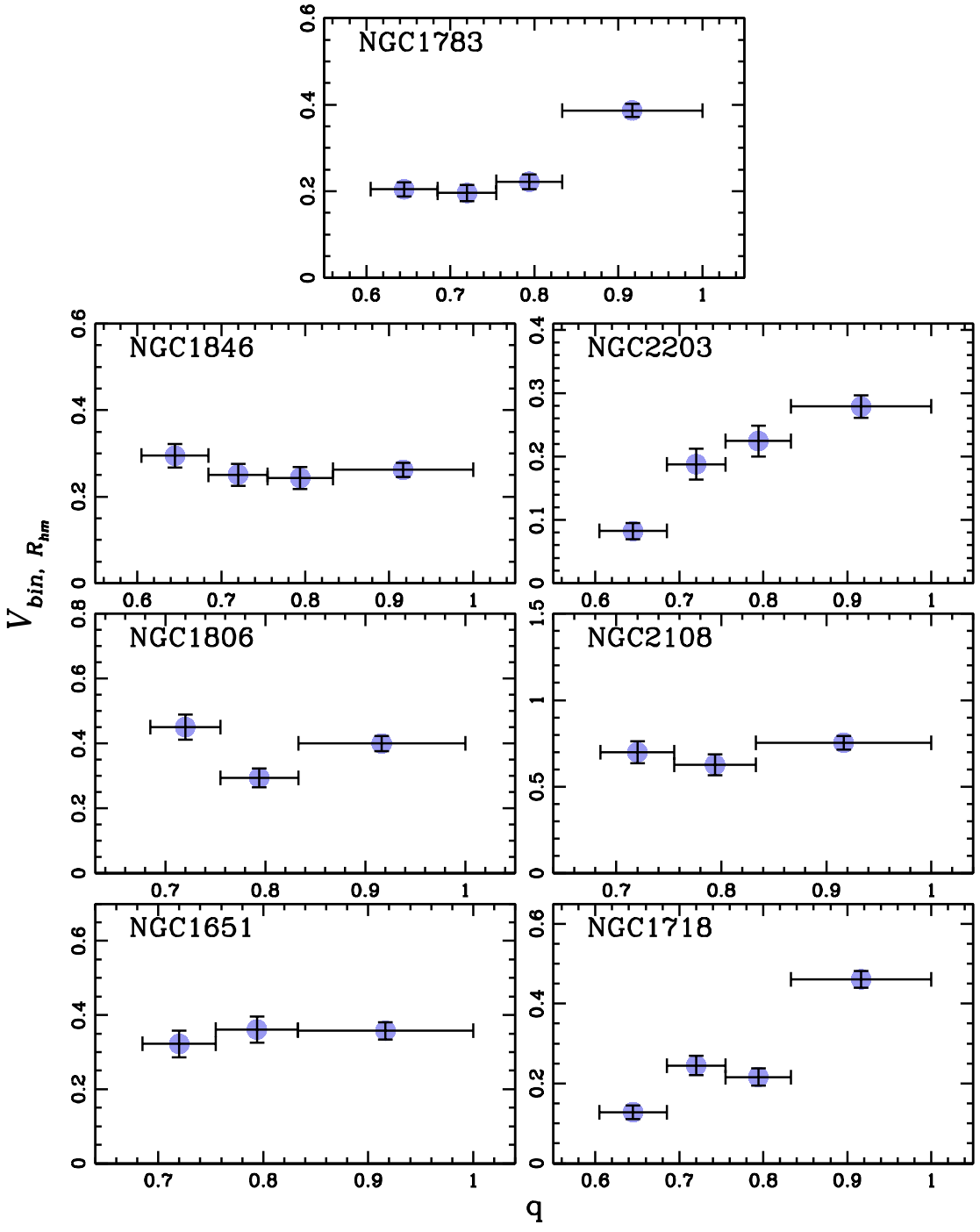

FIGURE 5.7: Binary fraction and mass ratio parameter. The frequency of binaries is plotted as a function of the mass ratio. The horizontal bars mark the mass-ratio intervals corresponding to each point.

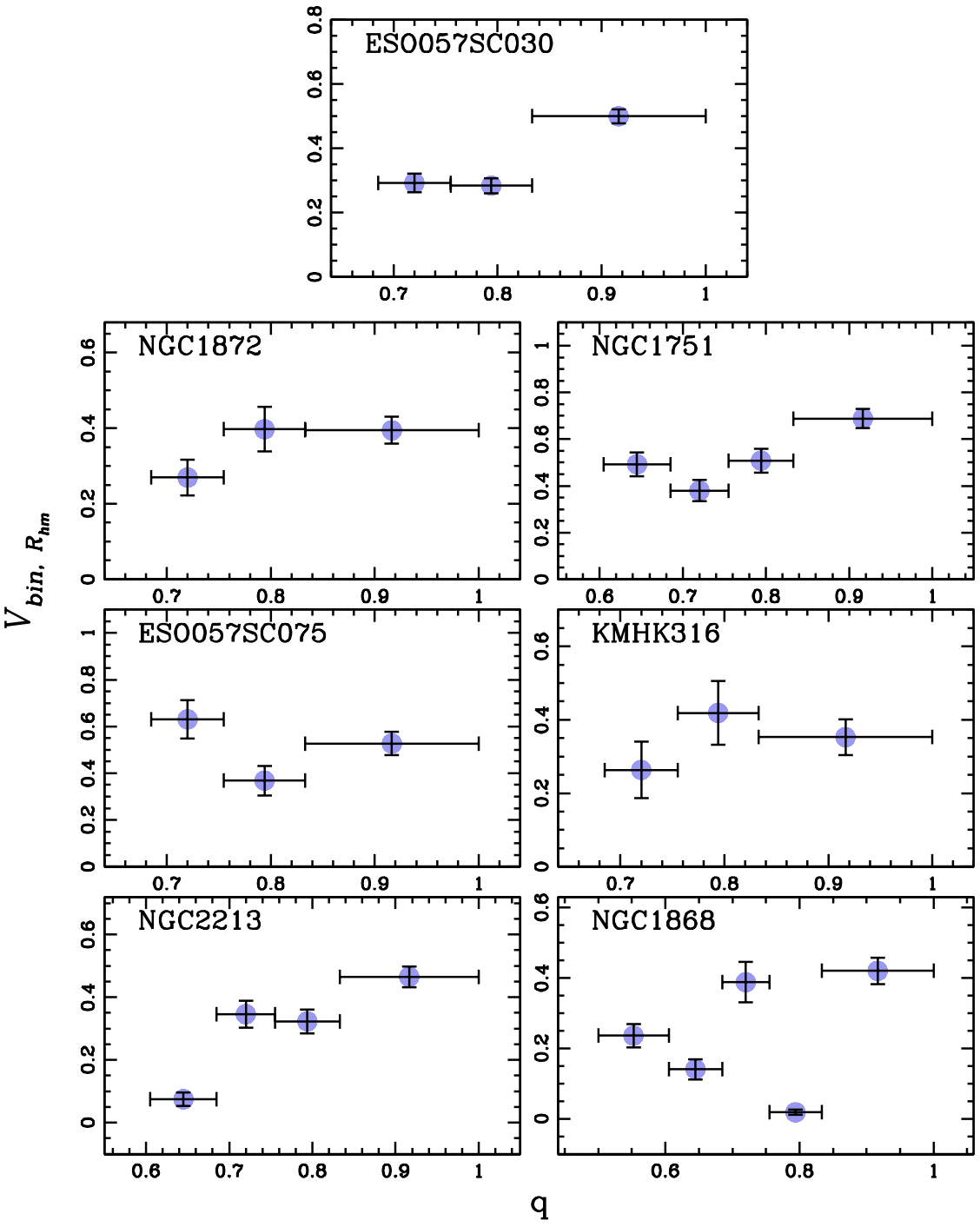

FIGURE 5.8: Continuation from Figure 5.7.

arrived at a flat mass ratio distribution. However, Jadhav et al. (2021) claims the mass-ratio distribution is unlikely to be flat in OCs. Based on Hipparcos data, Raghavan et al. (2010) found a preference for equal mass binaries in a data set of solar-type stars in the solar neighbourhood. Duquennoy and Mayor (1991) also reported an increase in binary fraction with a decrease in mass-ratio for G-dwarf stars in the solar neighbourhood. Moe and Di Stefano (2017) claimed that the mass-ratio distribution is a function of the period of the binary system. The dynamics of binaries are influenced by their mass and interaction cross-section, which is related to their period. They categorised mass ratio distribution in the studied O-type to B-type binaries into three categories depending on their period ranges.

To constrain the relation between binary population and mass ratio, we calculated the binary fraction in different mass ratio bins and with $r \leq R_{hm}$ [2]. The q-intervals are selected within region B of the CMD with a prerequisite that the strips formed by the different q-loci should occupy the same area in the CMD. Therefore, we have selected loci of q values 0.6, 0.685, 0.755, 0.833, and 1. Though the subsequent q values are not in equal increments, they form equal-area strips in the CMD as shown in Figure 5.6.

We calculated the fraction of binaries in each mass ratio interval and derived the equivalent binary fraction,

$$V_{bin} = \frac{F_{bin}}{\Delta q}, \tag{5.1}$$

where F_{bin} is the fraction of binaries in a given mass ratio interval, Δq.

The values of $V_{bin,R_{hm}}$ are plotted against q, as shown in Figure 5.7 and Figure 5.8. The corresponding χ^2 and $P - values$ are provided in Table 5.1. We note that

[2]This section is taken from Section 5.2 of Mohandasan et al. (2024).

some clusters such as NGC1718, NGC2203, and NGC2213 (all with $P - value = 0$) manifest an increase in the frequency of binaries with higher mass ratios, while others, such as NGC 1651 ($P - value \geq 0.5$) and NGC1846 ($P - value \sim 0.5$), exhibit a nearly flat distribution.

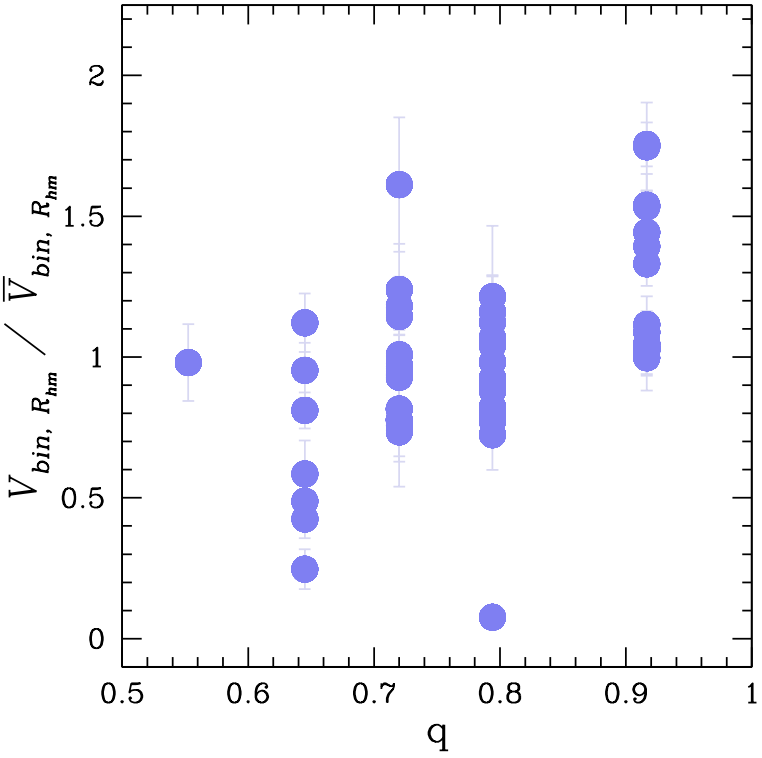

FIGURE 5.9: Frequency of binaries as a function of the mass-ratio for all the studied clusters (Mohandasan et al., 2024).

By combining the distributions from all clusters, Figure 5.9 investigates the overall trend between binary fraction and mass ratio in the analysed MC GCs. To properly compare the different clusters, we have normalised the fraction of binaries by its average value. The distribution is nearly flat with a Spearman's rank correlation coefficient of $+0.4$.

5.4 Chromosome map of binaries

To obtain the complete binary fraction and distribution with respect to mass-ratio parameters in star clusters, it is imperative to know the number of binaries belonging to every mass ratio range, from 0 to 1. However, we are limited to higher mass-ratio binaries because of photometric uncertainties. The CMDs used for binary analysis in this study are constructed using the optical filters available in HST. The locus binaries with $q > 0.7$ are found to be well separated in these optical CMDs and were used for the study. As evident in Figure 5.6, more than 60% of the area between the MSFL and the equal mass binary line is occupied by binaries with $q > 0.5$. Hence, the loci of binaries with lower q values are congested together and appear in the vicinity of MSFL. The photometric error present in the magnitude estimation of stars in MSFL put an additional uncertainty in the estimation of the fraction of lower q binaries.

Properties of CMDs show variations depending on the filters used to construct them. Even though optical CMDs show crowding of lower q binaries, CMDs constructed with ultraviolet or infrared filters are found to show different degrees of crowding in these areas. By tuning the contribution from ultraviolet, optical, and infrared filters in the colour and magnitude axes, the crowding around different q ranges in the CMD can be controlled and mitigated.

We have simulated the CMD of NGC2213 in the JWST filter and have investigated the colour error compared to the observation error, as demonstrated in the right panel of Figure 5.10. To investigate binaries with low qs, we need to limit the observational error in such a way that the CMDs are sharp enough to distinguish single stars from the lowest q binaries. The optical and UV filters aboard HST are not specific to low mass stars and the high observational error makes it impossible

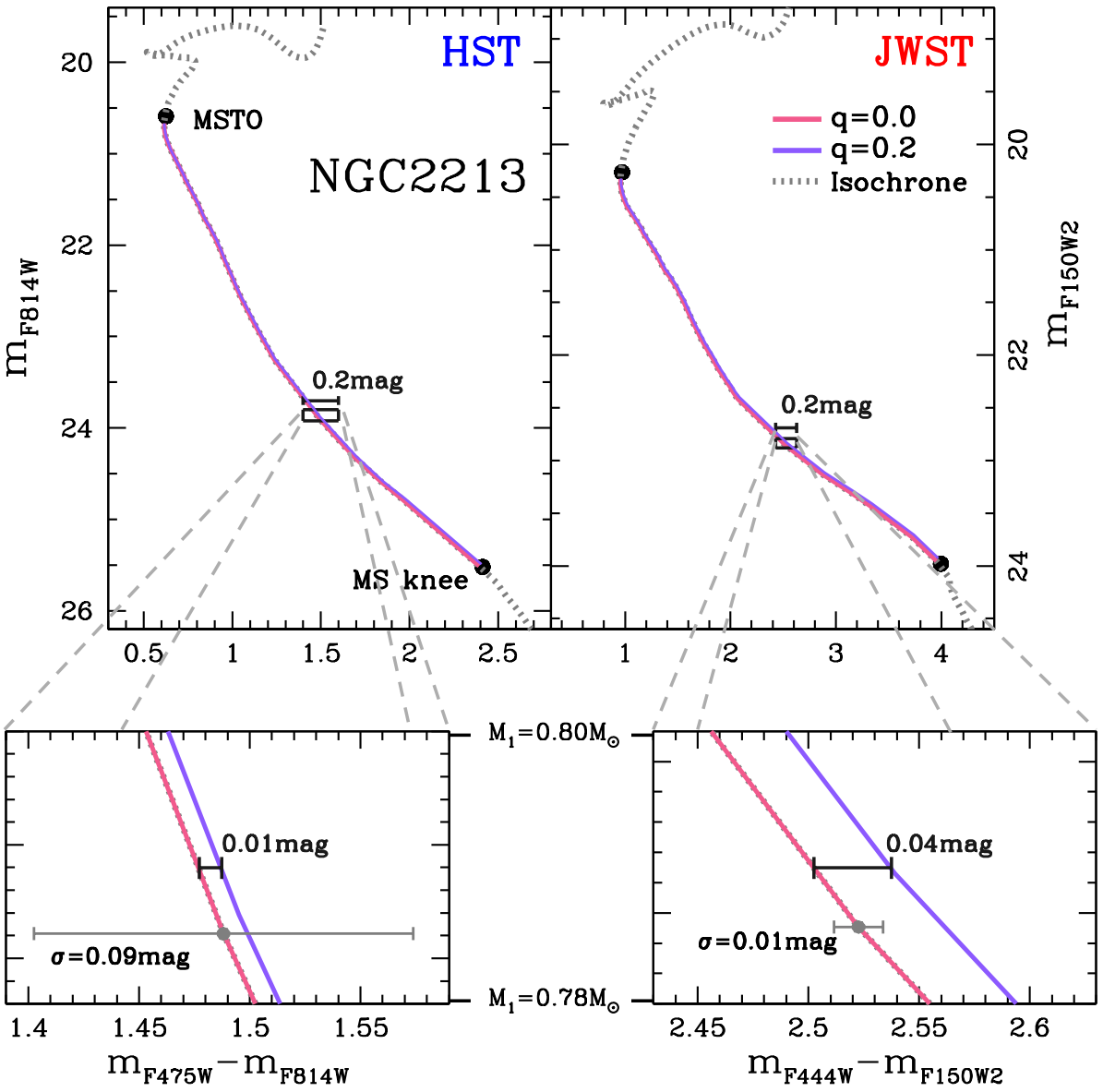

FIGURE 5.10: The plot shows the main sequence part of the colour-magnitude diagram of the cluster NGC2213. The left and right panels show the CMD with HST, and the simulated CMD with JWST, respectively. Zoom-in images of a 0.2 mag window show the colour separation between $q = 0$ and $q = 0.2$ lines (denoted in a black horizontal line) and the associated observational error (σ, denoted in a grey horizontal line) for a certain mass range as denoted in the figure.

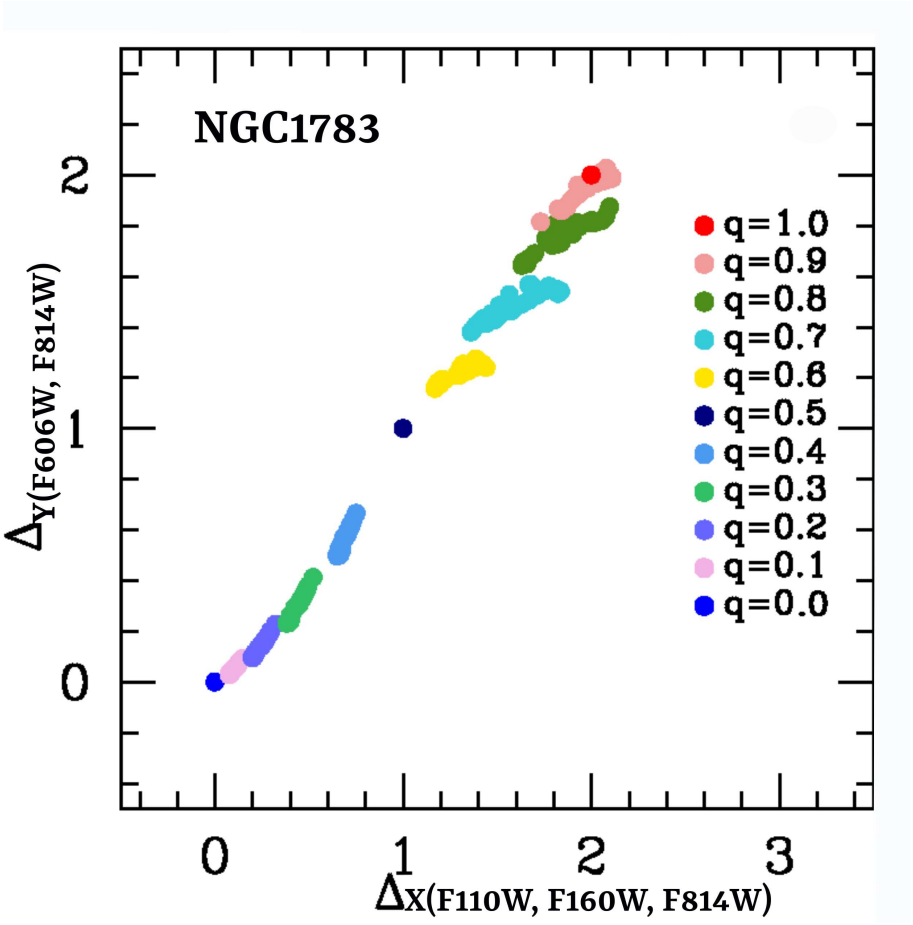

FIGURE 5.11: Chromosome map for binaries constructed using a F814 v/s (F110W-F160W) CMD and F814W v/s (F606W-F814W) CMD of the NGC1783. The Loci of binaries with different qs are colour-coded as denoted in the figure.

to separate low q binaries from single stars. In the HST-based m_{F814W} v/s m_{F475W} - m_{F814W} CMD of cluster NGC2213, the observational error is a staggering 9 times the colour difference between the locus of binaries with $q = 0.2$ and single star MSFL denoted by the $q = 0$ line (refer to the left panel of Figure 5.10). We have simulated the CMD in JWST/NIRCam filters, as shown in the right panel of Figure 5.10. The observational error is 1/4th of the colour difference between MSFL and the binary locus with $q = 0.2$. This is a 36-fold improvement which will potentially help us to explore low q binaries, and further help in obtaining the complete q distribution of binaries.

To better disentangle binaries belonging to different q loci, we have constructed a plot similar to the Chromosome map, a popular analysis method to characterise multiple populations in star clusters. We followed the recipe prescribed by Milone et al. (2017) to construct the Chromosome maps. The adopted procedure can be summarised as follows. Two CMDs, with the same magnitude axes and different colour axes, are generated for the same cluster. A filter combination for each of these two CMDs is selected such that we obtain better separation of binaries belonging to different q ranges. Each target q locus in each of the CMDs is subjected to verticalisation with 2 reference lines, for example, $q = 0$ and $q = 1$ loci. The colour difference of the target q locus is calculated in each CMD with respect to the respective reference lines. Thus obtained colour difference from each CMD is plotted against each other to create the Chromosome maps.

Figure5.11 shows a Chromosome map constructed using best-fitting isochrones of the cluster NGC1783. Double normalisation has been performed here to increase the separation of different q loci. The first normalisation is done with $q = 0$ and $q = 0.5$ as the reference lines while the subsequent verticalisation is done with $q = 0.5$ and $q = 1$ as the reference lines. The loci of different mass ratio binaries are denoted with different colours in the figure and they appear to be well separated to facilitate an accurate calculation of their fraction.

Chromosome map of binaries helps in (i) studying binaries of lower q values and (ii) optimising the separation of larger q loci. Multiple verticalisation procedures and multi-wavelength analysis offer a holistic approach to control the separation between different q loci. By incorporating the lower q binary fractions, we can approach the complete binary fraction and attain a comprehensive view of the mass-ratio distribution of binaries in star clusters.

5.5 The radial distribution of binaries

The radial distribution of binaries is the result of various processes leading to the formation, migration, and evaporation of binaries. The environmental conditions in different radial ranges are different which changes the amount of binaries present there. Dense cluster cores witness higher interaction rates, including collision, which accelerates the binary disruptions processes there compared to cluster outskirts. On the other hand, mass segregation builds up the concentration of binaries in the core.

The radial distribution of BSSs has been found useful in the context of a 'dynamical clock' to date the dynamical history of the host stellar system (Ferraro et al., 2012). Li et al. (2013) found the radial distribution of binaries in two chronologically coeval clusters in LMC, NGC1818, and NGC1805 of age $\sim$ 30Myr, to have different radial distributions. Different dynamical ages were advocated to explain the observed difference. Similarly, MS binaries population in non-relaxed systems such as the Galactic GC NGC6101 shows no evidence of mass segregation (Dalessandro et al., 2015).

Lanzoni et al. (2016) claim the radial distribution of the binary system in clusters can be generalised to bimodal where the position of the is associated with the dynamical stage of evolution (Dalessandro et al., 2011; Beccari et al., 2013). A study using detailed N-body modelling by Geller et al. (2013) supports this claim. They find that in the very early phase of cluster evolution, just a few Myr from the formation, a bimodal radial distribution of binaries can be observed and the minima between the two peaks progressively move to larger radial values until it reaches cluster outskirts and the distribution becomes unimodal with a single central peak.

The following section details our investigation of the radial distribution of MC GCs and their potential dynamical significance.

The radial distribution of binaries is examined by dividing the cluster region within the radial distance of R_{2f} into five annuli, each with an equal number of MS stars [3]. The binary fraction in each annulus is calculated using the procedure mentioned in Chapter 4 and is plotted as a function of the mean radial distance of the stars in that annulus from the cluster centre, as in Figure 5.12 and Figure 5.13. The corresponding χ^2 and $P-values$ are reported in Table 5.1.

We find that in some clusters, such as ESO057SC075 and NGC 1868, which are the studied clusters with a higher dynamical age of 7 and 10 respectively, the binaries are centrally concentrated. However, the binaries of other clusters, including NGC 1751 and NGC 2108, show a flat distribution with $P-values \sim 1$ whereas NGC1872 shows hints of a secondary peak.

The radial distribution of binaries from all the clusters is combined, as shown in the left panel of Figure 5.14, where we normalise the fraction of binaries to the fraction of binaries in the core and express the radial distance in the units of the core radius. We do not find evidence for a correlation between the fraction of binaries and the radial distance from the cluster centre, as denoted by the correlation rank of -0.3. However, when we separate the clusters into two groups with ages either smaller or greater than five times their half-mass relaxation time, t_{rh} (middle and right panels of Figure 5.14, respectively), a pattern emerges. With a correlation rank of -0.6, most dynamically old clusters exhibit some hints of binary segregation into the centre, while the dynamically younger ones exhibit a flat distribution with a correlation rank of 0.

[3]This extract is taken from Section 5.3 of Mohandasan et al. (2024).

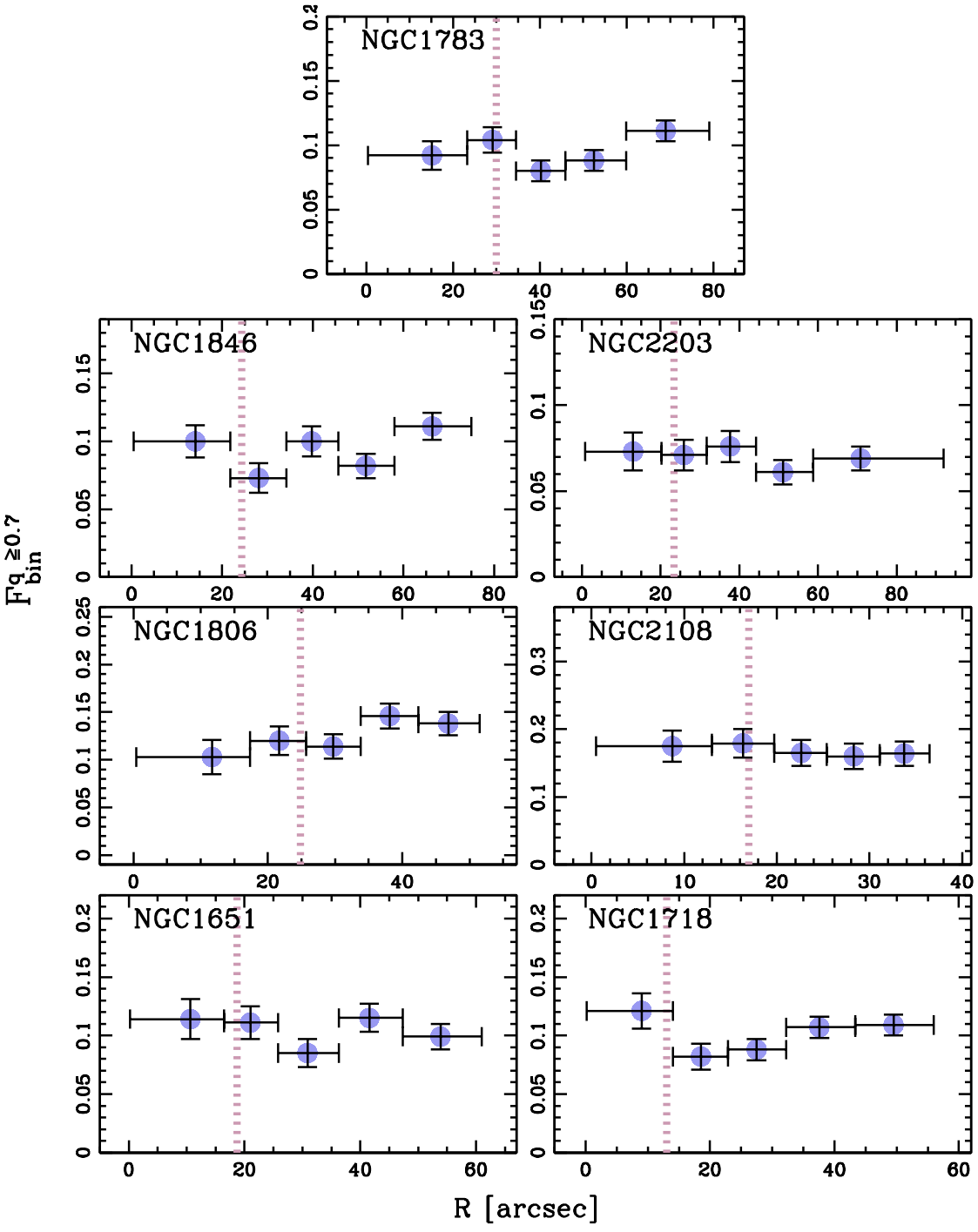

FIGURE 5.12: Radial distribution of binaries in Magellanic Cloud star clusters. The core radii of the studied clusters are denoted with a dotted pink line.

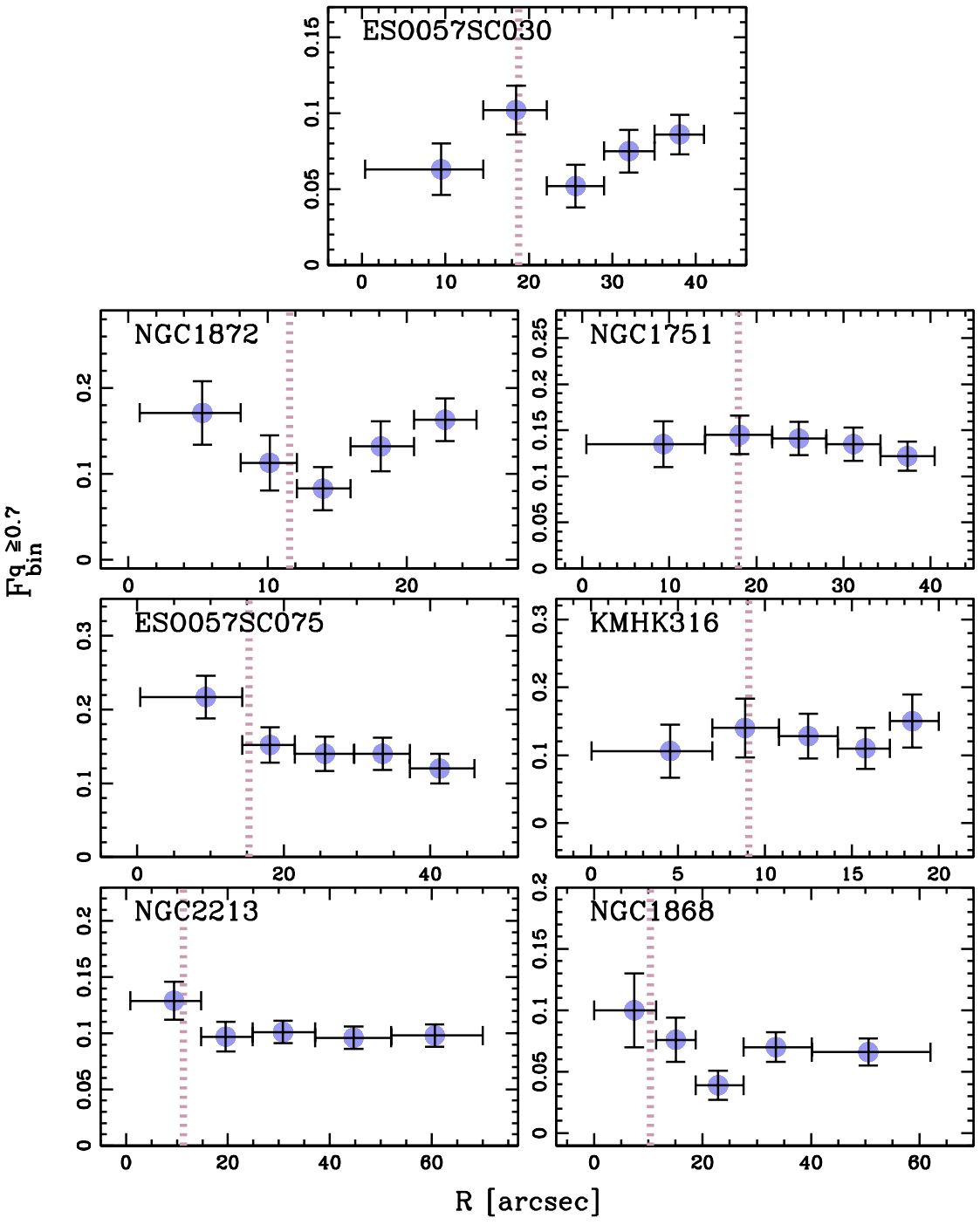

FIGURE 5.13: Continuation from Figure 5.12.

5.6 Comparison with Galactic clusters

Galactic and extra-galactic clusters provide different environmental conditions such as density and concentration. The stellar populations in them, including binaries, are expected to reflect such differences. Binaries in Galactic clusters, both OCs (Cordoni et al., 2023; Jadhav et al., 2021) and GCs (Milone et al., 2012, 2016; Sollima et al., 2007), are extensively studied in this context. Galactic GCs are predominantly old and massive, whereas Galactic OCs have a large number of young and less massive clusters.

To compare the binary fractions of MC star clusters and Galactic open and globular clusters, we combined the results of this work with results from the literature where binaries were analysed homogeneously [4]. The results are illustrated in Figure 5.15 which compares the core binary fraction with $q \geq 0.7$ derived in this paper (purple dots) and those measured in Galactic GCs (green dots, Milone et al., 2012, 2016) and Galactic OCs (pink dots, Cordoni et al., 2023). The left panel of Figure 5.15 shows the fraction of binary as a function of the cluster mass in the logarithmic scale. We used mass and t_{rh} values for Galactic GCs from Baumgardt and Hilker (2018), except for NGC 6637, NGC 6652, NGC 6981, and Palomar 1, for which the adopted values come from McLaughlin and van der Marel (2005). The MC star clusters studied in our paper span a mass interval between 10^4 and 10^5 $M_\odot$, which are poorly populated by the clusters studied in the previous works.

Considering all clusters together, we find an anti-correlation between the binary fraction in the core and the cluster mass. This observation is supported by theoretical models by Sollima (2008) where they suggest the energy and rate of collisions in the core increases with the mass of the cluster which in turn accelerates the

[4] This section is taken from section 5.5 of Mohandasan et al. (2024).

binary disruption processes there. However, for a fixed cluster mass, the binary fraction spans a wide range of values. In particular, the MC clusters studied in this paper exhibit a larger fraction of binaries than the bulk of Galactic GCs with similar masses. Conversely, as shown in the middle and right panel of Figure 5.15, there is no evidence of a correlation between the fraction of binaries and the cluster age or the ratio between cluster age and t_{rh}.

5.7 Summary

I have investigated binary fractions in young and intermediate-age MC star clusters as a function of different cluster and stellar parameters. The obtained results were compared to the homogeneous studies on Galactic OCs and GCs. The main results are as follows,

- Binary fraction did not show any strong correlation with cluster parameters such as chronological age, dynamical age, metallicity, mass, density, or concentration. However, a small number of clusters show a decrease in binary fraction with an increase in cluster mass and dynamical age. An increase in binary disruption processes with the increase in cluster mass has been predicted by theoretical models (Sollima, 2008).

- The mass distribution of binaries appears to be flat. The result is in agreement with the results from homogeneous studies on Galactic GCS (Milone et al., 2012) and OCs (Cordoni et al., 2023).

- Distribution of binaries with respect to the mass ratio of the systems did not show any strong correlation. The results are in agreement with the homogeneous studies on Galactic OCs (Cordoni et al., 2022) and Gcs (Milone et al., 2012).

- An innovative method titled 'Chromosome map of binaries' has been introduced to analyse binaries of different mass-ratio. This method appears quite promising to optimise the seperation between different mass-ratio and is quite advantageous for studying lower mass-ratio binaries which are hard to disentangle otherwise.

- The radial distribution shows two kinds of patterns.
  (i) The dynamically older clusters, with an age greater than five times their t_{rh}, show a concentration of binaries towards the centre. Similar central concentrations of binaries have been observed in a homogeneous study of old Galactic GCs by Milone et al. (2012).
  (ii) Dynamically younger clusters, with an age less than five times their t_{rh}, show no correlation between binary fraction and radial distance. Studies on Galactic OCs have reported different radial distributions for clusters of different ages (Cordoni et al., 2023).

We have combined the results obtained in the case of MC GCs with homogeneous studies on Galactic clusters (Milone et al., 2012; Cordoni et al., 2022) which enabled us to increase the cluster parameter range of MS binary fraction investigation. We find a decrease in binary fraction with an increase in cluster mass as predicted by theoretical models (Sollima, 2008). However, for a fixed cluster mass, the binary fraction spans a wide range of values. Additionally, we did not find any connection between the observed binary fraction in the core and either the chronological or dynamical age of the cluster.

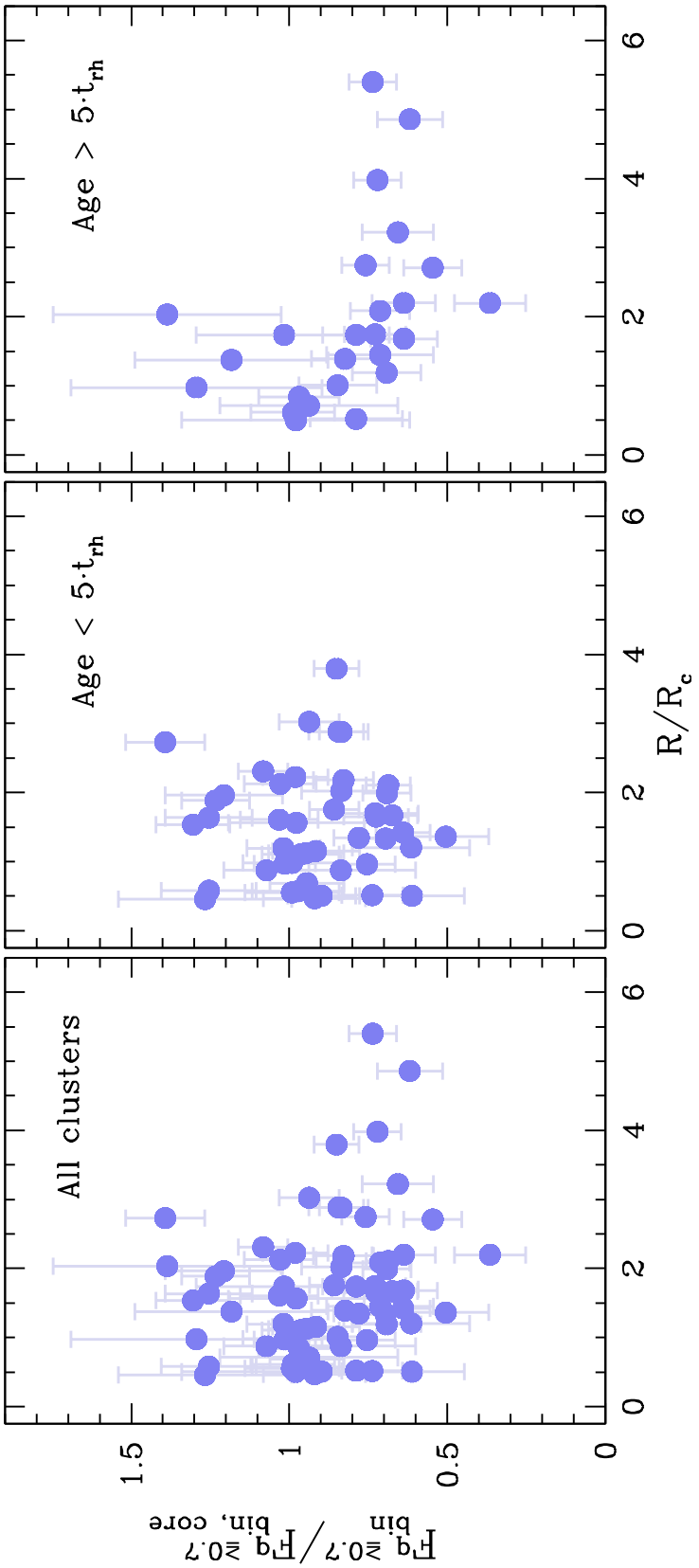

FIGURE 5.14: Difference types of radial distribution. Binary fraction, normalised to the binary fraction in the core, as a function of the radial distance in the unit of core radius (Mohandasan et al., 2024). (*left panel*) All the analysed Magellanic Cloud clusters. (*middle panel*) Dynamically younger clusters. (*right panel*) Dynamically older clusters.

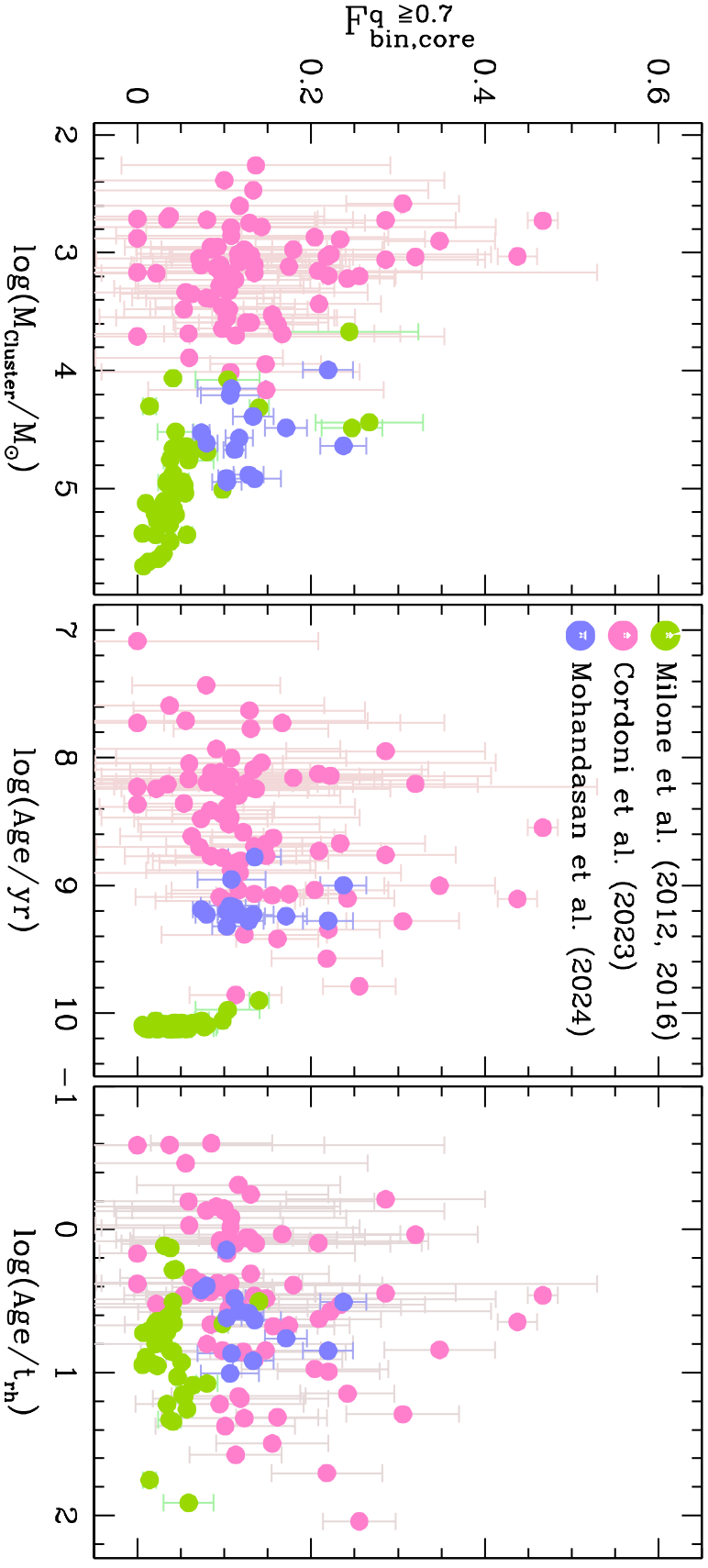

FIGURE 5.15: Binary fraction in different environments (Mohandasan et al., 2024). The plot compares the core binary fraction for clusters belonging to different environments. Galactic GCs, Galactic open clusters, and the Magellanic Clouds globular clusters studied in this paper are denoted in lime green, magenta, and violet, respectively. Binary fractions in these clusters are explored as a function of mass (*left panel*), age (*middle panel*), and dynamical age (*right panel*) on a logarithmic scale.

Chapter 6

Blue straggler stars

6.1 The interesting case of blue straggler stars

Blue straggler stars were first discovered in the CMD of Galactic GC M3 by Allen Sandage (Sandage, 1953). The occurrence of such bright and massive stars in old systems like GCs is quite puzzling. Their existence is at odds with single stellar evolution models as such a massive object should have exhausted its nuclear fuel and evolved long ago to become a white dwarf. However, BSSs were identified and studied later in different stellar systems such as GCs (e.g., Piotto et al., 2004), OCs (e.g., Chen and Han, 2008), dwarf galaxies (e.g., Salinas et al., 2012), galactic field region (e.g., Preston and Sneden, 2000)), MC (e.g., Sun et al., 2018; Li and Hong, 2018). Gaia and other modern astrometric and photometric surveys have led to a significant rise in the detection of BSSs (Li et al., 2023). It is now widely accepted that BSSs are commonly observed in star clusters older than 1 Gyr.

BSSs represent a population of rejuvenated stars formed through the evolution of old stellar populations in star clusters. BSSs are younger and hotter than the

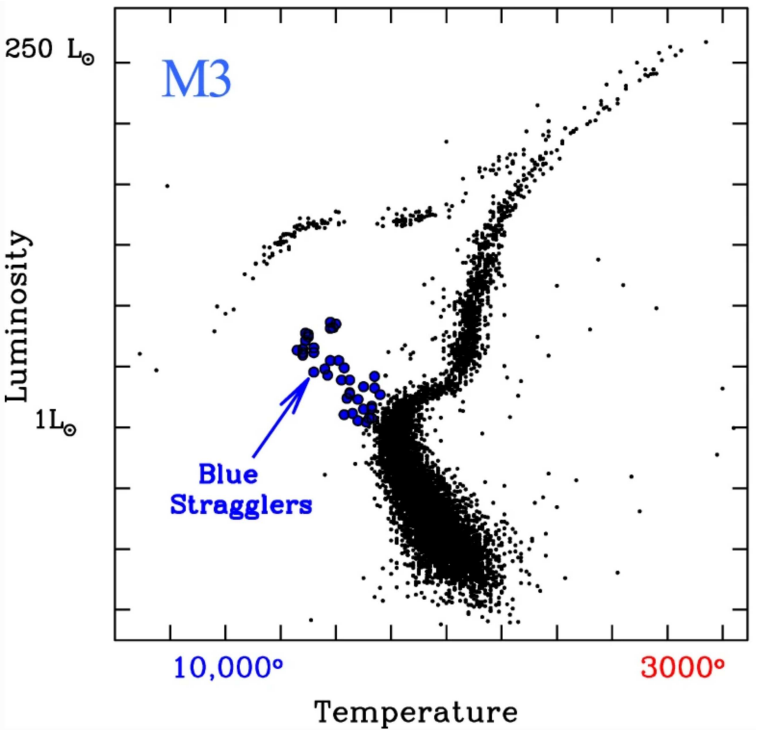

FIGURE 6.1: Blue straggler stars identified in the Hertzsprung-Russel diagram of Galactic globular cluster M3 (Ferraro et al., 2020).

normal cluster members and have masses up to twice that of turn-off stars (Li and Hong, 2018; Fiorentino et al., 2014). Radial distribution of BSSs was found to carry dynamical implications regarding the star cluster (Stryker, 1993; Ferraro et al., 2009). In the CMD of a cluster, BSSs populate a region in the upper and bluer side of the MSTO and appear as an extension of the MS stars, as shown in Figure 6.1 (Ferraro et al., 1999b). Two main, non-exclusive formation scenarios have been identified to unravel the mystery regarding their formation; (i) collisional stellar mergers (Hills and Day, 1976) and (ii) mass transfer in a binary system (McCrea, 1964). The discovery of a double BSS sequence in the CMD of a candidate post-core collapse GC (refer to Figure 6.2) and the subsequent implication that each of these sequences is linked to one of the two major formation channels (Ferraro et al., 2009; Cadelano et al., 2022) make the photometric ventures into BSSs further compelling.

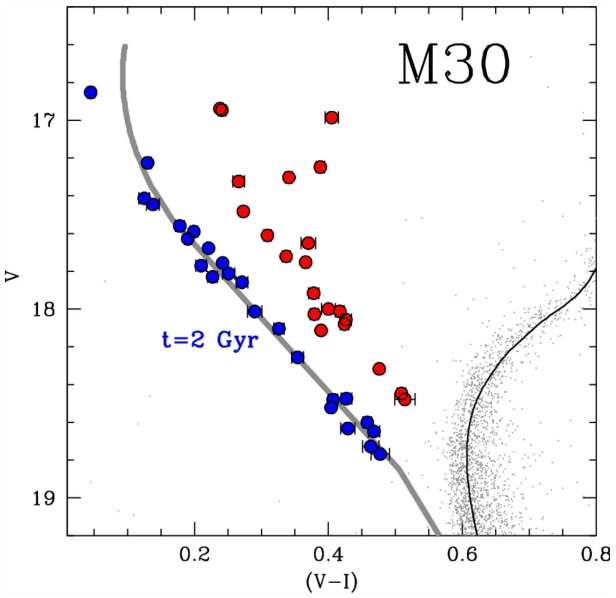

FIGURE 6.2: Double sequence of blue straggler stars observed in the colour-magnitude diagram of Galactic globular cluster M30 (Ferraro et al., 2009).

6.1.1 Blue straggler stars: Formation scenarios

Binary mass transfer (McCrea, 1964) and direct stellar collisions (Hills and Day, 1976) are identified as competing evolutionary scenarios leading to the formation of BSSs in star clusters (refer to Figure 6.3). The temperature and luminosity spread of the BSS population observed in the CMD is mapped to the mass transfer process in primordial binaries, which is present irrespective of the environment. However, the detection of a double sequence of BSSs supports the co-existence of mass transfer and collisional formation scenarios. Core collapse triggers the formation of BSSs through binary and collisional channels. The observed distribution of BSSs in CMDs can be reproduced through collisional models of MS binaries (Sills et al., 2009) and binary mass transfer models (Jiang et al., 2017). Observational pieces of evidence can be a deciding factor in determining the relative importance of these processes.

Many of the observational studies on Galactic BSSs have been produced in recent

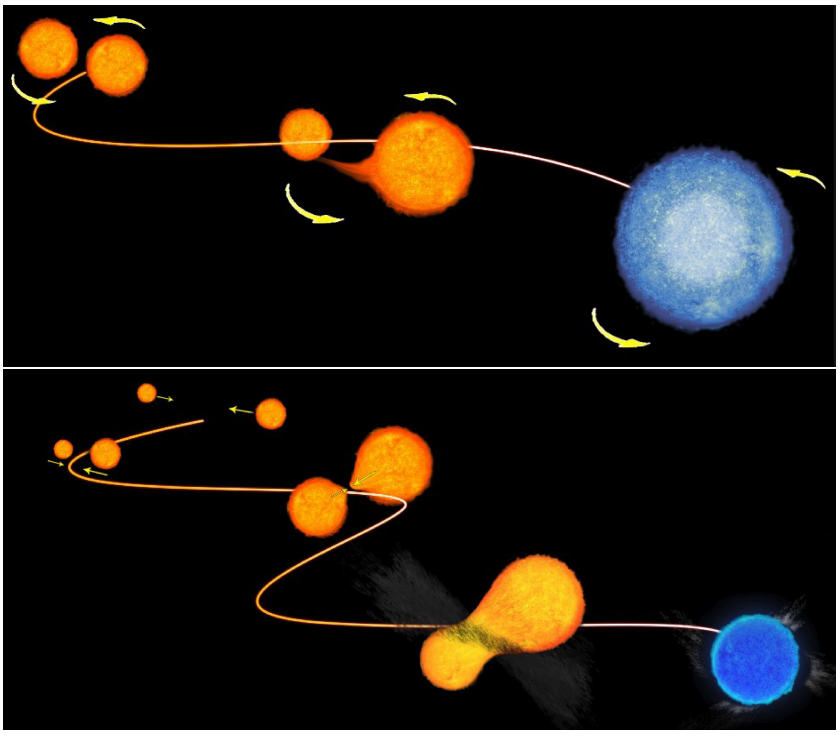

FIGURE 6.3: Artistic illustration of blue straggler star formation through (*Top panel*) binary mass transfer channel and (*Bottom panel*) stellar collision channel (Ferraro et al., 2020).

years and some of them have conflicting conclusions. Ferraro et al. (2003) studied central regions of six Galactic GCs of varying densities and metallicity in the context of the BSS population. They found good agreement between the observed number of BSSs and the predicted number through collisional models. Piotto et al. (2004) studied BSSs in 56 Galactic GCs and did not find any statistically significant relation between BSS frequency and the collision rate. However, they found an anti-correlation between the relative frequency of BSSs and the total absolute luminosity. On the other hand, Andronov et al. (2006) suggests the predicted number of BSS from MS mergers is comparable to the observed number in GCs. They also claim such mergers are responsible for at least one-third of the BSSs in OCs and found agreement between the observed number of BSSs and the estimated MS merger rates in the OC M67. Knigge et al. (2009) found a sub-linear relation between the BSS number in the cluster core of GCs and the core mass. Binary

fraction is also found to be dependent on core mass in Galactic GCs (Milone et al., 2012), suggesting the dominance of binary interaction in BSS production. Mapelli et al. (2006) inferred that the dominant formation channel can be a function of spatial distribution, especially in clusters with a significant radial gradient of density. By studying the radial distribution of BSSs in 4 GCs and comparing them with numerical simulations, they surmise that the BSSs found near the cluster core most likely formed through collisional interactions while those in the outskirts almost exclusively formed from mass transfer in primordial binaries. Since the ecology of formation holds immense importance in the preferred formation scenario, studying BSSs from different environments is crucial to constrain their formation scenarios.

6.1.2 Blue straggler stars in Magellanic Cloud star clusters

Most of the studies on BSSs were focused on Galactic clusters. They offer better photometry with low-field contamination. However, most Galactic clusters are old and massive. For a better understanding of the formation scenarios of BSSs, we need to increase the sample size and include clusters with different ages and evolutionary stages. The star clusters in the LMC and SMC are suitable for achieving this objective as they are the only systems that contain clusters at all stages of evolution while being close enough to study the resolved stellar populations in them. Unlike the Galactic clusters, clusters in MC span a wide range of ages and densities (McLaughlin and van der Marel, 2005; Mackey and Gilmore, 2003). They have lower density and hence a lower probability for collisional interactions compared to that of the MW clusters.

The studies on BSSs in extragalactic clusters are limited in number (Li and Hong, 2018; Li et al., 2018a). Sun et al. (2018) studied the BSS population in 24 MC GCs and compared it with collision rates and mass of the core. They found a correlation between the mass of the core and the number of BSSs in the core. The mass-normalised number of BSSs depends only weakly (or perhaps not at all) on the collision rate, implying that the binary-driven BSS formation channel dominates. Li et al. (2019) studied the radial distribution of BSSs in 7 MC GCs in the contest of the dynamical clock framework proposed for the Galactic clusters. They did not find a strong agreement between dynamical age and radial distribution of BSSs. Additionally, Li and Hong (2018) found no mass segregation in the LMC cluster NGC2213 compared to the giant stars, though it was dynamically old. Through numerical simulations, they argue that the disagreement between the dynamical age and the radial profile of BSSs can be attributed to the presence of potential black holes or binary disruption processes present in the clusters which delay mass segregation. A robust conclusion requires further observational studies on the BSS populations in MC star clusters.

6.2 Blue straggler star fraction

The CMDs of the analysed 14 MC star clusters have a sequence of stars in the blue and brighter side of the MSTO [1]. This region of the CMD is populated by the BSSs, whose origins are traditionally associated with stellar mergers or the evolution of binary stars (e.g. Sun et al., 2018, and references therein). However, recent works argue that the sequences of blue stars observed in some intermediate-age LMC star clusters correspond to young stellar populations that emerged from the

[1]This session discusses the results from session 5.4 of Mohandasan et al. (2024).

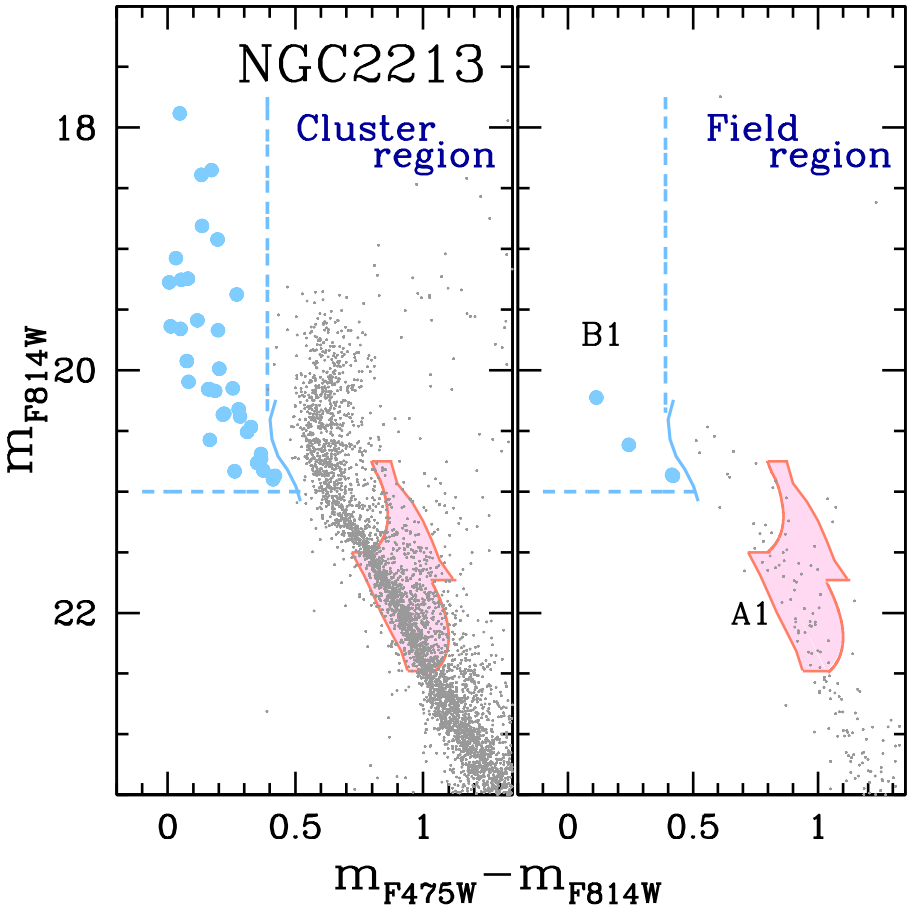

FIGURE 6.4: Figure demonstrates the procedure to derive the blue straggler star fraction in the upper MS region of the $m_{\rm F814W}$ vs. $m_{\rm F475W} - m_{\rm F814W}$ CMD of NGC 2213 for stars in the (*left panel*) cluster region and (*right panel*) field region (Mohandasan et al., 2024). The pink-shaded areas mark region A1 which is populated by MS stars, while region B1 hosts the candidate blue straggler stars which are marked with azure dots. The azure solid and dotted lines denote the boundaries of region B1. See the text for details.

merging events in the MC (Li et al., 2016; Hong et al., 2017; Hammer et al., 2021). Understanding the origin of these stars is beyond the purposes of our study. Here, we focus on determining some of their observational properties.

To derive the fraction of candidate BSSs in each cluster, we defined two regions in their CMD, namely A1 and B1, as illustrated in Figure 6.4 for the cluster NGC 2213. The A1 region (pink-shaded area) hosts MS stars. It is similar to the region A of the CMD introduced in Chapter 4, but spans an interval of one magnitude in the filter

F814W along the magnitude axes. The B1 region corresponds to the portion of the CMD that hosts the candidate BSSs and is limited by the azure solid and dotted lines. The continuous azure line corresponds to the MSFL shifted by four times σ to the blue side, where σ is the colour uncertainty associated with MSFL. The vertical azure dotted line has the same colour as the MSTO, whereas the horizontal azure dotted line is 0.25 mag fainter than the brightest limit of region A1.

The fraction of candidate BSSs is defined as,

$$F_{BSS} = \frac{N^{B1}_{cluster} - N^{B1}_{field}}{N^{A1}_{cluster} - N^{A1}_{field}}, \tag{6.1}$$

where $N^{A1}_{cluster}$ and $N^{B1}_{cluster}$ are the numbers of stars in the regions A1 and B1 of the cluster-region CMD obtained after giving correction for completeness. N^{A1}_{field} and N^{B1}_{field} are the corresponding quantities for the field-region CMD that have been normalised by the ratio between the areas of cluster-region and the field-region, as explained in Chapter 4.

The BSS fraction obtained for the analysed clusters is listed in Table 6.1. The fraction of candidate BSSs within the half-mass radius of the cluster ranges from a minimum of 0.1%, in the cluster NGC 2108, to a maximum of 2% in clusters NGC 1806 and NGC2213. The fraction in the core is higher than $F_{BSS,R_{hm}}$ and it ranges from a minimum of 0.1% in clusters NGC1872 and NGC2108 up to a maximum of 4% in cluster NGC2213. NGC2213, the cluster with the highest fraction, is one of the dynamically old clusters in the list with an age of more than eight times its t_{rh}, while NGC2108, the cluster with the lowest fraction, is one of the dynamically young clusters in the list, with an age of three times its t_{rh}.

Figure 6.5 reveals the lack of correlation between the fraction of candidate BSSs in the core and the cluster age or metallicity, as expressed by Spearman's rank

TABLE 6.1: Fraction of candidate blue straggler stars for the studied clusters (Mohandasan et al., 2024).

Cluster ID	$F_{BSS,R_{hm}}$	F_{BSS,R_c}	A^+
ESO057SC075	0.010 ± 0.005	0.012 ± 0.006	0.12 ± 0.00
ESO057SC030	0.006 ± 0.006	0.017 ± 0.008	0.02 ± 0.01
KMHK316	0.007 ± 0.009	0.018 ± 0.015	0.16 ± 0.04
NGC1651	0.009 ± 0.003	0.014 ± 0.006	0.25 ± 0.03
NGC1718	0.012 ± 0.004	0.019 ± 0.006	0.07 ± 0.02
NGC1751	0.012 ± 0.007	0.005 ± 0.009	0.04 ± 0.02
NGC1783	0.016 ± 0.003	0.016 ± 0.003	-0.16 ± 0.01
NGC1806	0.021 ± 0.003	0.019 ± 0.004	0.06 ± 0.01
NGC1846	0.018 ± 0.004	0.026 ± 0.007	0.06 ± 0.01
NGC1868	0.006 ± 0.003	0.018 ± 0.008	0.19 ± 0.07
NGC1872	0.000 ± 0.002	0.001 ± 0.002	-0.07 ± 0.01
NGC2108	0.001 ± 0.004	0.001 ± 0.005	0.15 ± 0.03
NGC2203	0.008 ± 0.002	0.005 ± 0.003	0.00 ± 0.01
NGC2213	0.021 ± 0.006	0.040 ± 0.012	0.30 ± 0.03

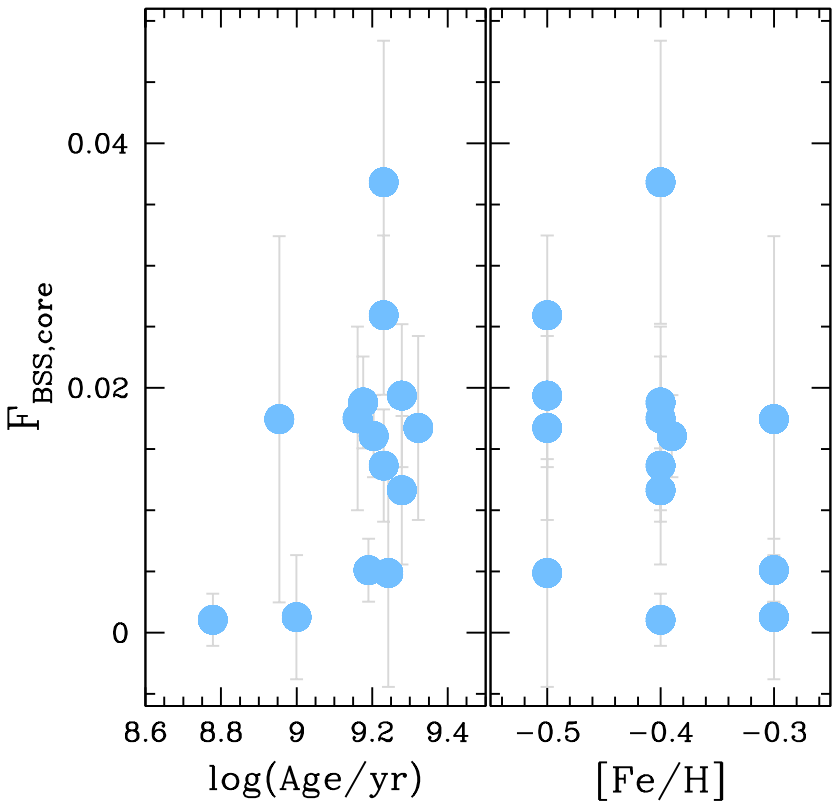

FIGURE 6.5: BSS fraction and cluster parameters (Mohandasan et al., 2024). The fraction of candidate Blue straggler stars in the core is plotted as a function of (*left panel*) cluster age and (*right panel*) iron abundance.

correlation coefficients of 0.3 and −0.3, respectively. The BSS fraction showed a correlation rank of 0.1 and -0.1 with the dynamical age and mass of the clusters, as demonstrated respectively in the left and right panels of Figure 6.6. Nevertheless, we confirm that clusters younger than $\sim$ 1 Gyr are unlikely to host BSSs (Rain et al., 2021; Cordoni et al., 2023). Also, we did not observe any double-sequence in the distribution of BSSs as expected for the analysed pre-core collapse clusters. However, recent studies have documented the existence of bi-sequences of BSSs in a young LMC cluster NGC 2173 of age 1.58 Gyr (Li et al., 2018b). While this finding remains contentious (Dalessandro et al., 2019), additional proper-motion-based analysis is required to ascertain cluster membership of the stars forming the sequence.

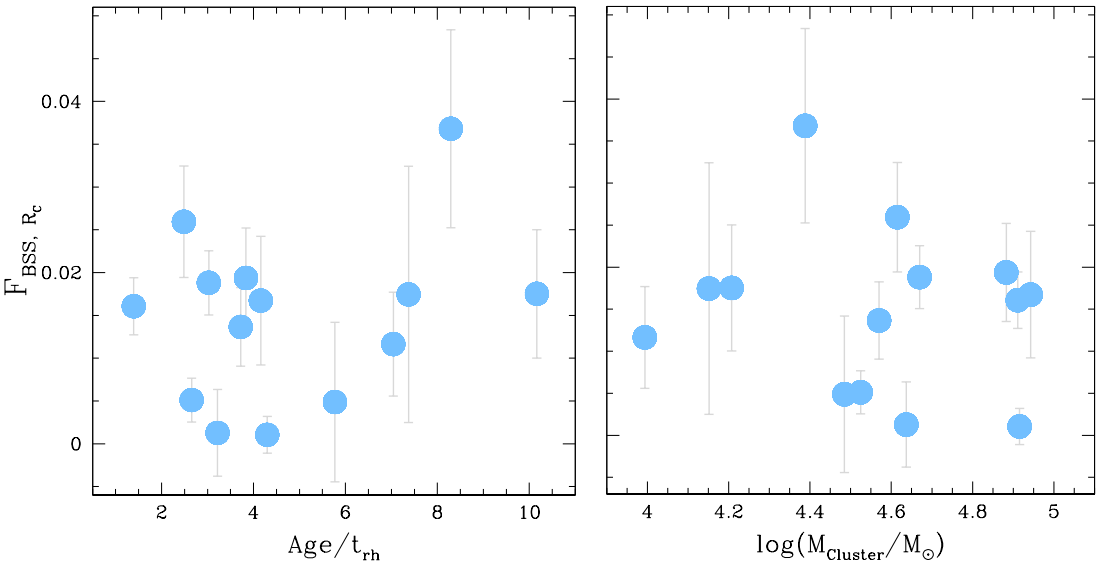

FIGURE 6.6: The relation between blue straggler star friction with (*left panel*) dynamical age and (*right panel*) mass of the cluster.

6.3 Blue straggler stars and MS binaries

Mass transfer in a binary and coalescence of companion stars in a binary–binary or binary–single star systems are competing scenarios of BSS formation (Chen and Han, 2008). Therefore, the amount of BSSs is expected to be correlated with the number of MS binaries in a cluster. The fraction of BSSs was found to show a strong correlation with the fraction of binaries in the case of old Galactic GCs (Milone et al., 2012; Sollima et al., 2008). Figure 6.7 demonstrates the correlation obtained between the core MS binary fraction with $q \geq 0.5$ and the number of BSSs normalised to a luminosity standard. With Spearman's rank correlation coefficient of ~ 0.9, the BSSs in these old clusters are expected to have an evolutionary link with MS binaries in them.

The BSS fraction in the MC GCs under study is explored as a function of the MS binary fraction in them. Figure 6.8 shows the variation of the BSS fraction as a function of the binary fraction with $q \geq 0.7$, within the half-mass radius of

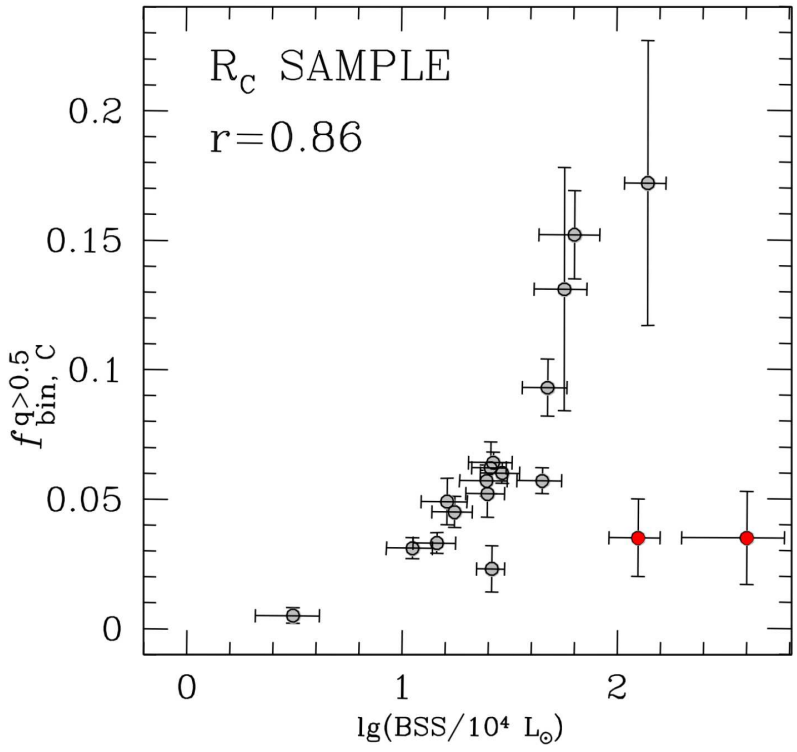

FIGURE 6.7: The relation between the normalised number of blue straggler stars and binary fraction in old Galactic globular clusters (Milone et al., 2012). Spearman's rank of the relation is denoted in the figure.

the cluster. There is no evidence of a correlation between the BSS fraction and MS binary fraction in these young and intermediate age clusters. This lack of correlation is similar to what has been observed in the case of young Galactic OCs, as reported by Cordoni et al. (2023). Figure 6.9 demonstrates the variation of the BSS fraction in them with MS binary fraction.

Figure 6.8 shows that the clusters with higher density are distributed around a vertical strip centred at a binary fraction of 0.1. Whereas the lower-density clusters are spread out along a line with an obtuse angle with the horizontal direction. Higher and lower-density clusters are found to populate different regions in young Galactic clusters as well, as demonstrated in Figure 6.9.

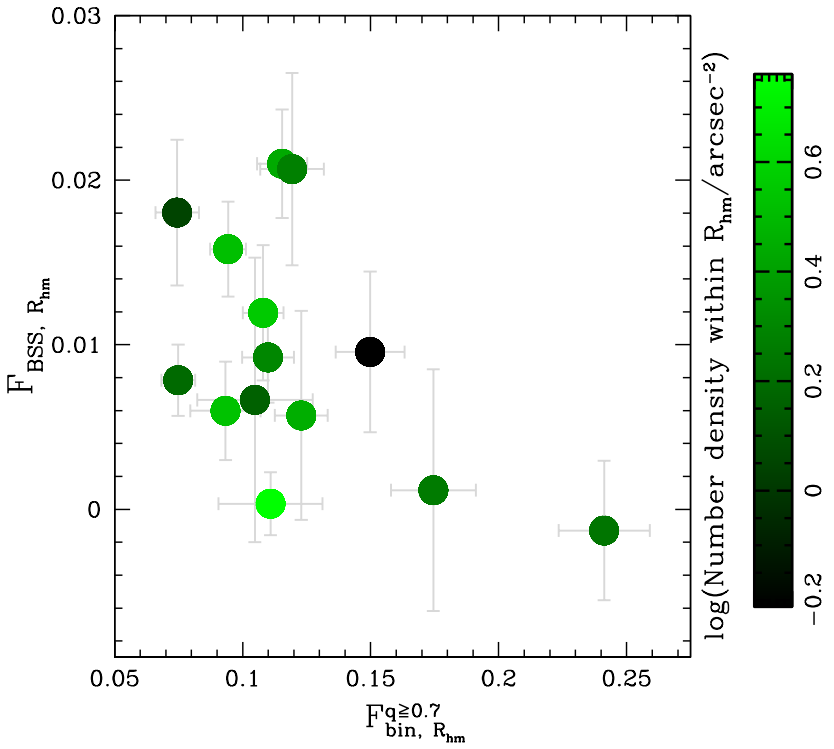

FIGURE 6.8: Fraction of candidate blue straggler stars as a function of the fraction of binaries with mass ratio, q$\geq$ 0.7 in Magellanic Cloud star clusters (Mohandasan et al., 2024). The clusters are colour-coded based on their density, as indicated in the colour bar.

6.4 Cluster dynamics and A^+ Parameter

BSSs have an average mass of $\sim$ 1.2 - 1.5 $M_\odot$ which is quite high for an average GC member (Sollima, 2008). In a dynamically active system such as GC, they are prone to dynamical friction which is an effect that sinks objects with above-average masses towards the centre of the gravitational potential. This gravitational sedimentation has a stronger and more immediate effect on the objects near the centre. However, eventually, the effect spreads to the whole radial range of the cluster (Ferraro et al., 2009; Lanzoni et al., 2016). The extent of this mass segregation, which is visible from the radial distribution of massive objects such as BSSs, is closely linked with the dynamic evolution of the cluster (Ferraro et al., 2009).

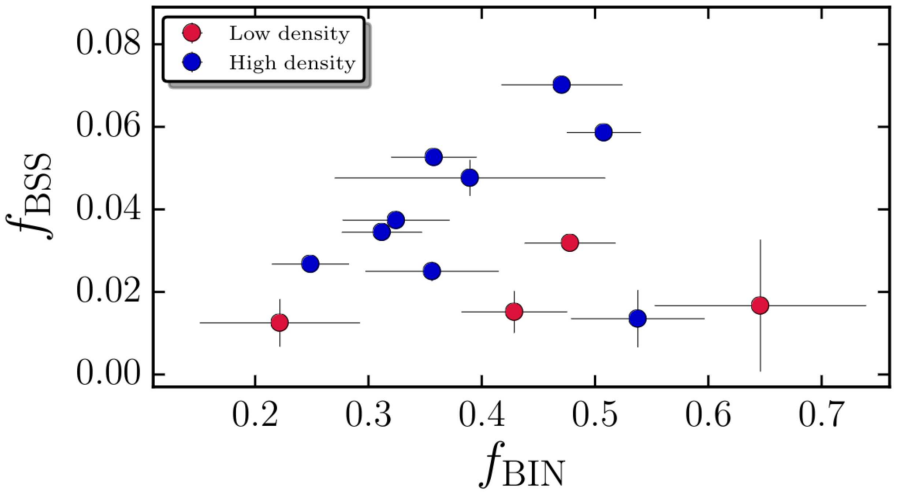

FIGURE 6.9: The variation of blue straggler fraction and binary fraction in young Galactic open clusters (Cordoni et al., 2023). The points are colour-coded depending on their density range.

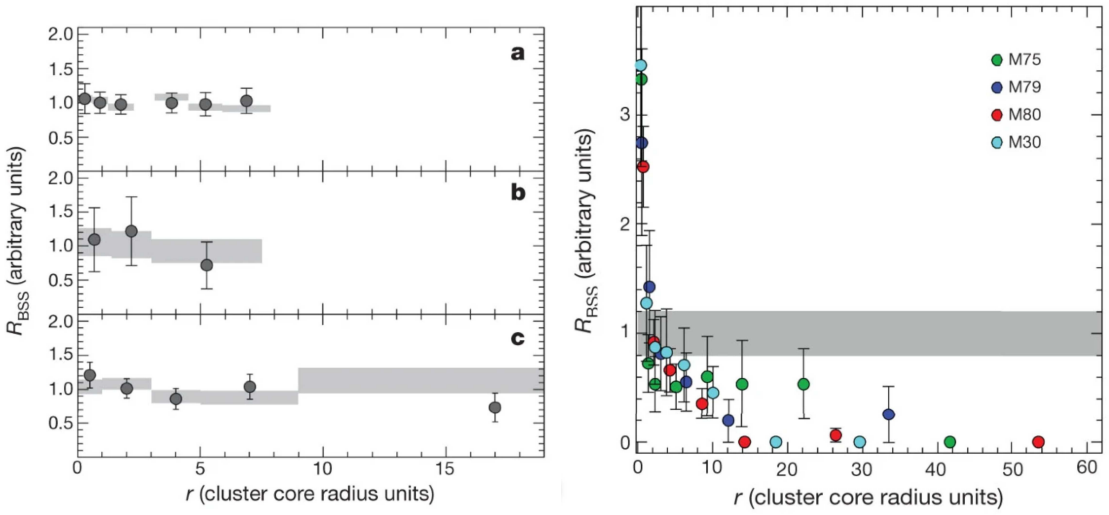

FIGURE 6.10: Radial distribution of blue straggler stars in (*left panel*) young and (*right panel*) old clusters (Ferraro et al., 2012).

6.4.1 Dynamical implications of radial distribution of blue straggler stars

The radial distribution of BSSs is expected to be flat in dynamically young clusters with ages less than their t_{rh}. Dynamic friction has not influenced the stars in these young systems. Eventually, when the dynamic sinking has affected the vicinity of

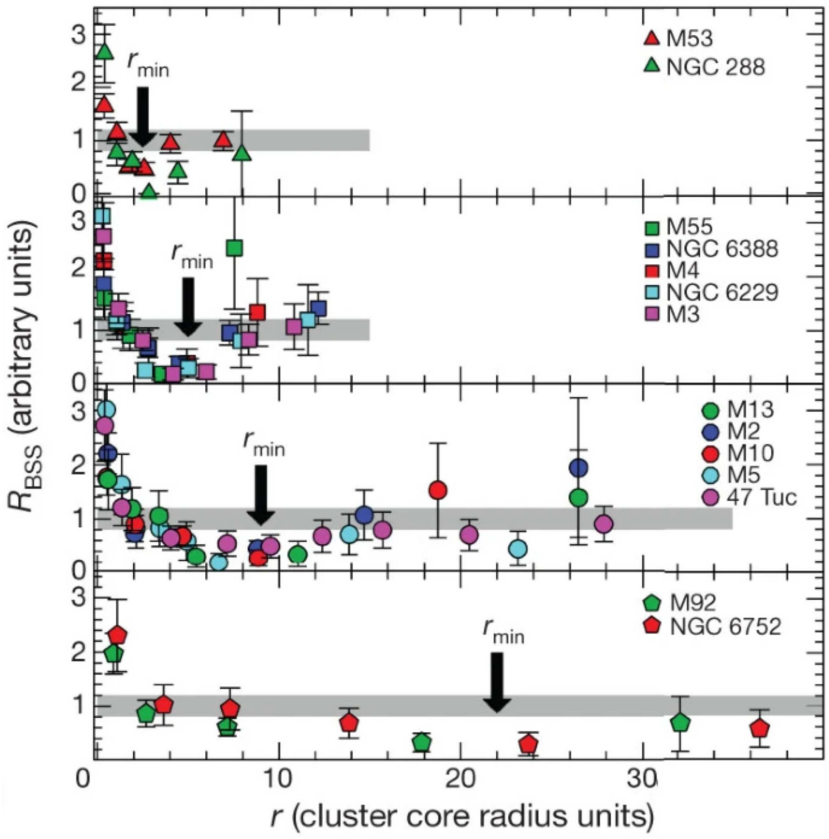

FIGURE 6.11: Radial distribution of blue straggler stars in intermediate-age clusters (Ferraro et al., 2012). r_{min} denotes the position of the dip.

the cluster centre but not the outskirts, a bimodal distribution starts to emerge. Clusters with an age in between t_{rh} and 5 $\times$ t_{rh} are expected to demonstrate such a radial behaviour (Dalessandro et al., 2008). In dynamically old clusters with an age greater than 5 $\times$ t_{rh}, the mass segregation has influenced the whole radial range of the cluster and the radial distribution of BSSs is expected to have a peak in the centre followed by a monotonous decrease. Besides BSSs, massive systems such as binaries are also found to follow a similar radial profile for clusters in different evolutionary stages, as shown with detailed N-body simulations in the case of LMC cluster NGC1818 in Geller et al. (2013).

Dynamically old Galactic clusters are found to have a higher concentration of BSSs

in their core (refer to the right panel of Figure 6.10). Ferraro et al. (1999b) observed one of the most numerous and mass-segregated populations of BSSs in the old Galactic GC M80. Many of them are expected to be formed from collisional interactions which also is expected to put off the impending core collapse in such dense systems. MS binaries and BSS populations in non-relaxed systems such as the Galactic GC NGC6101 show no evidence of mass segregation (Dalessandro et al., 2015). The left panel of Figure 6.10 shows the flat distribution observed in dynamically young clusters. Many intermediate-age clusters, such as Hodge 11, are found to host bimodal distribution of BSS fraction (Li et al., 2013). Figure 6.11 demonstrates the radial profile of BSSs in different intermediate-age clusters along with the position of the dip between the two peaks. Bimodal distribution has been proposed as a general template of BSS radial distribution (Dalessandro et al., 2008). The position of the dip progressively moves from the cluster centre to the outskirts, changing the radial profile from flat to one with a central peak. Hence, the position of the dip has been associated with the dynamical age of the cluster (Ferraro et al., 2012).

Though observed in a large number of clusters, bimodal distribution is unstable in predictions made using analytical models and N-body simulations (Miocchi et al., 2015). Categorising BSS radial distribution into three major dynamical phases is found to be subjective at times, especially in systems with a low number of BSSs. Field contamination and other artefacts pose further hurdles to an accurate determination (Dalessandro et al., 2019). $A+$ parameter-based categorisation offers a statistically robust estimation of the relative segregation of BSSs.

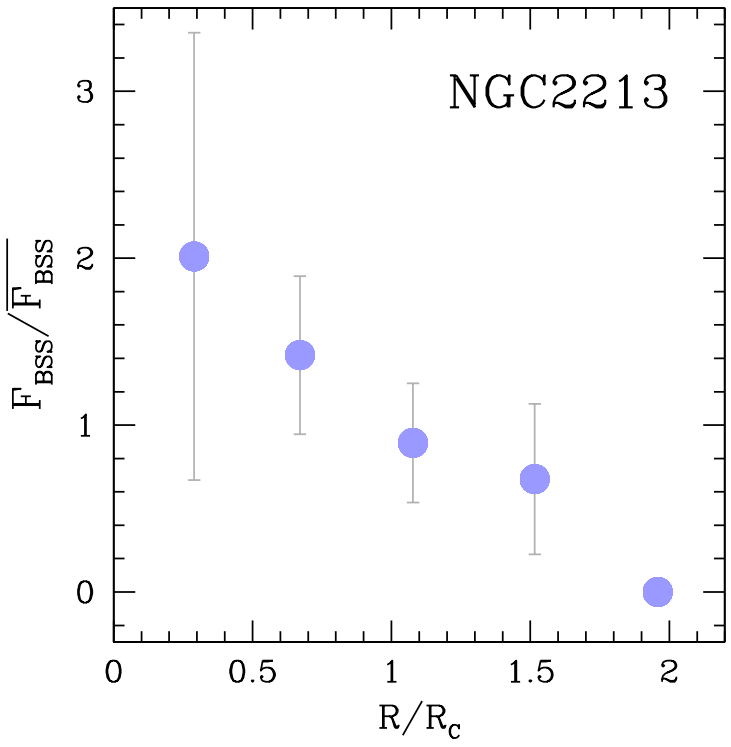

FIGURE 6.12: The normalised radial distribution of blue straggler star fraction in the case of the cluster NGC2213.

6.4.2 A^+ parameter

With the help of N-body simulations, Alessandrini et al. (2016) introduced a quantity called $A+$ as a measure of relative segregation of BSSs in a cluster. It is defined as the difference between the cumulative distribution of BSSs and that of a lighter stellar population. They argue that the time evolution of $A+$ is a better measure of the dynamical evolution of the stellar system compared to the normal radial profile of BSSs. A dynamically young cluster with no effective mass segregation is expected to have an A^+ closer to 0. With the progress in mass segregation, the value of A^+ increases (Lanzoni et al., 2016).

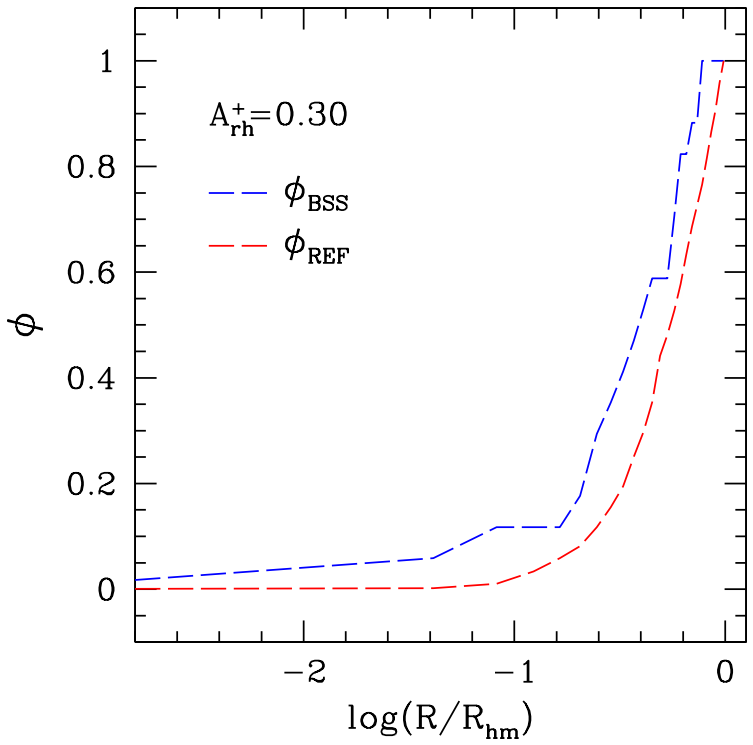

FIGURE 6.13: The figure shows the cumulative distributions of the blue straggler stars and the reference population in cluster NGC2213 in blue and red colour respectively. The corresponding A parameter is denoted in the figure.

To investigate the dynamical significance of the BSSs in the analysed clusters, we derived the A^+ parameter for them. The A^+ parameter is defined as:

$$A^+(x) = \int_{x_{min}}^{x} \phi_{BSS}(x')dx' - \int_{x_{min}}^{x} \phi_{REF}(x')dx', \tag{6.2}$$

where $x = log(R/R_{hm})$ and x_{min} is the minimum value that we sampled. We limited the analysis to stars within the R_{hm}. ϕ_{BSS} is the cumulative distribution of BSSs while ϕ_{REF} denotes the cumulative distribution of a reference population of stars with smaller masses. Consistent with the BSS fraction calculation, we adopted the MS stars in region A1 of the CMD as the reference population, as illustrated in Figure 6.4 for the cluster NGC 2213.

To account for the effect of field stars on the determination of A^+, we adopted a

method based on the distributions of 1,000 groups of BSSs and reference stars. To define each group, we first randomly associated each field-region star that populates the regions B1 and A1 of the CMD with a random position within the R_{hm} of the cluster. Then, we excluded them from the sample of BSSs and reference-population stars. We derived a value of A^+ by using the remaining stars. The best determination of A^+ and the corresponding uncertainty are provided by the respective mean and root mean square (RMS) of the 1,000 determinations.

Figure 6.12 shows the normalised radial distribution of the BSS fraction in the cluster NGC2213. Annular regions of analysis are the same as in the radial distribution of MS binary. Figure 6.13 demonstrates the corresponding cumulative distribution of the BSS population and the reference population. The $A+$ parameter is calculated from the relative difference in their distribution, within the R_{hm} of the cluster. The calculated A^+ parameters for the analysed MC GCs are listed in Table 6.1. A^+ ranges from a minimum of ~ -0.16 in cluster NGC 1783 to a maximum of 0.30 in cluster NGC 2213. Eleven out of the fourteen clusters have positive A^+ values. Moreover, we find a mild correlation between A^+ and the cluster dynamical age that yields a Spearman's rank correlation coefficient of 0.6. This finding would provide constraints on the origin of the candidate BSSs as well (e.g. Li et al., 2016), by supporting the binary formation scenario for the detected candidate BSSs in the analysed MC GCs.

6.5 Summary

The population of candidate BSSs was analysed in the studied 14 MC GCs. Their fraction was compared in terms of structural parameters and MS binary fraction

in the cluster. The dynamical implication of their radial distribution was explored using the A^+ parameter. The main results are summarised below;

- The core BSS fraction ranges from a minimum of 0.1 % in clusters NGC2108 and NGC1872 to a maximum of 4% in cluster NGC2213.
- The BSS fraction did not correlate with either age, metallicity, mass, or dynamical age of the cluster. However, clusters younger than $\sim$ 1Gyr are found unlikely to host BSSs.
- The fraction of BSSs did not show any correlation with MS binary fraction in the analysed clusters, similar to what has been observed in young Galactic OCs and unlike in old Galactic GCs.
- A^+ parameter is found to be positive for 11 of the 14 analysed MC GCs. Moreover, the values of the A^+ parameter show evidence of a mild correlation with the dynamical age of the clusters.

Chapter 7

Red clump binaries

7.1 Red clump stars

Red clump (RC) is one of the distinctive features observed in the CMD of intermediate age clusters and nearby galaxies (Girardi, 2016). Yet, studies focusing on RC stars are few in number and have started to emerge in only recent decades. Cannon (1970) was the first to recognize RC as a real CMD feature and a result of the post-Red Giant Branch (RGB) evolution of low-mass stars. Helium is converted to Carbon and Oxygen in their convective cores. The cores are surrounded by a radiative Hydrogen-burning shell that migrates outwards and an H-rich convective envelope. Because their core masses are very similar for a range of turnoff ages, the differences in their luminosity and effective temperature are constrained (Girardi, 2016). Though in the same evolutionary stage as the Horizontal branch (HB) stars, RC stars do not spread over a range of surface temperatures. They appear redder as an over-density in a spot close to the first ascent RGB, which was later termed as RC region (Cannon, 1970). Binarity and rotation are expected to

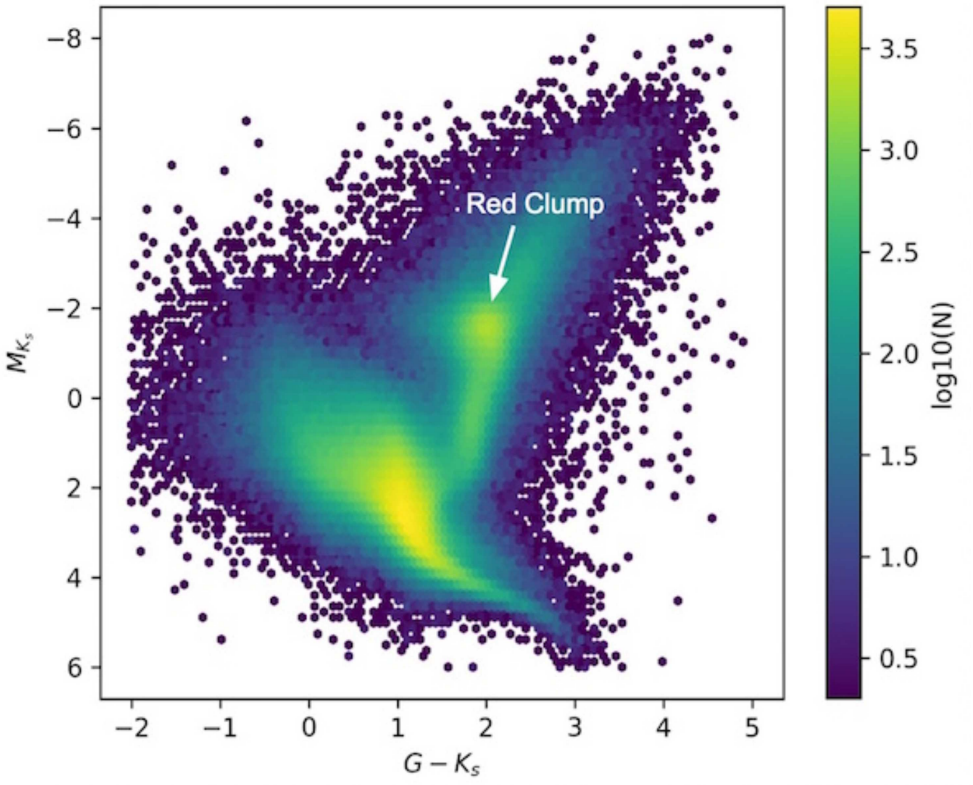

FIGURE 7.1: Color-magnitude diagram of stars with well-measured parallax, common to the TGAS and 2MASS catalogues (Hawkins et al., 2017). The diagram is colour-coded with the number of stars on a logarithmic scale.

bring other uncertainties in the position of stars in RC. However, their effects have not been investigated due to the unavailability of detailed models (Girardi, 2016).

The uniqueness and narrowness in the characteristics of RCs make them easily recognizable from spectroscopic and asteroseismic surveys such as Hipparcos, Gaia, or LSST. Figure 7.1 shows the CMD obtained using stars that have well-measured parallaxes in both Gaia survey-based Tycho-Gaia Astrometric Solutions (TAGS) and Two Micron All-Sky Survey (2MASS). They are quite abundant that about 30% of the red giants in any star-forming galaxies are expected to be in RC (Girardi et al., 2005). They are widely used to accurately measure different properties of the host cluster, such as kinematics and chemical abundances. The near consistency in the absolute magnitude of the RC stars, irrespective of their age or chemical

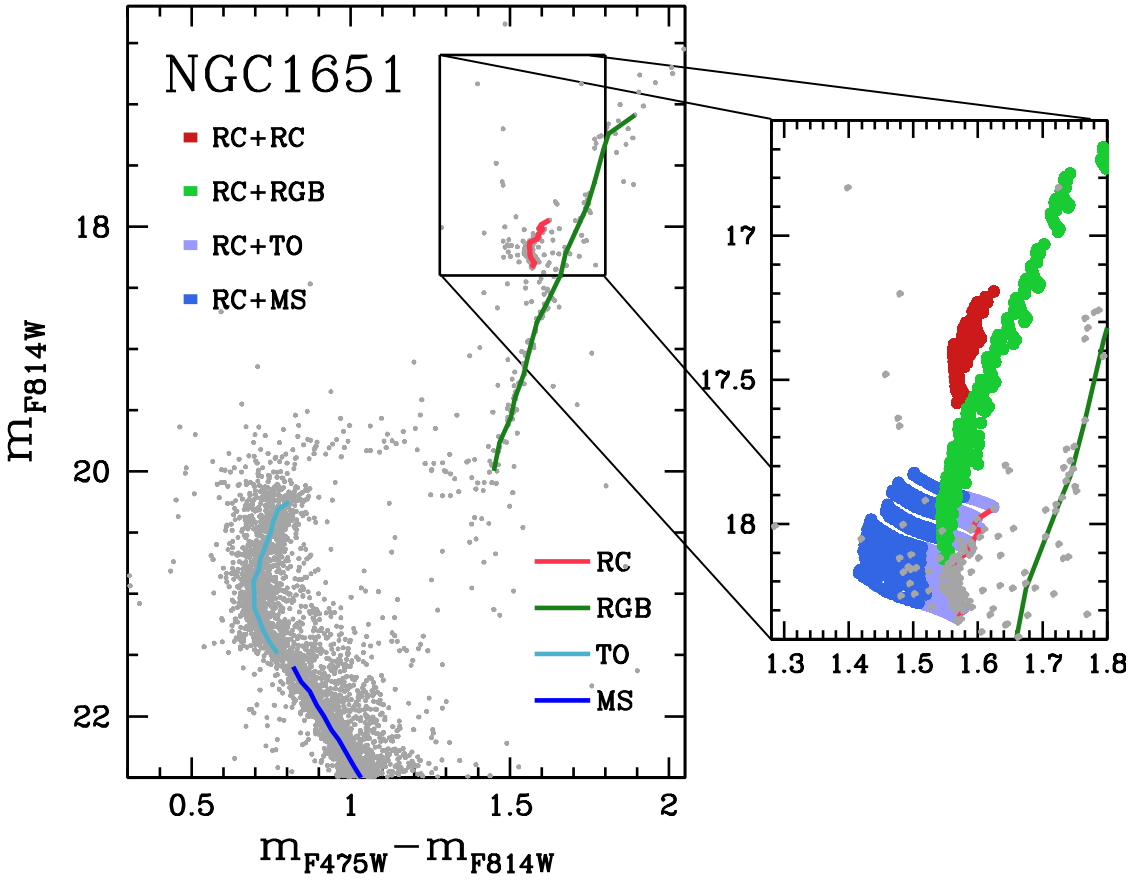

FIGURE 7.2: The CMD of the cluster NGC1651. Observed stars are denoted using grey points. Fiducial lines constructed from the red clump, main sequence, turn-off, and red giant branch stars are denoted in different colours, as indicated in the figure. Zoomed-in window highlights the position of simulated binaries constructed with red clump stars and a companion star. A companion star can be a star from a red clump, main sequence, turn-off, or red giant branch. The binary combinations are represented in different colours as indicated in the figure.

composition, has led to them being used as standard crayons to determine the true colour and reddening maps (Nidever et al., 2014; Nataf et al., 2016). They are also widely used as standard candles for astronomical distance measurements (Hawkins et al., 2017; Ting et al., 2018), particularly in MC and MW bulge. They are used to measure distances larger than what is measurable using white dwarfs. Near-infrared I band observations are found to be free of statistical uncertainties and offer more precise distance estimation than using giant stars.

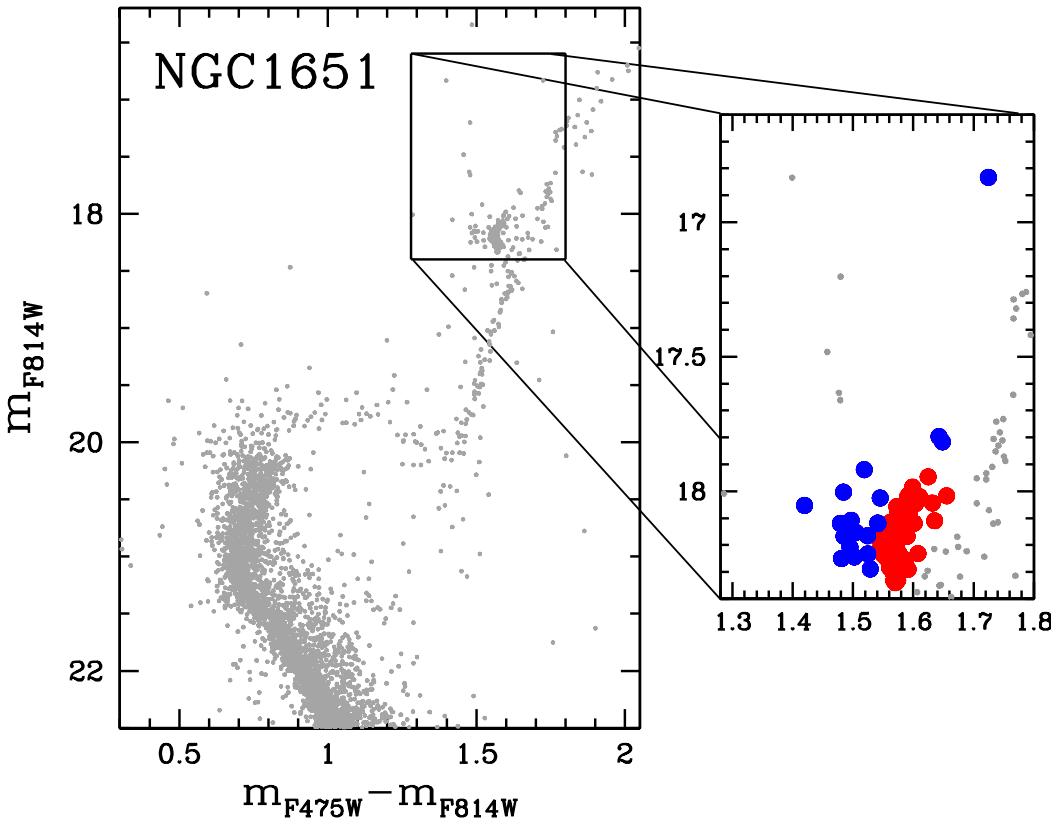

FIGURE 7.3: The CMD of the cluster NGC1651. The red clump region is zoomed in the right panel. The red clump stars are identified in red colour. The potential red clump binaries are denoted in blue.

7.2 Potential red clump binaries

MC clusters have well-constrained distances and foreground extinction. The large number of stars relative to the field and the availability of high-quality observations make them an ideal candidate for RC studies. High-quality HST observations used to study the MC clusters in this work ensured the visibility of RC stars in their CMDs, largely unaffected by photometric errors. Interestingly, a population of stars was consistently present in the region just above the RC region. To understand more about these populations, we have tried to characterise them as a function of cluster parameters and explored potential formation scenarios.

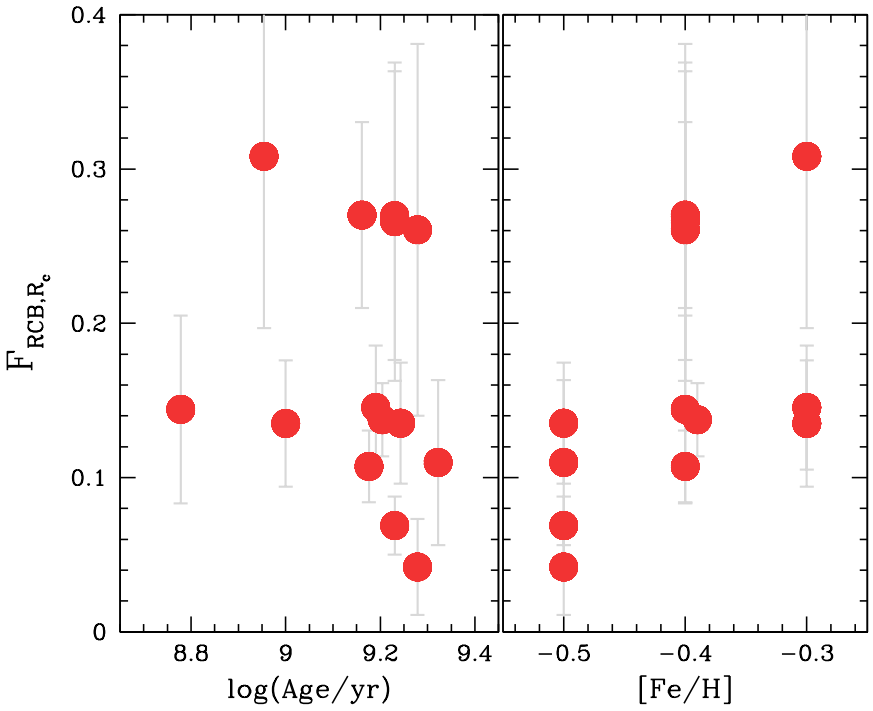

FIGURE 7.4: The plot shows variation of the red clump binary fraction within the cluster core, as a function of cluster age and metallicity.

Appearance of this population above the RC was compared with MS binary distribution for possible analogy. We have first explored the possibility of binaries consisting of two RC stars populating the above-mentioned region. However, the observed spread was not confined within the 0.7526 magnitude interval, as prescribed by Equation 4.1. To account for the binaries appearing outside this region, we have considered binaries with companion stars belonging to diverse evolutionary phases, such as TO, RGB, and MS. We have investigated their positions in the CMD by simulating such binaries. We constructed the fiducial lines corresponding to RC, RGB, TO, and MS regions of the CMD and randomly selected points from them to constitute a set of 1000 binaries in each combination. The magnitudes of resulting binaries are calculated using Equation 4.1 and are plotted in the CMD. The constructed fiducials and the position of binaries arising from different combinations are visualised in Figure 7.2. The considered four binary combinations

were found to span different non-exclusive regions above the RC region, as shown in the figure.

To quantify the population of these potential binaries, which will be referred to by the name potential RC binaries (RCBs) for the rest of the analysis, we have introduced a quantity called RCB fraction, F_{RCB}, which is the ratio of the number of RCBs to the number of RC stars in the cluster. F_{RCB} is calculated after accounting for the field star contamination in the region, following the method prescribed in Chapter 4. I have identified the RCBs under investigation and RC stars in the CMD of MC GC NGC1651 in Figure 7.3. I have denoted them in colours blue and red respectively.

F_{RCB} is calculated for different MC clusters analysed in this study and the results within the core radius and half mass radius are reported in Table 7.1. F_{RCB} within R_{hm} ranges from a minimum of 4 $\%$ in the cluster NGC1846 to a maximum of $\sim 20\%$ in the cluster KMHK316. The fraction is comparatively higher in the core, with a minimum of $\sim 4\%$ in NGC1718 and a maximum of $\sim 30\%$ in clusters KMHK316. Being massive, RCBs are more likely to undergo mass segregation towards the centre than RC stars. This mass segregation is expected to cause the observed increase in F_{RCB} within R_c compared to that within R_{hm} of the cluster.

We have investigated the effect of cluster parameters on the formation of the evolution of RCBs which may be reflected in the calculated F_{RCB}. Figure 7.4 demonstrates the variation of F_{RCB} within R_c as a function of the age and metallicity of the cluster. F_{RCB} shows no strong correlation with either age or metallicity of the clusters, as demonstrated by Spearman's rank correlation coefficient of -0.4 and 0.5 respectively. Within R_{hm}, the correlation coefficients are -0.3 and 0.4, respectively. On average, the clusters with higher F_{RCB} are found to have a higher dynamical age as well. Figure 7.5 shows the variation of F_{RCB} with the cluster's

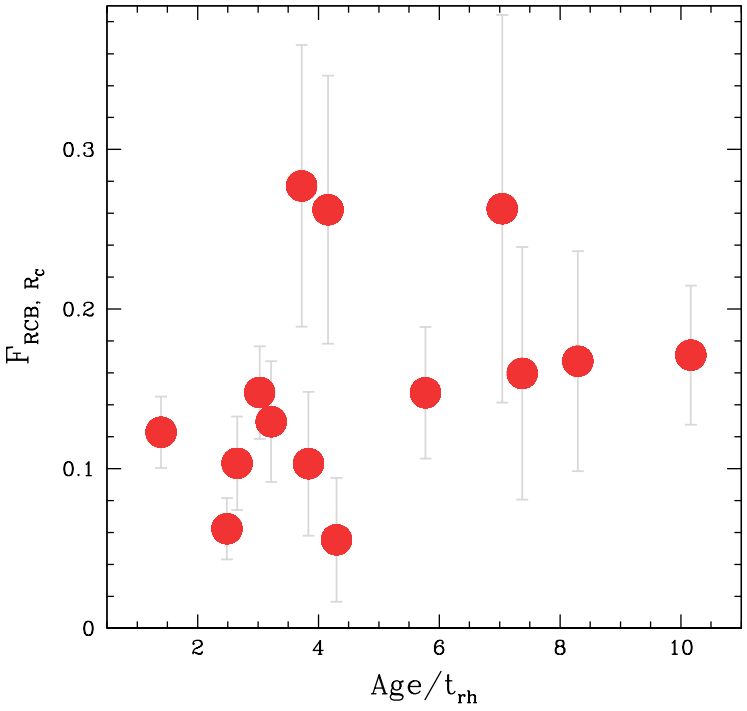

FIGURE 7.5: The plot shows the variation of the red clump binary fraction within the core as a function of the dynamical age of the cluster.

TABLE 7.1: Fraction of potential red clump binaries of the studied clusters.

Cluster ID	F_{RCB,R_c}	$F_{RCB,R_{hm}}$
ESO057SC075	0.261 ± 0.121	0.189 ± 0.079
ESO057SC030	0.110 ± 0.054	0.057 ± 0.040
KMHK316	0.308 ± 0.111	0.211 ± 0.064
NGC1651	0.270 ± 0.094	0.189 ± 0.062
NGC1718	0.042 ± 0.031	0.066 ± 0.027
NGC1751	0.135 ± 0.039	0.117 ± 0.030
NGC1783	0.138 ± 0.024	0.112 ± 0.019
NGC1806	0.107 ± 0.023	0.093 ± 0.022
NGC1846	0.069 ± 0.019	0.041 ± 0.010
NGC1868	0.270 ± 0.060	0.150 ± 0.034
NGC1872	0.144 ± 0.061	0.139 ± 0.053
NGC2108	0.135 ± 0.041	0.114 ± 0.031
NGC2203	0.145 ± 0.040	0.106 ± 0.027
NGC2213	0.266 ± 0.103	0.182 ± 0.052

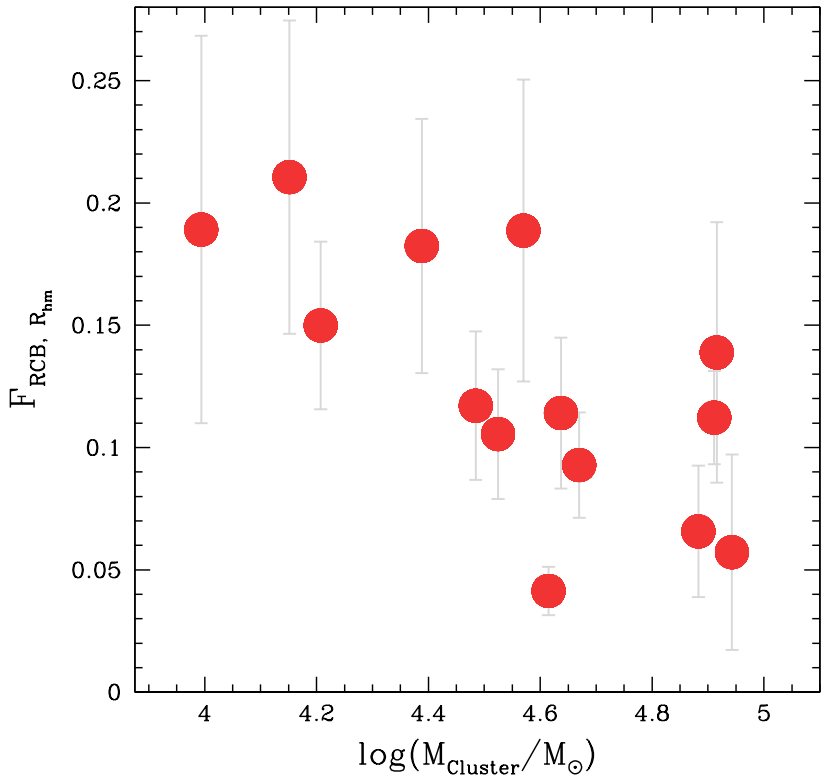

FIGURE 7.6: The plot shows the variation of the red clump binary fraction within the half mass radius of the cluster as a function of the cluster's mass.

dynamical age. They show evidence of a correlation with a Spearman's rank correlation coefficient of 0.7. The core BSS fraction shows an anti-correlation with the mass of the cluster with a correlation rank of -0.7 (Figure 7.6). In conclusion, the mass and dynamical age of the cluster appear to have the strongest contribution in driving the RCBs in the cluster where the former increases the fraction while the latter brings it down.

7.3 Potential red clump binaries: Origin

Though high-quality HST data of these bright stars largely eliminate such possibilities, photometric errors and blends may lead to the appearance of HB stars,

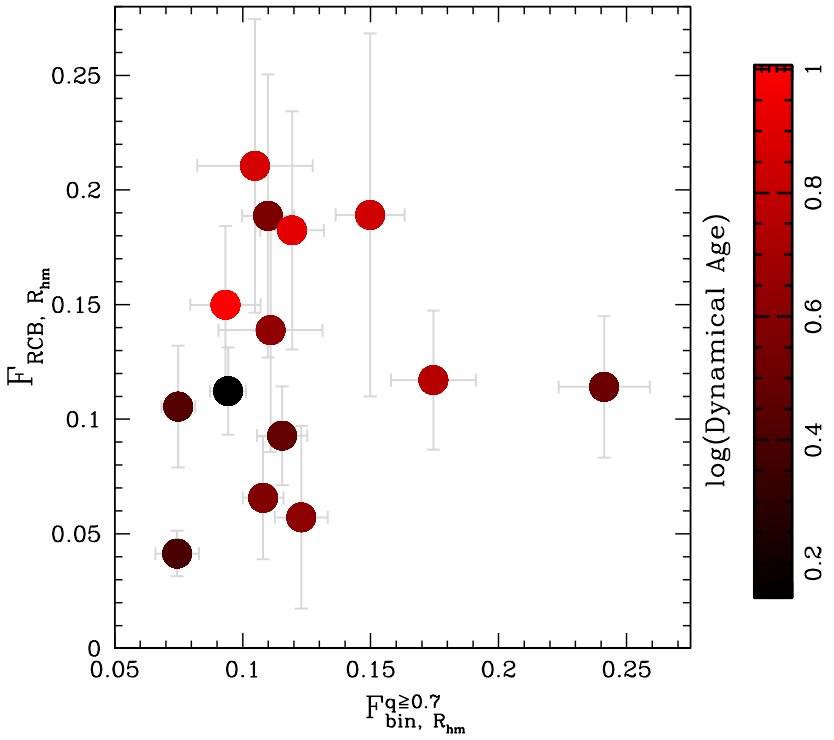

FIGURE 7.7: Variation of potential Red clump binary fraction with the global binary fraction with $q > 0.7$. The points are colour-coded according to the dynamical age of the cluster.

RGB stars, sub-giant branches, or even MSTO stars close to the RC regions. These stars may be related to the neighbouring RC stars with modifications made to their temperature and luminosity as a result of variations in their mass or metallicity. With the possibility of mass transfer and rotation, binarity in the life of RC stars can be a competing contributor to such behaviours. A non-contact binary system consisting of one or two RC stars and evolved BSSs formed out of mass transfer and/or collisions in binary systems are competing scenarios to explain the origin of this peculiar population of stars.

7.3.1 Potential red clump binaries and MS binaries

A non-contact binary system consisting of RC stars may be responsible for the observed stellar population above the RC region. Binary systems may be formed with two RC stars or one RC star with a companion belonging to other evolutionary stages such as MSTO, giants, or MS. The possibility that these binary systems evolved from the MS binary population in the cluster where each companion star evolved separately into an RC star is interesting and can be investigated in this study. To investigate the potential relation connecting the two, F_{RCB} is explored as a function of the F_{bin} calculated in Chapter 4.

Figure 7.7 demonstrates the variation of RCB fraction with respect to MS binary fraction. With Spearman's correlation rank coefficient of 0.2, F_{RCB} shows no evidence of a correlation with F_{bin} within the half-mass radius of the cluster. This may indicate a potential evolutionary connection between MS binaries and RCBs. However, the correlation was less significant within the core of the cluster, with a Spearman's rank correlation coefficient of 0, the distribution is flat. This may be due to the stronger and more frequent interactions in the core which often leads to binary disruption. The points in the figure are colour-coded according to the dynamical age of the cluster on a logarithmic scale. However, no clear distinction can be observed in the distribution of points in terms of the relaxation state of the clusters.

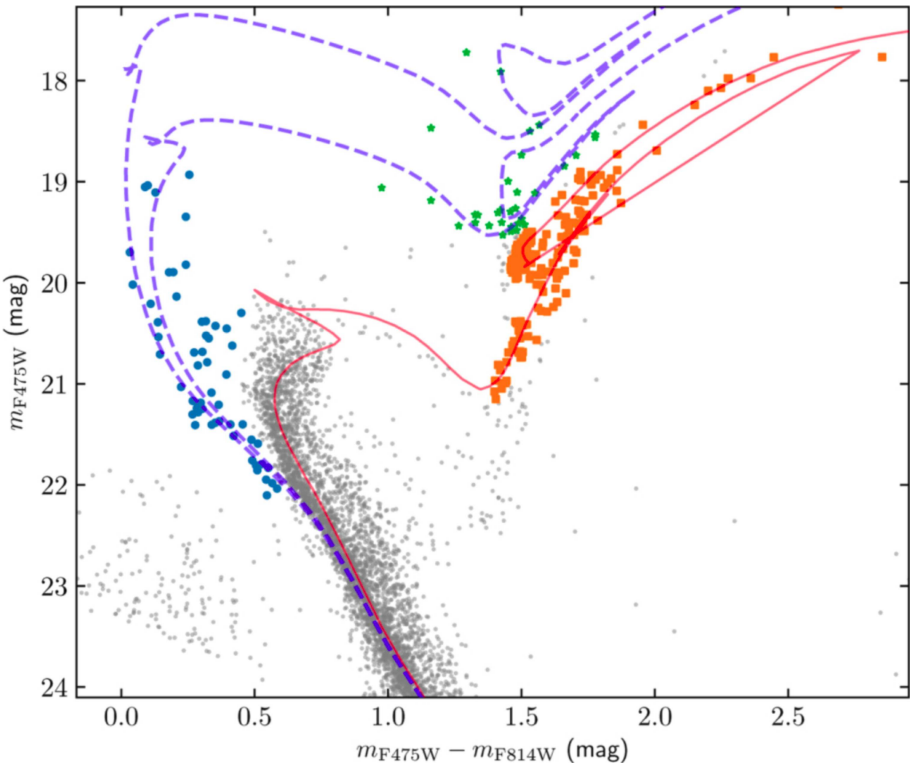

FIGURE 7.8: The colour-magnitude-diagram of the LMC cluster NGC2173. The position of Blue straggler stars (in blue), evolved Blue straggler stars (in green), and giant stars (in orange) are denoted. The orange solid line denotes the best-fitting isochrone for the cluster and the blue dashed lines denote the isochrones for younger populations (Sun et al., 2018).

7.3.2 Potential red clump binaries and evolved blue straggler stars

Binaries with mass transfer are also explored for their potential relation with RCBs. BSSs have evolutionary scenarios linked with binary mass transfer and collisions and they have a significant population in analysed MC clusters. Studies post-MS evolution using collisional models have shown that the BSSs in advanced evolutionary stages, known as evolved BSSs (eBSSs), can appear quite close to the RC region in the CMD (Sills et al., 2009). By accounting for the observed ratio between BSSs and eBSSs in different clusters, they suggest a lifetime of 1-2 Gyr for the BSSs. Figure 7.8 shows the CMD of the LMC cluster NGC2213 with its

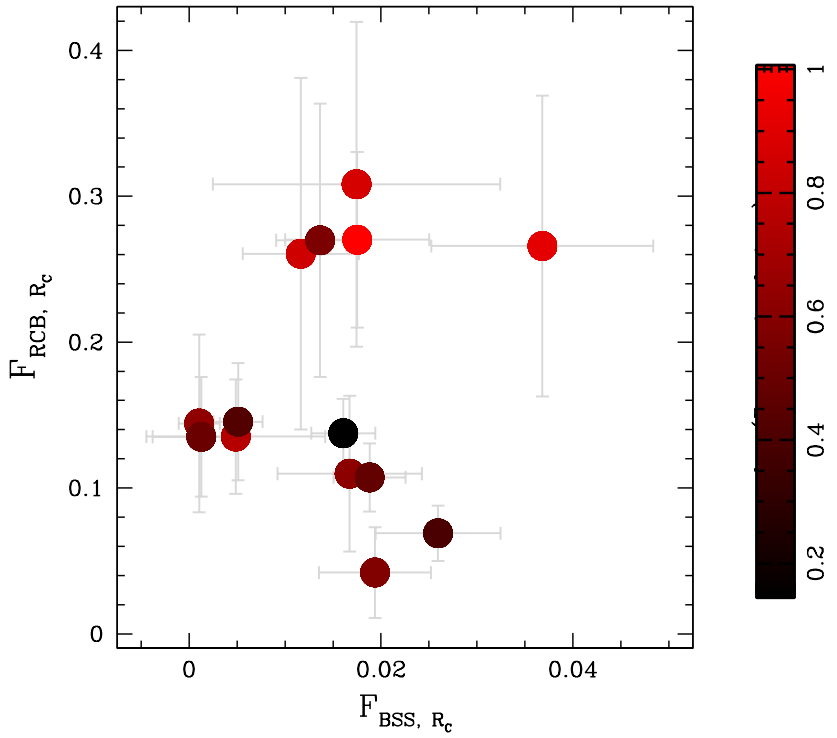

FIGURE 7.9: The plot demonstrates the relation between the fraction of potential red clump binaries and the fraction of blue straggler stars in a cluster. The points are colour-coded following the dynamical age of the cluster.

BSSs, eBSSs, and some giant stellar populations (RGB and RC) which are identified in different colours (Sun et al., 2018). The orange solid line denotes the best-fitting isochrone for the cluster and the blue dashed lines denote the isochrones for younger populations. A concentration of eBSSs can be seen in the RCB region.

To understand the effect of eBSSs on F_{RCB} in the present dataset, we have plotted F_{RCB,R_c} as a function of F_{BSS,R_c}, which is taken as a proxy for eBSSs in the cluster. Figure 7.9 demonstrates that there is no evidence of correlations between them. The points in Figure 7.9 are colour-coded with the dynamical age of the cluster on a logarithmic scale. The clusters with higher dynamical ages tend to have higher $F_{RCB,R_{hm}}$. The observed lack of correlation questions the previous assumption regarding contamination of RCB region by eBSSs. Analysed MC clusters are younger

compared to the expected lifetime of BSSs. Hence, they may not host a significant number of eBSSs to produce a strong correlation.

7.4 Summary

A stellar population, termed RCBs, has been identified in a region above the RC stars in the analysed MC GCs. I have quantified their number and explored the potential scenarios of their origin, particularly the ones connected to binary stars. The findings can be summarised as follows;

- The fraction of RCBs ranges from a minimum of 4 $\%$ in clusters NGC1846 to a maximum of $\sim 20\%$ in KMHK316, within R_{hm} of the clusters. The fraction in the core has a minimum of $\sim$ 4% in NGC1718 and a maximum of $\sim$ 30% in clusters KMHK316.
- Although the fraction did not show any strong correlation with either age or metallicity of the cluster, it was observed to vary with the mass and dynamical age of the cluster. With a Spearman's rank correlation coefficient of 0.7, the RCB fraction was found to increase with the dynamical age of the cluster. However, an increase in cluster mass is associated with a decrease in RCB fraction, as clarified by Spearman's correlation rank of -0.7 respectively.
- The RCB fraction in the clusters did not show any strong correlation with either the fraction of binaries or BSSs in the cluster.

Any strong conclusion regarding the origin of RCBs has not been achieved in this study. Detailed studies considering different formation scenarios are needed to shed light on this peculiar population.

Chapter 8

Summary and Conclusions

From promoting alternate stellar evolution scenarios to detecting accurate masses, binaries shed light on a multitude of phenomena in astronomy. With their higher masses and higher interaction cross sections, binaries play a major role in kinetic energy distribution, mass segregation, and the production of exotic objects, among others, in star clusters. Information regarding the fraction and distribution of binaries is needed in calculating several structural and dynamical parameters of the cluster. A proper understanding of binarity facilitates a glimpse into their dynamical and chemical evolution. To extend our understanding of the same, we have dwelled on the population of MS binaries and related stellar populations in 14 MC GCs in this thesis.

We used high-precision data collected with the WFC3/UVIS and ACS/WFC cameras on board *HST* to investigate the same. The studied cluster spanned a wide age and density range and a mass range that is not spanned by the Galactic clusters. Moreover, we determined the structure parameters of the star clusters, including the core radius, half mass radius, and central density, and estimated the mass function and the total mass of the cluster by fitting the density profile with an EFF

profile.

Binary fraction in star clusters

Binary fraction analysis depends on different detection methods that are specific to the type of binaries under study. The photometric analysis relies on the combined flux of the unresolved companion stars in a binary and their feasible identification in the CMD of a star cluster. They are suitable for non-interacting systems such as the binaries comprised of two MS stars with a head-on view. In this work, the MS binary fraction in young and intermediate-age MC GCs is successfully computed within core and half mass radii of the cluster, for mass ratios greater than 0.7, and 0.6 whenever possible. The selected clusters span a mass interval unexplored in the Galactic cluster. Fraction has been subjected to corrections for field star contamination, scattering effects, and incompleteness of the data set. The distribution of binary fraction with respect to different stellar and cluster parameters is investigated and the obtained results were compared to the homogeneous studies on Galactic OCs and GCs. The main results on binaries can be summarised as follows,

- Within half mass radius and for a mass-ratio greater than 0.7, the fraction ranges from $\sim$ 7% in NGC1846 to more than $\sim$ 24% in NGC2108. These values correspond to a total binary fraction between $\sim$ 20% and 70%, by assuming a flat mass-ratio distribution. We obtain similar results for the binaries in the cluster cores.

- When we combine the results from all clusters, we find no evidence for correlations between the fraction of binaries and either the mass of the primary star or the mass ratio. However, we notice various remarkable exceptions. As an example, the binary fraction decreases towards large stellar masses in

NGC 2108, while NGC 1806 follows a flat distribution. Moreover, NGC 1718, NGC 2203, and NGC 2213 exhibit a predominance of binaries with large mass ratios, whereas the fractions in NGC1651 and NGC1846 are distributed homogeneously. The obtained results are in agreement with homogeneous studies on Galactic OCs (Cordoni et al., 2023) and GCs (Milone et al., 2012).

- There is no evidence for significant differences in the radial distribution of binaries in most studied clusters. However, in clusters that are significantly older in comparison to their t_{rh}, the binaries are more centrally concentrated than single stars as observed in the case of Galactic GCs (Milone et al., 2012). Dynamically younger clusters demonstrate a flat distribution. Homogeneous studies on Galactic OCs (Cordoni et al., 2023) have also observed a difference in the radial distribution of binaries depending on the age of the cluster.

Comparison with Galactic clusters

We have combined results on MC clusters with those by a recent paper where we have performed a similar analysis on 78 Galactic OCs (Cordoni et al., 2023) and with results on 67 Galactic GCs (Milone et al., 2012, 2016). In total, binaries have been now homogeneously studied in 159 star clusters.

The fraction of binaries was found to not correlate with either the cluster age or with the dynamical age. Conversely, we find a significant anti-correlation between the fraction of binaries in the core and the mass of the host cluster. This observation is supported by theoretical models by Sollima (2008) which suggest the energy and rate of collisions in the core increases with the mass of the cluster which in turn accelerates the binary disruption processes happening there. Our

observations agree with the conclusions of Sollima et al. (2010) that binary disruption processes are the dominant factor in determining the binary fraction in star clusters.

However, clusters with similar masses exhibit a range of binary fractions that is wider than the observational errors. As an example, the star clusters studied in this work typically host higher binary fractions than the Galactic GCs with similar masses. This fact indicates that at least another parameter, in addition to cluster mass, has an influence on the fraction of binaries in the core.

Blue straggler stars

Out of the several exotic objects present in the GCs, BSS are the most populous and they have evolutionary links with MS binaries. We have studied the BSS population in the analysed MC GCs. Their fraction is quantified with respect to a reference population selected in one magnitude bin of filter F814W in the upper MS. Their fraction was compared in terms of the structural parameters of the cluster and the MS binary fraction present within. The dynamical implication of their radial distribution was explored using the A^+ parameter, as prescribed in Lanzoni et al. (2016).

The BSS fraction in the core was found to range from a minimum of 0.1% in clusters NGC2108 and NGC1872 to a maximum of 4 % in cluster NGC2213. It did not show any strong correlation with physical parameters of the cluster such as age, metallicity, mass, or dynamical age of the cluster. However, clusters younger than $\sim$ 1Gyr are found unlikely to host BSSs. However, the A^+ parameter shows

evidence of mild correlation with the dynamical age of the clusters. The A^+ parameter is found to be positive for 11 of the 14 analysed clusters denoting the segregation of BSSs relative to a reference population.

There is no correlation between the fraction of binaries and the fraction of candidate BSSs in the analysed MC GCs of young and intermediate age and intermediate masses. The results are in agreement with homogeneous studies done on young and less massive Galactic OCs (Cordoni et al., 2023) and are contrary to observations in the case of old and massive Galactic GCs (Milone et al., 2012).

Potential red clump binaries

A population of stars was identified above the RC region in the analysed clusters. Their fraction was determined, for the first time, with respect to the RC stars in the clusters. The fraction is further explored with respect to different cluster parameters. To shed light on their formation scenarios, non-contact binary systems with one or more RC stars which may have evolutionary links with MS binaries and contact systems leading to the production of objects such as BSSs were considered.

Their fraction was found to range from a minimum of 4% in the cluster NGC1846 to a maximum of $\sim$ 20% in KMHK316, within the half-mass radius of the clusters. Within the cluster core, the fraction ranges from a minimum of 4% in the cluster NGC1718 to a maximum of $\sim$ 30% in KMHK316. The fraction did not show any strong correlation with either age or metallicity of the cluster. However, the fraction showed evidence of correlation with dynamical age and anti-correlation with the mass of the cluster.

The fraction did not show any evidence of correlation with MS binary fraction or with BSS fraction in the clusters. In the absence of any strong correlation, the

questions regarding their formation scenarios remain unanswered. More studies are required to better understand the origin and evolution of these systems.

Exploring lower mass-ratio binaries with Chromosome map of binaries

This thesis introduces a unique method called the 'Chromosome map of binaries', which provides a better way to separate binaries with varying mass ratios. This method is particularly effective in resolving binaries of lower mass ratios from the single stars in MSFL and in optimising the separation between higher mass-ratio binaries. The availability of ultraviolet, optical, and infrared data sets from telescopes such as the JWST and HST is quite promising for this strategy. I intend to employ this method in the future to investigate the complete mass-ratio distributions in MW and MC clusters. This allows us to approach the complete MS binary fraction in the cluster.

Future work

Though much has been studied about binaries, much more is left to be explored. We have explored the areas of MS binaries and the BSS population in this thesis. However, certain areas require further exploration. Particularly, the thesis draws research focus into the following areas.

1. The chromosome map put forward in this thesis is one area that is quite promising for future studies on binaries and stellar populations in star clusters. We require a multi-wavelength exploration to dwell in the regime of lower mass binaries. Data from JWST and upcoming space telescopes will be quite advantageous for these studies.

2. Though we explored the peculiar population spotted over RC of the CMD, their formation scenarios are yet to be constrained. Extension of the study on candidate RC binaries into more clusters and comparing them with state-of-the-art models of binaries with evolved companion stars are essential for a comprehensive understanding.

3. Binaries with companion stars in different evolutionary stages are another area that offers a lot of potential for future studies. We have explored the region of occurrence of binaries formed out of stars from RC, MSTO, RGB, and MS part of the CMD (refer to Figure 7.2). However, models and simulations are required to account for the complex interactions between the evolved companions and verify the predictions based on the observational and numerical approaches. Such approaches will better constrain the position of such binaries in CMD and facilitate a better understanding of their fraction.

An accurate binary fraction determination holds immense gravity in stellar and cluster studies. More research on extragalactic clusters will undoubtedly aid future efforts in that direction. Studying binaries in lower mass ranges and at different phases of evolution would considerably improve our understanding of cluster evolution. More studies are needed regarding stellar populations associated with binaries, aside from BSSs. Adopting homogeneous analytic methodologies will assist in efficiently comparing distinct studies. With new and upcoming telescopes and enhanced data reduction techniques, the scope of the proposed study is certain to expand. Robust multi-wavelength studies of binaries are sure to emerge, revealing many secrets about these fascinating objects.

List of Publications

Articles Published in International Journals

1. Photometric binaries in 14 Magellanic Cloud star clusters

   - Mohandasan, A., A. P. Milone, G. Cordoni, E. Dondoglio, E. P. Lagioia, M. Vittoria Legnardi, T. Ziliotto, S. Jang, A. F. Marino & M. Carlos, 2024, 681, A42

2. Photometric binaries, mass functions, and structural parameters of 78 Galactic open clusters

   - Milone, A. P., G. Cordoni, A. F. Marino, F. D'Antona, A. Bellini, M. Di Criscienzo, E. Dondoglio, E. P. Lagioia, N. Langer, M. V. Legnardi, M. Libralato, H. Baumgardt, M. Bettinelli, Y. Cavecchi, R. de Grijs, L. Deng, B. Hastings, C. Li, A. Mohandasan, A. Renzini, E. Vesperini, C. Wang, T. Ziliotto, M. Carlos, G. Costa, F. Dell'Agli, S. Di Stefano, S. Jang, M. Martorano, M. Simioni, M. Tailo, & P. Ventura, 2023, A&A, 672, A161

3. Hubble Space Telescope survey of Magellanic Cloud star clusters. Photometry and astrometry of 113 clusters and early results

   - Milone, A. P., G. Cordoni, A. F. Marino, F. Muratore, F. D'Antona, M. Di Criscienzo, E. Dondoglio, E. P. Lagioia, M. V. Legnardi, A. Mohandasan, T. Ziliotto, F. Dell'Agli, M. Tailo, & P. Ventura, 2023, MNRAS, 524, 6149

4. Hubble Space Telescope survey of Magellanic Cloud star clusters: UV-dim stars in young clusters

   - Milone, A. P., G. Cordoni, A. F. Marino, F. Muratore, F. D'Antona, M. Di Criscienzo, E. Dondoglio, E. P. Lagioia, M. V. Legnardi, A. Mohandasan, T. Ziliotto, F. Dell'Agli, M. Tailo, & P. Ventura, 2023, MNRAS, 524, 6149

5. NGC1818 unveils the origin of the extended main-sequence turn-off in young Magellanic Clouds clusters

   - Cordoni, G., A. P. Milone, A. F. Marino, M. Cignoni, E. P. Lagioia, M. Tailo, M. Carlos, E. Dondoglio, S. Jang, A. Mohandasan, & M. V. Legnardi, 2022, NatCo, 13, 4325

6. Differential reddening in the direction of 56 Galactic globular clusters

   - Legnardi, M. V., A. P. Milone, G. Cordoni, E. P. Lagioia, E. Dondoglio, A. F. Marino, S. Jang, A. Mohandasan, & T. Ziliotto, 2023, MNRAS, 522, 367

7. Mass-loss law for red giant stars in simple population globular clusters

   - Tailo, M., A. P. Milone, E. P. Lagioia, F. D'Antona, S. Jang, E. Vesperini, A. F. Marino, P. Ventura, V. Caloi, M. Carlos, G. Cordoni, E. Dondoglio, A. Mohandasan, J. E. Nastasio, & M. V. Legnardi, 2021, MNRAS, 503, 694

8. Constraining the original composition of the gas forming first-generation stars in globular clusters

   - Legnardi, M. V., A. P. Milone, L. Armillotta, A. F. Marino, G. Cordoni, A. Renzini, E. Vesperini, F. D'Antona, M. McKenzie, D. Yong, E. Dondoglio, E. P. Lagioia, M. Carlos, M. Tailo, S. Jang, & A. Mohandasan, 2022, MNRAS, 513, 735

9. Multiple Stellar Populations in Metal-poor Globular Clusters with JWST: A NIRCam View of M92

   - Ziliotto, T., A. Milone, A. F. Marino, A. L. Dotter, A. Renzini, E. Vesperini, A. Karakas, G.

Cordoni, E. Dondoglio, M. V. Legnardi, E. P. Lagioia, A. Mohandasan, & S. Baimukhametova, 2023, ApJ, 953, 62

10. Multiple stellar populations in globular clusters with JWST: an NIRCam view of 47 Tucanae

    - Milone, A. P., A. F. Marino, A. Dotter, T. Ziliotto, E. Dondoglio, G. Cordoni, S. Jang, E. P. Lagioia, M. V. Legnardi, A. Mohandasan, M. Tailo, D. Yong, S. Baimukhametova, & M. Carlos, 2023, MNRAS, 522, 2429

11. Multiple stellar populations found outside the tidal radius of NGC 1851 via Gaia DR3 XP spectra

    - Cordoni, G., A. F. Marino, A. P. Milone, E. Dondoglio, E. P. Lagioia, M. V. Legnardi, A. Mohandasan, S. Jang, & T. Ziliotto, 2023, A&A, 678, A155

12. Integrated Photometry of Multiple Stellar Populations in Globular Clusters

    - Jang, S., A. P. Milone, E. P. Lagioia, M. Tailo, M. Carlos, E. Dondoglio, M. Martorano, A. Mohandasan, A. F. Marino, G. Cordoni, & Y.-W. Lee, 2021, ApJ, 920, 129

13. Chromosome maps of globular clusters from wide-field ground-based photometry

    - Jang, S., A. P. Milone, M. V. Legnardi, A. F. Marino, A. Mastrobuono-Battisti, E. Dondoglio, E. P. Lagioia, L. Casagrande, M. Carlos, A. Mohandasan, G. Cordoni, E. Bortolan, & Y.-W. Lee, 2022, MNRAS, 517, 5687

14. A deep dive into the Type II globular cluster NGC 1851

    - Dondoglio, E., A. P. Milone, A. F. Marino, F. D'Antona, G. Cordoni, M. V. Legnardi, E. P. Lagioia, S. Jang, T. Ziliotto, M. Carlos, F. Dell'Agli, A. Karakas, A. Mohandasan, Z. Osborn, M. Tailo, & P. Ventura, 2023, MNRAS, 526, 2960

15. Survey of Multiple Populations in Globular Clusters among Very-low-mass Stars

- Dondoglio, E., A. P. Milone, A. Renzini, E. Vesperini, E. P. Lagioia, A. F. Marino, A. Bellini, M. Carlos, G. Cordoni, S. Jang, M. V. Legnardi, M. Libralato, A. Mohandasan, F. D'Antona, M. Martorano, F. Muratore, & M. Tailo, 2022, ApJ, 927, 207

16. The chemical compositions of multiple stellar populations in the globular cluster NGC 2808

    - Carlos, M., A. F. Marino, A. P. Milone, E. Dondoglio, S. Jang, M. V. Legnardi, A. Mohandasan, G. Cordoni, E. P. Lagioia, A. M. Amarsi, & H. Jerjen, 2023, MNRAS, 519, 1695

Presentations and Proceedings in International Conferences

1. **Contributed talk at the EAS 2023**: Photometric Binaries in Extragalactic Star Clusters.

   The annual meeting of the European Astronomical Society (EAS) of the year 2023, was conducted at the ICE congress center in Krakow from 10-14 July.

   Link: https://eas.unige.ch/EAS2023/

2. **Contributed talk at MPA**: Photometric Binaries in Extragalactic Star Clusters.

   The conference titled 'The Impact of Binaries on Stellar Evolution' was held at Max Plank Institute for Astrophysics (MPA), Garching from 14-18 Nov 2022.

   Link: https://indico.ph.tum.de/event/7022/

3. **Contributed talk**: Photometric Binaries in Magellanic Cloud Globular Clusters.

   The conference titled 'A Multiwavelength View on Globular Clusters Near and Far: From JWST to the ELT' organized at Sexten from 3-7 July 2023.

   Link: https://www.sexten-cfa.eu/event/a-multi-wavelength-view-on-globular-clusters-near-and-far-from-jwst-to-the-elt/

4. **Contributed talk**: Photometric Binaries in Galactic and Extragalactic Globular Clusters.

   The conference titled 'Wheel of Star Formation' was held at the Charles University, Prague from 12-16 September 2022.

   Link: https://janfest2022.asu.cas.cz/

List of Tables

List of Figures

References

Aarseth, S. J. and Hills, J. G. (1972). The Dynamical Evolution of a Stellar Cluster with Initial Subclustering. *A&A*, 21:255.

Alessandrini, E., Lanzoni, B., Ferraro, F. R., Miocchi, P., and Vesperini, E. (2016). Investigating the Mass Segregation Process in Globular Clusters with Blue Straggler Stars: The Impact of Dark Remnants. *ApJ*, 833(2):252.

Alves, F. O., Caselli, P., Girart, J. M., Segura-Cox, D., Franco, G. A. P., Schmiedeke, A., and Zhao, B. (2019). Gas flow and accretion via spiral streamers and circumstellar disks in a young binary protostar. *Science*, 366(6461):90–93.

Anderson, J. and Bedin, L. R. (2010). An Empirical Pixel-Based Correction for Imperfect CTE. I. HST's Advanced Camera for Surveys. *PASP*, 122(895):1035.

Anderson, J. and King, I. R. (2000). Toward High-Precision Astrometry with WFPC2. I. Deriving an Accurate Point-Spread Function. *PASP*, 112(776):1360–1382.

Anderson, J. and King, I. R. (2006). PSFs, Photometry, and Astronomy for the ACS/WFC. Instrument Science Report ACS 2006-01, 34 pages.

Anderson, J., Sarajedini, A., Bedin, L. R., King, I. R., Piotto, G., Reid, I. N., Siegel, M., Majewski, S. R., Paust, N. E. Q., Aparicio, A., Milone, A. P., Chaboyer, B.,

and Rosenberg, A. (2008). The Acs Survey of Globular Clusters. V. Generating a Comprehensive Star Catalog for each Cluster. *AJ*, 135(6):2055–2073.

Andronov, N., Pinsonneault, M. H., and Terndrup, D. M. (2006). Mergers of Close Primordial Binaries. *ApJ*, 646(2):1160–1178.

Aparicio, A., Bertelli, G., Chiosi, C., and Garcia-Pelayo, J. M. (1991). CCD UBVR photometry of two open clusters : King 11 and Be 42. Comparison with theoretical models. *Astronomy and Astrophysics, Supplement*, 88:155.

Battinelli, P. and Capuzzo-Dolcetta, R. (1991). Formation and evolutionary properties of the galactic open cluster system. *MNRAS*, 249:76.

Baumgardt, H. and Hilker, M. (2018). A catalogue of masses, structural parameters, and velocity dispersion profiles of 112 Milky Way globular clusters. *MNRAS*, 478(2):1520–1557.

Beccari, G., Dalessandro, E., Lanzoni, B., Ferraro, F. R., Sollima, A., Bellazzini, M., and Miocchi, P. (2013). Deep Multi-telescope Photometry of NGC 5466. I. Blue Stragglers and Binary Systems. *ApJ*, 776(1):60.

Bellini, A., Anderson, J., and Bedin, L. R. (2011). Astrometry and Photometry with HST WFC3. II. Improved Geometric-Distortion Corrections for 10 Filters of the UVIS Channel. *PASP*, 123(903):622.

Bellini, A., Anderson, J., Bedin, L. R., King, I. R., van der Marel, R. P., Piotto, G., and Cool, A. (2017). The State-of-the-art HST Astro-photometric Analysis of the Core of ω Centauri. I. The Catalog. *ApJ*, 842(1):6.

Bolte, M. (1992). CCD Photometry in the Globular Cluster NGC 288. I. Blue Stragglers and Main-Sequence Binary Stars. *Astrophysical Journal, Supplement*, 82:145.

Bressan, A., Marigo, P., Girardi, L., Salasnich, B., Dal Cero, C., Rubele, S., and Nanni, A. (2012). PARSEC: stellar tracks and isochrones with the PAdova and TRieste Stellar Evolution Code. *MNRAS*, 427(1):127–145.

Cadelano, M., Ferraro, F. R., Dalessandro, E., Lanzoni, B., Pallanca, C., and Saracino, S. (2022). Discovery of a Double Sequence of Blue Straggler Stars in the Core-collapsed Globular Cluster NGC 6256. *ApJ*, 941(1):69.

Cannon, R. D. (1970). Red giants in old open clusters. *MNRAS*, 150:111.

Chen, X. and Han, Z. (2008). Binary coalescence from case A evolution: mergers and blue stragglers. *MNRAS*, 384(4):1263–1276.

Cool, A. M., Grindlay, J. E., Cohn, H. N., Lugger, P. M., and Slavin, S. D. (1995). Discovery of Candidate Cataclysmic Variables in the Post–Core-Collapse Globular Cluster NGC 6397. *ApJ*, 439:695.

Cordoni, G., Milone, A. P., Marino, A. F., Cignoni, M., Lagioia, E. P., Tailo, M., Carlos, M., Dondoglio, E., Jang, S., Mohandasan, A., and Legnardi, M. V. (2022). NGC1818 unveils the origin of the extended main-sequence turn-off in young Magellanic Clouds clusters. *Nature Communications*, 13:4325.

Cordoni, G., Milone, A. P., Marino, A. F., Vesperini, E., Dondoglio, E., Legnardi, M. V., Mohandasan, A., Carlos, M., Lagioia, E. P., Jang, S., and Ziliotto, T. (2023). Photometric binaries, mass functions, and structural parameters of 78 Galactic open clusters. *A&A*, 672:A29.

Dalessandro, E., Ferraro, F. R., Bastian, N., Cadelano, M., Lanzoni, B., and Raso, S. (2019). The double blue-straggler sequence in NGC 2173: an artifact of field contamination. *A&A*, 621:A45.

Dalessandro, E., Ferraro, F. R., Massari, D., Lanzoni, B., Miocchi, P., and Beccari, G. (2015). No Evidence of Mass Segregation in the Low-mass Galactic Globular Cluster NGC 6101. *ApJ*, 810(1):40.

Dalessandro, E., Lanzoni, B., Beccari, G., Sollima, A., Ferraro, F. R., and Pasquato, M. (2011). The Binary Fraction in the Globular Cluster M10 (NGC 6254): Comparing Core and Outer Regions. *ApJ*, 743(1):11.

Dalessandro, E., Lanzoni, B., Ferraro, F. R., Rood, R. T., Milone, A., Piotto, G., and Valenti, E. (2008). Blue Straggler Stars in the Unusual Globular Cluster NGC 6388. *ApJ*, 677(2):1069–1079.

Dondoglio, E., Milone, A. P., Renzini, A., Vesperini, E., Lagioia, E. P., Marino, A. F., Bellini, A., Carlos, M., Cordoni, G., Jang, S., Legnardi, M. V., Libralato, M., Mohandasan, A., D'Antona, F., Martorano, M., Muratore, F., and Tailo, M. (2022). Survey of Multiple Populations in Globular Clusters among Very-low-mass Stars. *ApJ*, 927(2):207.

Dorn-Wallenstein, T. Z. and Levesque, E. M. (2020). A Comparison of Rotating and Binary Stellar Evolution Models: Effects on Massive Star Populations. *ApJ*, 896(2):164.

Dotter, A. (2016). MESA Isochrones and Stellar Tracks (MIST) 0: Methods for the Construction of Stellar Isochrones. *Astrophysical Journal, Supplement*, 222(1):8.

Dotter, A., Chaboyer, B., Jevremović, D., Kostov, V., Baron, E., and Ferguson, J. W. (2008). The Dartmouth Stellar Evolution Database. *Astrophysical Journal, Supplement*, 178(1):89–101.

Dotter, A., Sarajedini, A., Anderson, J., Aparicio, A., Bedin, L. R., Chaboyer, B., Majewski, S., Marín-Franch, A., Milone, A., Paust, N., Piotto, G., Reid, I. N.,

Rosenberg, A., and Siegel, M. (2010). The ACS Survey of Galactic Globular Clusters. IX. Horizontal Branch Morphology and the Second Parameter Phenomenon. *ApJ*, 708(1):698–716.

Duquennoy, A. and Mayor, M. (1991). Multiplicity among Solar Type Stars in the Solar Neighbourhood - Part Two - Distribution of the Orbital Elements in an Unbiased Sample. *A&A*, 248:485.

Edmonds, P. D., Gilliland, R. L., Camilo, F., Heinke, C. O., and Grindlay, J. E. (2002). A Millisecond Pulsar Optical Counterpart with Large-Amplitude Variability in the Globular Cluster 47 Tucanae. *ApJ*, 579(2):741–751.

Elson, R. A. W., Fall, S. M., and Freeman, K. C. (1987). The Structure of Young Star Clusters in the Large Magellanic Cloud. *ApJ*, 323:54.

Ferraro, F. R. (2006). Exotic populations in Galactic Globular Clusters. *arXiv e-prints*, pages astro–ph/0601217.

Ferraro, F. R., Beccari, G., Dalessandro, E., Lanzoni, B., Sills, A., Rood, R. T., Pecci, F. F., Karakas, A. I., Miocchi, P., and Bovinelli, S. (2009). Two distinct sequences of blue straggler stars in the globular cluster M 30. *Nature*, 462(7276):1028–1031.

Ferraro, F. R., Lanzoni, B., and Dalessandro, E. (2020). The "dynamical clock": dating the internal dynamical evolution of star clusters with Blue Straggler Stars. *Rendiconti Lincei. Scienze Fisiche e Naturali*, 31(1):19–31.

Ferraro, F. R., Lanzoni, B., Dalessandro, E., Beccari, G., Pasquato, M., Miocchi, P., Rood, R. T., Sigurdsson, S., Sills, A., Vesperini, E., Mapelli, M., Contreras, R., Sanna, N., and Mucciarelli, A. (2012). Dynamical age differences among coeval star clusters as revealed by blue stragglers. *Nature*, 492(7429):393–395.

Ferraro, F. R., Messineo, M., Fusi Pecci, F., de Palo, M. A., Straniero, O., Chieffi, A., and Limongi, M. (1999a). The Giant, Horizontal, and Asymptotic Branches of Galactic Globular Clusters. I. The Catalog, Photometric Observables, and Features. *AJ*, 118(4):1738–1758.

Ferraro, F. R., Paltrinieri, B., Rood, R. T., and Dorman, B. (1999b). Blue Straggler Stars: The Spectacular Population in M80. *ApJ*, 522(2):983–990.

Ferraro, F. R., Sills, A., Rood, R. T., Paltrinieri, B., and Buonanno, R. (2003). Blue Straggler Stars: A Direct Comparison of Star Counts and Population Ratios in Six Galactic Globular Clusters. *ApJ*, 588(1):464–477.

Fijma, S., Castro Segura, N., Degenaar, N., Knigge, C., Higginbottom, N., Hernández Santisteban, J. V., and Maccarone, T. J. (2023). A transient ultraviolet outflow in the short-period X-ray binary UW CrB. *MNRAS*, 526(1):L149–L154.

Fiorentino, G., Lanzoni, B., Dalessandro, E., Ferraro, F. R., Bono, G., and Marconi, M. (2014). Blue Straggler Masses from Pulsation Properties. I. The Case of NGC 6541. *ApJ*, 783(1):34.

Fregeau, J. M., Cheung, P., Portegies Zwart, S. F., and Rasio, F. A. (2004). Stellar collisions during binary-binary and binary-single star interactions. *MNRAS*, 352(1):1–19.

Geller, A. M., de Grijs, R., Li, C., and Hurley, J. R. (2013). Consequences of Dynamical Disruption and Mass Segregation for the Binary Frequencies of Star Clusters. *ApJ*, 779(1):30.

Girardi, L. (2016). Red clump stars. *Annual Review of Astronomy and Astrophysics*, 54(1):95–133.

Girardi, L., Groenewegen, M. A. T., Hatziminaoglou, E., and da Costa, L. (2005). Star counts in the Galaxy. Simulating from very deep to very shallow photometric surveys with the TRILEGAL code. *A&A*, 436(3):895–915.

Hammer, F., Wang, J., Pawlowski, M. S., Yang, Y., Bonifacio, P., Li, H., Babusiaux, C., and Arenou, F. (2021). Gaia EDR3 Proper Motions of Milky Way Dwarfs. II Velocities, Total Energy, and Angular Momentum. *ApJ*, 922(2):93.

Hawkins, K., Leistedt, B., Bovy, J., and Hogg, D. W. (2017). Red clump stars and Gaia: calibration of the standard candle using a hierarchical probabilistic model. *MNRAS*, 471(1):722–729.

Heggie, D. and Hut, P. (2003). *The Gravitational Million-Body Problem: A Multidisciplinary Approach to Star Cluster Dynamics*.

Heggie, D. C. (1975). Binary evolution in stellar dynamics. *MNRAS*, 173:729–787.

Hills, J. G. and Day, C. A. (1976). Stellar Collisions in Globular Clusters. *Astrophysics Letters*, 17:87.

Hong, J., de Grijs, R., Askar, A., Berczik, P., Li, C., Wang, L., Deng, L., Kouwenhoven, M. B. N., Giersz, M., and Spurzem, R. (2017). The dynamical origin of multiple populations in intermediate-age clusters in the Magellanic Clouds. *MNRAS*, 472(1):67–77.

Huang, S. S. and Struve, O. (1956). The radii and masses of eclipsing binary stars. *AJ*, 61:300–309.

Hut, P., McMillan, S., Goodman, J., Mateo, M., Phinney, E. S., Pryor, C., Richer, H. B., Verbunt, F., and Weinberg, M. (1992). Binaries in Globular Clusters. *PASP*, 104:981.

Ishak, B. (2019). The impact of binary stars on stellar evolution. *Contemporary Physics*, 60(2):196–196.

Jadhav, V. V., Roy, K., Joshi, N., and Subramaniam, A. (2021). High Mass-Ratio Binary Population in Open Clusters: Segregation of Early Type Binaries and an Increasing Binary Fraction with Mass. *AJ*, 162(6):264.

Jiang, D., Chen, X., Li, L., and Han, Z. (2017). Contribution of Primordial Binary Evolution to the Two Blue-straggler Sequences in Globular Cluster M30. *ApJ*, 849(2):100.

Kaluzny, J., Kubiak, M., Szymański, M., Udalski, A., Krzemiński, W., and Mateo, M. (1996). OGLE Eclipsing and SX Phe Stars in ω Cen and 47 Tuc. In Milone, E. F. and Mermilliod, J. C., editors, *The Origins, Evolution, and Destinies of Binary Stars in Clusters*, volume 90 of *Astronomical Society of the Pacific Conference Series*, page 38.

Kim, E., Kim, D.-W., Fabbiano, G., Lee, M. G., Park, H. S., Geisler, D., and Dirsch, B. (2006). Low-Mass X-Ray Binaries in Six Elliptical Galaxies: Connection to Globular Clusters. *ApJ*, 647(1):276–292.

King, I. (1962). The structure of star clusters. I. an empirical density law. *AJ*, 67:471.

Knigge, C., Leigh, N., and Sills, A. (2009). A binary origin for 'blue stragglers' in globular clusters. *Nature*, 457(7227):288–290.

Kuiper, G. P. (1938). The Empirical Mass-Luminosity Relation. *ApJ*, 88:472.

Lanzoni, B., Ferraro, F. R., Alessandrini, E., Dalessandro, E., Vesperini, E., and Raso, S. (2016). Refining the Dynamical Clock for Star Clusters. *Astrophysical Journal, Letters*, 833(2):L29.

Latham, D. W. (1996). Radial Velocity Techniques. In Milone, E. F. and Mermilliod, J. C., editors, *The Origins, Evolution, and Destinies of Binary Stars in Clusters*, volume 90 of *Astronomical Society of the Pacific Conference Series*, page 31.

Legnardi, M. V., Milone, A. P., Cordoni, G., Lagioia, E. P., Dondoglio, E., Marino, A. F., Jang, S., Mohandasan, A., and Ziliotto, T. (2023). Differential reddening in the direction of 56 Galactic globular clusters. *MNRAS*, 522(1):367–380.

Li, C., de Grijs, R., Deng, L., Geller, A. M., Xin, Y., Hu, Y., and Faucher-Giguère, C.-A. (2016). Formation of new stellar populations from gas accreted by massive young star clusters. *Nature*, 529(7587):502–504.

Li, C., de Grijs, R., Deng, L., and Liu, X. (2013). Blue Straggler Evolution Caught in the Act in the Large Magellanic Cloud Globular Cluster Hodge 11. *Astrophysical Journal, Letters*, 770(1):L7.

Li, C., Deng, L., Bekki, K., Hong, J., de Grijs, R., and For, B.-Q. (2018a). Blue Straggler Stars Beyond the Milky Way. III. Detection of Evolved Blue Straggler Candidates in Large Magellanic Cloud Clusters. *AJ*, 156(3):110.

Li, C., Deng, L., de Grijs, R., Jiang, D., and Xin, Y. (2018b). An Unexpected Detection of Bifurcated Blue Straggler Sequences in the Young Globular Cluster NGC 2173. *ApJ*, 856(1):25.

Li, C. and Hong, J. (2018). Blue straggler stars beyond the Milky Way: a non-segregated population in the Large Magellanic Cloud cluster NGC 2213. *MNRAS*, 476(4):5274–5283.

Li, C., Sun, W., Hong, J., Deng, L., de Grijs, R., and Sills, A. (2019). Blue Straggler Stars beyond the Milky Way. IV. Radial Distributions and Dynamical Implications. *ApJ*, 871(2):171.

Li, C., Zhong, J., Qin, S., and Chen, L. (2023). The new detection of blue straggler stars in 50 open clusters using Gaia DR3. *A&A*, 672:A81.

Mackey, A. D. and Gilmore, G. F. (2003). Surface brightness profiles and structural parameters for 53 rich stellar clusters in the Large Magellanic Cloud. *MNRAS*, 338(1):85–119.

Mapelli, M., Sigurdsson, S., Ferraro, F. R., Colpi, M., Possenti, A., and Lanzoni, B. (2006). The radial distribution of blue straggler stars and the nature of their progenitors. *MNRAS*, 373(1):361–368.

McCrea, W. H. (1964). Extended main-sequence of some stellar clusters. *MNRAS*, 128:147.

McLaughlin, D. E. and van der Marel, R. P. (2005). Resolved Massive Star Clusters in the Milky Way and Its Satellites: Brightness Profiles and a Catalog of Fundamental Parameters. *Astrophysical Journal, Supplement*, 161(2):304–360.

Milone, A. P., Bedin, L. R., Piotto, G., and Anderson, J. (2009). Multiple stellar populations in Magellanic Cloud clusters. I. An ordinary feature for intermediate age globulars in the LMC? *A&A*, 497(3):755–771.

Milone, A. P., Cordoni, G., Marino, A. F., D'Antona, F., Bellini, A., Di Criscienzo, M., Dondoglio, E., Lagioia, E. P., Langer, N., Legnardi, M. V., Libralato, M., Baumgardt, H., Bettinelli, M., Cavecchi, Y., de Grijs, R., Deng, L., Hastings, B., Li, C., Mohandasan, A., Renzini, A., Vesperini, E., Wang, C., Ziliotto, T., Carlos, M., Costa, G., Dell'Agli, F., Di Stefano, S., Jang, S., Martorano, M., Simioni, M., Tailo, M., and Ventura, P. (2023a). Hubble Space Telescope survey of Magellanic Cloud star clusters. Photometry and astrometry of 113 clusters and early results. *A&A*, 672:A161.

Milone, A. P., Cordoni, G., Marino, A. F., Muratore, F., D'Antona, F., Di Criscienzo, M., Dondoglio, E., Lagioia, E. P., Legnardi, M. V., Mohandasan, A., Ziliotto, T., Dell'Agli, F., Tailo, M., and Ventura, P. (2023b). Hubble Space Telescope survey of Magellanic Cloud star clusters: UV-dim stars in young clusters. *MNRAS*, 524(4):6149–6158.

Milone, A. P. and Marino, A. F. (2022). Multiple Populations in Star Clusters. *Universe*, 8(7):359.

Milone, A. P., Marino, A. F., Bedin, L. R., Dotter, A., Jerjen, H., Kim, D., Nardiello, D., Piotto, G., and Cong, J. (2016). The binary populations of eight globular clusters in the outer halo of the Milky Way. *MNRAS*, 455(3):3009–3019.

Milone, A. P., Piotto, G., Bedin, L. R., Aparicio, A., Anderson, J., Sarajedini, A., Marino, A. F., Moretti, A., Davies, M. B., Chaboyer, B., Dotter, A., Hempel, M., Marín-Franch, A., Majewski, S., Paust, N. E. Q., Reid, I. N., Rosenberg, A., and Siegel, M. (2012). The ACS survey of Galactic globular clusters. XII. Photometric binaries along the main sequence. *A&A*, 540:A16.

Milone, A. P., Piotto, G., Bedin, L. R., and Sarajedini, A. (2008). Photometric binaries in 50 globular clusters. *Mem. Societa Astronomica Italiana*, 79:623.

Milone, A. P., Piotto, G., Renzini, A., Marino, A. F., Bedin, L. R., Vesperini, E., D'Antona, F., Nardiello, D., Anderson, J., King, I. R., Yong, D., Bellini, A., Aparicio, A., Barbuy, B., Brown, T. M., Cassisi, S., Ortolani, S., Salaris, M., Sarajedini, A., and van der Marel, R. P. (2017). The Hubble Space Telescope UV Legacy Survey of Galactic globular clusters - IX. The Atlas of multiple stellar populations. *MNRAS*, 464(3):3636–3656.

Miocchi, P., Pasquato, M., Lanzoni, B., Ferraro, F. R., Dalessandro, E., Vesperini, E., Alessandrini, E., and Lee, Y. W. (2015). Probing the Role of Dynamical

Friction in Shaping the BSS Radial Distribution. I. Semi-analytical Models and Preliminary N-body Simulations. *ApJ*, 799(1):44.

Moe, M. and Di Stefano, R. (2017). Mind Your Ps and Qs: The Interrelation between Period (P) and Mass-ratio (Q) Distributions of Binary Stars. *Astrophysical Journal, Supplement*, 230(2):15.

Mohandasan, A., Milone, A. P., Cordoni, G., Dondoglio, E., Lagioia, E. P., Vittoria Legnardi, M., Ziliotto, T., Jang, S., Marino, A. F., and Carlos, M. (2024). Photometric Binaries in 14 Magellanic Cloud Star Clusters. *A&A*, 681(A42):15.

Nataf, D. M., Gonzalez, O. A., Casagrande, L., Zasowski, G., Wegg, C., Wolf, C., Kunder, A., Alonso-Garcia, J., Minniti, D., Rejkuba, M., Saito, R. K., Valenti, E., Zoccali, M., Poleski, R., Pietrzyński, G., Skowron, J., Soszyński, I., Szymański, M. K., Udalski, A., Ulaczyk, K., and Wyrzykowski, Ł. (2016). Interstellar extinction curve variations towards the inner Milky Way: a challenge to observational cosmology. *MNRAS*, 456(3):2692–2706.

Nidever, D. L., Bovy, J., Bird, J. C., Andrews, B. H., Hayden, M., Holtzman, J., Majewski, S. R., Smith, V., Robin, A. C., García Pérez, A. E., Cunha, K., Allende Prieto, C., Zasowski, G., Schiavon, R. P., Johnson, J. A., Weinberg, D. H., Feuillet, D., Schneider, D. P., Shetrone, M., Sobeck, J., García-Hernández, D. A., Zamora, O., Rix, H.-W., Beers, T. C., Wilson, J. C., O'Connell, R. W., Minchev, I., Chiappini, C., Anders, F., Bizyaev, D., Brewington, H., Ebelke, G., Frinchaboy, P. M., Ge, J., Kinemuchi, K., Malanushenko, E., Malanushenko, V., Marchante, M., Mészáros, S., Oravetz, D., Pan, K., Simmons, A., and Skrutskie, M. F. (2014). Tracing Chemical Evolution over the Extent of the Milky Way's Disk with APOGEE Red Clump Stars. *ApJ*, 796(1):38.

Piotto, G., De Angeli, F., King, I. R., Djorgovski, S. G., Bono, G., Cassisi, S., Meylan, G., Recio-Blanco, A., Rich, R. M., and Davies, M. B. (2004). Relative Frequencies of Blue Stragglers in Galactic Globular Clusters: Constraints for the Formation Mechanisms. *Astrophysical Journal, Letters*, 604(2):L109–L112.

Preston, G. W. and Sneden, C. (2000). What Are These Blue Metal-Poor Stars? *AJ*, 120(2):1014–1055.

Raghavan, D., McAlister, H. A., Henry, T. J., Latham, D. W., Marcy, G. W., Mason, B. D., Gies, D. R., White, R. J., and ten Brummelaar, T. A. (2010). A Survey of Stellar Families: Multiplicity of Solar-type Stars. *Astrophysical Journal, Supplement*, 190(1):1–42.

Rain, M. J., Ahumada, J. A., and Carraro, G. (2021). A new, Gaia-based, catalogue of blue straggler stars in open clusters. *A&A*, 650:A67.

Romani, R. W. and Weinberg, M. D. (1991). Limits on Cluster Binaries. *ApJ*, 372:487.

Rubenstein, E. P. and Bailyn, C. D. (1997). Hubble Space Telescope Observations of the Post-Core-Collapse Globular Cluster NGC 6752. II. A Large Main-Sequence Binary Population. *ApJ*, 474(2):701–709.

Sabbi, E., Lennon, D. J., Anderson, J., Cignoni, M., van der Marel, R. P., Zaritsky, D., De Marchi, G., Panagia, N., Gouliermis, D. A., Grebel, E. K., Gallagher, J. S., I., Smith, L. J., Sana, H., Aloisi, A., Tosi, M., Evans, C. J., Arab, H., Boyer, M., de Mink, S. E., Gordon, K., Koekemoer, A. M., Larsen, S. S., Ryon, J. E., and Zeidler, P. (2016). Hubble Tarantula Treasury Project. III. Photometric Catalog and Resulting Constraints on the Progression of Star Formation in the 30 Doradus Region. *Astrophysical Journal, Supplement*, 222(1):11.

Salinas, R., Jílková, L., Carraro, G., Catelan, M., and Amigo, P. (2012). Structural parameters and blue stragglers in Sagittarius dwarf spheroidal galaxy globular clusters. *MNRAS*, 421(2):960–970.

Sana, H., de Mink, S. E., de Koter, A., Langer, N., Evans, C. J., Gieles, M., Gosset, E., Izzard, R. G., Le Bouquin, J. B., and Schneider, F. R. N. (2012). Binary Interaction Dominates the Evolution of Massive Stars. *Science*, 337(6093):444.

Sana, H., Rauw, G., and Gosset, E. (2001). HD 152248: Evidence for a colliding wind interaction. *A&A*, 370:121–135.

Sandage, A. R. (1953). The color-magnitude diagram for the globular cluster M 3. *AJ*, 58:61–75.

Santos, João F. C., J., Maia, F. F. S., Dias, B., Kerber, L. d. O., Piatti, A. E., Bica, E., Angelo, M. S., Minniti, D., Pérez-Villegas, A., Roman-Lopes, A., Westera, P., Fraga, L., Quint, B., and Sanmartim, D. (2020). The VISCACHA survey - II. Structure of star clusters in the Magellanic Clouds periphery. *MNRAS*, 498(1):205–222.

Sills, A., Karakas, A., and Lattanzio, J. (2009). Blue Stragglers After the Main Sequence. *ApJ*, 692(2):1411–1420.

Siraj, A. and Loeb, A. (2020). The Case for an Early Solar Binary Companion. *Astrophysical Journal, Letters*, 899(2):L24.

Skelton, P. and Smits, D. (2009). Modelling of w uma-type variable stars. *S. Afr. j. sci*, 105(3-4):120–126.

Sollima, A. (2008). The evolution of the binary population in globular clusters: a full analytical computation. *MNRAS*, 388(1):307–322.

Sollima, A., Beccari, G., Ferraro, F. R., Fusi Pecci, F., and Sarajedini, A. (2007). The fraction of binary systems in the core of 13 low-density Galactic globular clusters. *MNRAS*, 380(2):781–791.

Sollima, A., Carballo-Bello, J. A., Beccari, G., Ferraro, F. R., Pecci, F. F., and Lanzoni, B. (2010). The fraction of binary systems in the core of five Galactic open clusters. *MNRAS*, 401(1):577–585.

Sollima, A., Lanzoni, B., Beccari, G., Ferraro, F. R., and Fusi Pecci, F. (2008). The correlation between blue straggler and binary fractions in the core of Galactic globular clusters. *A&A*, 481(3):701–704.

Spitzer, L. (1987). *Dynamical evolution of globular clusters*.

Stryker, L. L. (1993). Blue Stragglers. *PASP*, 105:1081.

Sun, W., Li, C., de Grijs, R., and Deng, L. (2018). Blue Straggler Stars beyond the Milky Way. II. A Binary Origin for Blue Straggler Stars in Magellanic Cloud Clusters. *ApJ*, 862(2):133.

Tailo, M., Milone, A. P., Lagioia, E. P., D'Antona, F., Jang, S., Vesperini, E., Marino, A. F., Ventura, P., Caloi, V., Carlos, M., Cordoni, G., Dondoglio, E., Mohandasan, A., Nastasio, J. E., and Legnardi, M. V. (2021). Mass-loss law for red giant stars in simple population globular clusters. *MNRAS*, 503(1):694–703.

Ting, Y.-S., Hawkins, K., and Rix, H.-W. (2018). A Large and Pristine Sample of Standard Candles across the Milky Way: ∼100,000 Red Clump Stars with 3% Contamination. *ApJ*, 858(1):L7.

Trenti, M., Vesperini, E., and Pasquato, M. (2010). Tidal Disruption, Global Mass Function, and Structural Parameter Evolution in Star Clusters. *ApJ*, 708(2):1598–1610.